

University of Mississippi

eGrove

Electronic Theses and Dissertations

Graduate School

1-1-2014

Secondary Metabolite Production By An Endophytic Bacillus sp. from Platanus Occidentalis

Michael C. James
University of Mississippi

Follow this and additional works at: <https://egrove.olemiss.edu/etd>



Part of the [Pharmacy and Pharmaceutical Sciences Commons](#)

Recommended Citation

James, Michael C., "Secondary Metabolite Production By An Endophytic Bacillus sp. from Platanus Occidentalis" (2014). *Electronic Theses and Dissertations*. 1344.
<https://egrove.olemiss.edu/etd/1344>

This Thesis is brought to you for free and open access by the Graduate School at eGrove. It has been accepted for inclusion in Electronic Theses and Dissertations by an authorized administrator of eGrove. For more information, please contact egrove@olemiss.edu.

SECONDARY METABOLITE PRODUCTION BY AN ENDOPHYTIC *BACILLUS* SP. FROM
PLATANUS OCCIDENTALIS

A Thesis
presented in partial fulfillment of requirements
for the degree of Master of Science
in Pharmaceutical Sciences (Emphasis Pharmacognosy)
The University of Mississippi

by

Michael C. James

July 2014

Copyright Michael C. James 2014
ALL RIGHTS RESERVED

ABSTRACT

Endophytes are bacterial and fungal microbes that live inside of plant tissue without causing disease. Endophytes have applications in many industries including the pharmaceutical and food industries as producers of natural products. This potential was demonstrated by investigating the natural product production from a *Bacillus amyloliquefaciens* endophyte of *Platanus occidentalis* using a combination of MALDI-IMS, LC-MS, MS-MS, and NMR methods, by purifying nicotianamine from soy flour, and by reviewing natural product inhibitors of the hepatitis C virus (HCV).

The secondary metabolite production of the endophytic *B. amyloliquefaciens* was investigated under a variety of fermentation conditions. It was discovered that the endophyte produces rapamycin, a molecule previously reported only from *Streptomyces hygrosopicus* from Easter Island in the South Pacific. Other known natural products from the *Bacillus* genus were identified using LC-MS including the lipopeptide fengycins, surfactins, and iturins. Iturin A₃ was isolated and characterized from the endophyte, and found in the host *P. occidentalis*, as shown by LC-MS. The presence of a possible rapamycin analogue was discovered which would be indicative of a biotransformation process. Challenge experiments were conducted using MALDI-IMS in an attempt to understand host regulation of secondary metabolites. Iturin production increased as shown by MALDI-IMS.

The impetus for studying endophytes like *B. amyloliquefaciens* for natural products was further exemplified by purifying a natural metal chelator, nicotianamine, from soy flour. This is a possible candidate to replace ethylenediaminetetraacetic acid (EDTA), a synthetic metal

chelator used to prevent food spoilage. Further studies on possible endophytic production of nicotianamine could be of great importance to many food companies. The importance of studying endophytes was further shown by reviewing the number of novel and known natural products that have been reported with activity against the hepatitis C virus (HCV). There are numerous examples in the literature of metabolites being reported as plant-derived which are later identified as ultimately being produced by endophytic organisms. This review demonstrates the importance of studying new and known sources of HCV active metabolites for endophytic organisms.

DEDICATION

This thesis is dedicated to Shivangi Awasthi, and Mary Nell Butler. For Ms. Awasthi, for always being there to support me through the difficult times that occurred while completing my thesis. And for my grandmother, Mrs. Mary Nell Butler, whose courage while battling cancer was a true inspiration and whose love is always with me.

LIST OF ABBREVIATIONS AND SYMBOLS

EIC: extracted ion chromatogram

ESI: electrospray ionization

FDA: U.S. Food and Drug Administration

FTMS: Fourier transform mass spectrometry

HCV: hepatitis C virus

HP-20: high porous styrenic adsorbent resin

HPLC: high performance liquid chromatography

HRMS: high resolution mass spectrometry

IC₅₀: the half maximal inhibitory concentration

IMS: imaging mass spectrometry

LC/MS: liquid chromatography/ mass spectrometry

MALDI-IMS: matrix-assisted laser desorption/ionization imaging mass spectrometry

MS/MS: tandem mass spectrometry

NCBI: National Center for Biotechnology Information

NCNPR: National Center for Natural Products Research

NIH: National Institutes of Health

TEM: transmission electron microscopy

TIC: total ion chromatogram

TOF: time of flight

VLC: vacuum liquid chromatography

ACKNOWLEDGMENTS

First of all I would like to express my sincere gratitude to Dr. Mark Hamann for his support towards the research that was completed while earning my master's degree. I would also like to thank my committee members Dr. Stephen Cutler, Dr. Daneel Ferreira, and Dr. Ted Leininger for their advice and valuable suggestions with regards to this thesis.

I would also like to thank Dr. Yu-Dong Zhou, Dr. John Rimoldi, Dr. Daneel Ferreira, Christina Coleman, and other formal and informal teachers I have had the pleasure of learning from here at The University of Mississippi.

I would like to thank Dr. Dale Nagle and Dr. Jordan Zwjawiony for allowing me the great honor of being a teacher's assistant in their classes.

I would also like to thank Dr. Amala Dass and Nuwan Kothalawala for their collaborative efforts using MALDI-IMS. Also, I would like to thank Dr. Allen Place and Sabeena Nazar for their genome sequencing work and Ben Pharr at the Mississippi Center for Supercomputing Research for expanding our capabilities to do genome research in the lab.

Last but not least I would like to thank Shivangi Awasthi and my parents, Dr. William James and Deborah Butler, for all their emotional support.

TABLE OF CONTENTS

ABSTRACT.....	ii
DEDICATION.....	iv
LIST OF ABBREVIATIONS AND SYMBOLS.....	v
ACKNOWLEDGMENTS	vi
LIST OF TABLES.....	viii
LIST OF FIGURES	ix
CHAPTER ONE: INTRODUCTION.....	1
CHAPTER TWO: SECONDARY METABOLITE PRODUCTION FROM A <i>BACILLUS AMYLOLIQUEFACIENS</i> ENDOPHYTE OF <i>PLATANUS OCCIDENTALIS</i>	18
CHAPTER THREE: PURIFICATION OF NICOTIANAMINE FROM SOY FLOUR	52
CHAPTER FOUR: HCV REVIEW.....	61
CHAPTER FIVE: CONCLUSION.....	69
EXPERIMENTAL SECTION	74
BIBLIOGRAPHY.....	78
VITA.....	89

LIST OF TABLES

Table 1 Reported Enriched Sources of Nicotianamine.....	14
Table 2 <i>Bacillus</i> genome assembly.....	20
Table 3 CS20 Media ⁸³	24
Table 4 MRSA and <i>Staph. aureus</i> activity.....	26
Table 5 Extracts of <i>P. occidentalis</i> tissue.....	42
Table 6 Calibration of NA using LC-MS.....	53

LIST OF FIGURES

Figure 1 <i>Platanus occidentalis</i> species with leaf inset	3
Figure 2 MRSA active glycosides isolated from <i>P. occidentalis</i> leaf tissue	5
Figure 3 Transmission electron microscopy image of <i>Bacillus subtilis</i>	5
Figure 4 Representative examples of the families of lipopeptides produced by <i>Bacillus</i> spp.....	8
Figure 5 Representative examples of polyketides produced by <i>Bacillus</i> spp.	10
Figure 6 Rapamycin structure.....	11
Figure 7 Nicotianamine structure.....	13
Figure 8 Production of rapamycin and possible biotransformation to a putative rapamycin analogue	20
Figure 9 Isolation of iturin A ₃ from <i>B. amyloliquefaciens</i> and <i>P. occidentalis</i> host	21
Figure 10 Isolation of rapamycin from <i>B. amyloliquefaciens</i>	22
Figure 11 FTMS of rapamycin standard.....	22
Figure 12 FTMS of purified fraction from <i>B. amyloliquefaciens</i>	23
Figure 13 <i>B. amyloliquefaciens</i> morphology.....	25
Figure 14 Culturing and purification of endophytic <i>Bacillus</i> secondary metabolites.	26
Figure 15 Fengycin ions.....	27
Figure 16 Fengycin isoforms	29
Figure 17 Surfactin ion signals.	29
Figure 18 Surfactin homologues.....	30
Figure 19 Iturin ions.....	30

Figure 20 Iturin isolation scheme	31
Figure 21 Purification of iturin homologues.....	31
Figure 22 Iturin homologues.....	32
Figure 23 Purified iturin homologues.....	32
Figure 24 EIC of bacterial extract and rapamycin standard	33
Figure 25 MADLI-IMS of <i>Bacillus</i> endophyte.	35
Figure 26 Isolation scheme for rapamycin.....	36
Figure 27 Isolation scheme for rapamycin.....	37
Figure 28 HRMS of rapamycin from <i>Bacillus</i> sp.	37
Figure 29 HRMS of rapamycin standard	38
Figure 30 Rapamycin and <i>B. amyloliquefaciens</i> fraction ¹ H-NMR overlay experiment	39
Figure 31 Rapamycin and <i>B. amyloliquefaciens</i> fraction ¹ H-NMR overlay experiment	40
Figure 32 Rapamycin and <i>B. amyloliquefaciens</i> fraction ¹ H-NMR overlay experiment	40
Figure 33 Rapamycin and <i>B. amyloliquefaciens</i> fraction ¹ H-NMR overlay experiment.	41
Figure 34 Overlay of two extracted ion chromatograms of <i>P. occidentalis</i> extract and endophytic extract.....	42
Figure 35 Extraction of <i>P. occidentalis</i> wood material	43
Figure 36 Two EICs of putative rapamycin analog and rapamycin	43
Figure 37 Isolation of putative rapamycin analogue.....	44
Figure 38 Putative rapamycin analogue purification	45
Figure 39 HRMS of putative rapamycin analog.	45

Figure 40 MALDI-IMS iturin blank run.....	47
Figure 41 Extraction of <i>P. occidentalis</i> for MALDI-IMS challenge experiment.....	48
Figure 42 <i>Bacillus</i> sp. colony surrounded by host <i>P. occidentalis</i> extracts.....	48
Figure 43 Day one iturin production.....	49
Figure 44 <i>Bacillus</i> sp. colony surrounded by host <i>P. occidentalis</i> extracts.....	49
Figure 45 Day three iturin production.	50
Figure 46 Day four iturin production.....	51
Figure 47 Nicotianamine structure.....	52
Figure 48 Calibration curve for nicotianamine.....	54
Figure 49 Detection limits of nicotianamine	55
Figure 50 HRMS of nicotianamine.....	55
Figure 51 Comparision of nicotianamine from whole soybean precipitate, soy flour precipitate, and nicotianamine standard.....	56
Figure 52 Nicotianamine isolation scheme.....	58
Figure 53 Yield of nicotianamine from soy flour	59
Figure 54 Yield of nicotianamine from soy flour after multiple purification steps.....	59
Figure 55 Co-injection of nicotianamine and extract	60
Figure 56 Plant-derived inhibitors of HCV	65
Figure 57 Microbial-derived HCV inhibitors	67
Figure 58 Marine-derived inhibitors of HCV	68

CHAPTER ONE: INTRODUCTION

Endophytes are bacterial and fungal microbes that live inside of plant tissue without causing disease. Endophytes have applications in many industries including the pharmaceutical and food industries as producers of natural products. This potential was demonstrated by investigating the natural product production from a *Bacillus amyloliquefaciens* endophyte of *Platanus occidentalis* using a combination of MALDI-IMS, LC-MS, MS-MS, and NMR methods, by studying the production of nicotianamine from soy flour, and by reviewing natural product inhibitors of the hepatitis C virus (HCV).

The secondary metabolite production of the endophytic *Bacillus amyloliquefaciens* was investigated under a variety of fermentation conditions. It was discovered that the *B. amyloliquefaciens* produces rapamycin, a molecule previously reported only from *Streptomyces hygrosopicus* from Easter Island in the South Pacific. Other known natural products from *Bacillus* sp. were identified using LC-MS including the antifungal lipopeptide fengycins, surfactins, and iturins. Iturin A₃ was isolated and characterized from the endophytic *B. amyloliquefaciens*, and found in the host *P. occidentalis*, as shown by LC-MS. The presence of a possible rapamycin analogue was discovered which would be indicative of a biotransformation process. Challenge experiments were conducted using MALDI-IMS in an attempt to understand host regulation of secondary metabolites. Iturin production increased as shown by MALDI-IMS.

The impetus for studying endophytes like *B. amyloliquefaciens* for natural products was further exemplified by purifying a natural metal chelator, nicotianamine, from soy flour. This is a possible candidate to replace ethylenediaminetetraacetic acid (EDTA), which is a synthetic

metal chelator that is used to prevent food spoilage. Further studies on possible endophytic production of nicotianamine could be of great importance to many food companies. The importance of endophytes was further demonstrated by reviewing natural product hepatitis C virus (HCV) inhibitors. There are numerous examples in the literature of metabolites being reported as plant-derived which are later identified as ultimately being produced by endophytic organisms. This review demonstrates the importance of studying new and known sources of HCV active metabolites for endophytic organisms.

Platanus occidentalis* and *Bacillus amyloliquefaciens

Platanus occidentalis (American Sycamore) is an Eudicotyledon species of tree that has a native range that primarily exists east of the Great Plains region in the United States but also extends into parts of southern Ontario and the mountainous region of northeastern Mexico (**Figure 1**).¹ Fully mature trees are characterized by exfoliating bark that leaves portions of inner bark exposed and leads to a patchwork appearance with different areas of grey, brown, white, and green. Trees are deciduous and leaves are palmate-veined with three to five lobes per leaf and are among the largest trees in Eastern deciduous forests. American Sycamore is a fast-growing species often grown in plantations for pulp or dimensional lumber products.¹ It has been used in the rehabilitation of saturated soils and strip-mined land and is an early colonizer of waterway disposal sites and degraded stream banks. Ethnobotanic uses by Native Americans include the treatment of colds, respiratory ailments, as gastrointestinal and gynecological aids, and for uses in dermatological problems.¹ Previously, one known and three novel glycosides were isolated from *P. occidentalis* leaf tissue that showed significant activity against MRSA (**Figure 2**).² In order to more fully understand the pharmacological potential of this native tree, the secondary metabolite production of an endophyte that is involved in a mutualism with *P.*

occidentalis was studied.

Mutualism is an association between two organisms that benefits both organisms. These types of associations abound in nature and certain mutualistic relationships play important roles in plant health. For example, mycorrhizal fungi form symbiotic relationships with plant roots whereby plants gain increased surface area for mineral and water absorption from the soil while the fungal symbionts derive nutrition from plant-produced carbohydrates. Plants contributing in this symbiosis are more resistant to drought and disease.³⁻⁴ Plants benefit in a number of other ways through this association, many of which are still being researched. It is currently estimated that 80% of plant species and 92% of plant families



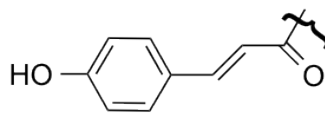
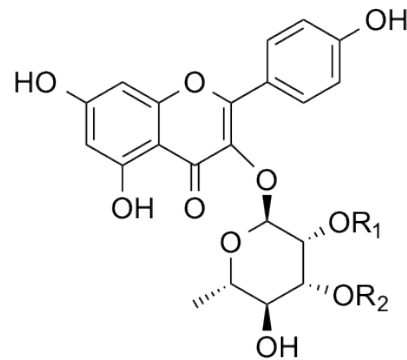
Figure 1 *Platanus occidentalis* species with leaf inset

have mycorrhizal associations with fungi.⁵ Another important mutualism exists between plants and nitrogen-fixing bacteria whereby bacteria dwelling inside the root nodules of certain plant

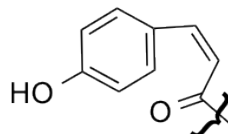
species fix nitrogen and make it available to the host plant and, after the host dies, to the soil.

Yet another important mutualism exists between bacterial and/or fungal microbes and their plant hosts.

Endophytes are bacteria and/or fungi that reside in living plant tissue without causing disease. There are examples of bacterial and fungal species that can exist as both endophytes and pathogens depending on many factors including different stages of the microorganism's life cycle or environmental conditions. Thus, the nature of the host-microbe association must be taken into account when labeling a microorganism as an endophyte.⁶ Although estimates vary, it is currently accepted that there are over 300,000 higher plants on Earth, and each species that has been examined for endophytes



E-p-coumaroyl



Z-p-coumaroyl

- 1, $R^1=R^2=E-p\text{-coumaroyl}$
- 2, $R^1=E-p\text{-coumaroyl}$, $R^2=Z-p\text{-coumaroyl}$
- 3, $R^1=Z-p\text{-coumaroyl}$, $R^2=E-p\text{-coumaroyl}$
- 4, $R^1=R^2=Z-p\text{-coumaroyl}$

Figure 2 MRSA active glycosides isolated from *P. occidentalis* leaf tissue has contained them. One of the best studied endophyte and plant host mutualisms occurs between fungal endophytes and various grasses. It has been shown in native grasses that the presence of fungal endophytes decreases herbivory.⁷ These fungal endophytes produce insecticidal alkaloids that have proven activity against both vertebrates and insect pests.⁸ The ecology of endophytes and how they contribute to plant health is an active and compelling area of research. One of the recognized functions of endophytes is to provide natural products to the host plant that aid in protection and survival. Many of these compounds have human uses in agriculture, industry, and in medicine as antibiotics, antimycotics, immunosuppressants, and as chemotherapeutic compounds.⁹ One of the endophytes that was isolated from *P. occidentalis* was identified by colony morphology, and later by 16S rRNA analysis, as *B. amyloliquefaciens*.

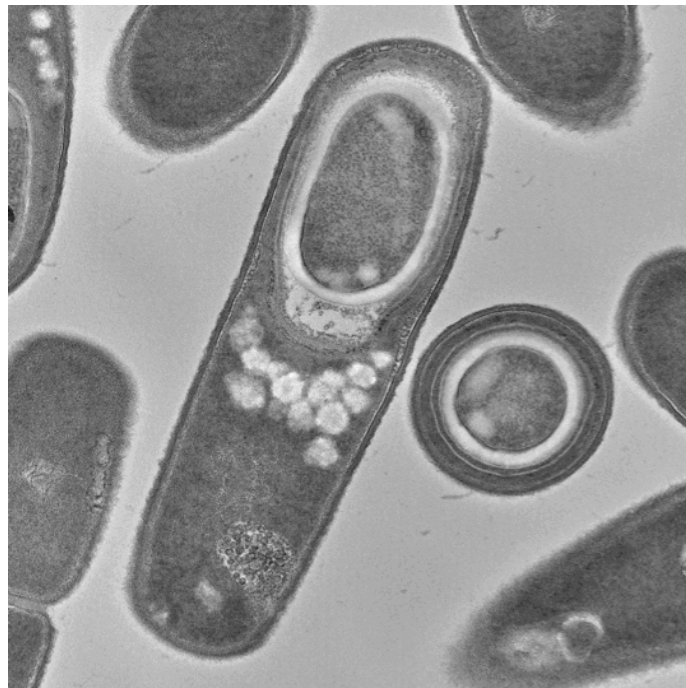


Figure 3 Transmission electron microscopy image of *Bacillus subtilis*. Endospore is shown. (Photo courtesy of NCI at Frederick: http://ncifrederick.cancer.gov/atp/cms/wp-content/uploads/2010/11/bacteria_021.jpg)

Bacillus spp. are rod-shaped, motile, and aerobic. They can produce endospores to survive unfavorable conditions and, until the advent of molecular phylogenetics, this was the defining characteristic that placed a bacterium within the genus.¹⁰ *B. subtilis* is used as a model organism for Gram-positive bacteria and is one of the most well known and studied Gram-positive species (**Figure 3**). The fact that *B. subtilis* and other *Bacillus* species can form such hardy spores, and that these spores are often dispersed by wind, has made characterizing the preferred environment of *B. subtilis* difficult.¹¹ However, there is mounting evidence that the environments where *B. subtilis* can survive are extremely diverse. These include soil, plant roots, and within the GI tract of animals.¹¹ Soil dwelling *B. subtilis* species have been shown to be involved in plant growth promotion.¹² The presence of *B. subtilis* spores in the GI tract of many animals including humans has been known for many years, and this was assumed to be due to the ingestion of food contaminated by spores. However, there is growing evidence that *B. subtilis* are actually involved in a mutualistic relationship with the host animal species.¹³ The full genome of *B. subtilis* was published in 1997.¹⁴ The genome was reported to contain 4,214,810 base pairs which correlated with 4,100 protein coding genes. Interestingly, a number of these genes are devoted to the production of proteins involved in the utilization of plant-derived molecules.¹⁴

Some other commonly known *Bacillus* species are *B. anthracis*, *B. thuringiensis*, and *B. cereus*. *B. anthracis* causes anthrax by producing the anthrax toxin that has been developed into a biological weapon by a number of countries. *B. thuringiensis* produces pesticidal crystal proteins and is the most widely used biorational pesticide.¹⁵ Certain *B. cereus* strains are responsible for a number of food poisoning cases.

The genome of *B. amyloliquefaciens* FZB42 strain was comparatively analyzed in

2007.¹⁶ The particular *B. amyloliquefaciens* strain that was analyzed, *B. amyloliquefaciens* FZB42, has been reported as a rhizobacterium. It was reported that more than 8.5% of the genome was devoted to synthesizing siderophores and antibiotics using non-ribosomal pathways.¹⁶ A number of genes that were previously identified as being involved in bacterium-plant interactions were also identified. These include genes involved in: the production of an exopolysaccharide that holds bacterial cells together; the production of surfactin for the colonization of plant surfaces; and the production of extra-cellular macromolecular depolymerases for growing on plant surfaces.¹⁶ A number of PKS and NRPS genes were also identified, although the putative synthetic secondary metabolites are unknown.¹⁶

The secondary metabolite production of *Bacillus* spp. was reviewed comprehensively by Sansinenea and Ortiz in 2011.¹⁷ *Bacillus* spp. produce a diverse array of natural products including bacteriocins, lantibiotics, lipopeptides, and polyketides.¹⁷ Bacteriocins are peptides or proteins that can vary in structure and molecular weight and typically are active against bacteria that are closely related to the producer organism. A *B. licheniformis* strain which was isolated from buffalo rumen produces lichenin, a bacteriocin with a mass of approximately 1400 daltons and length of 12 amino acids.¹⁸ A bacteriocin peptide of 44 residues called coagulins, produced by *B. coagulans*, has proven antilisterial activity.¹⁹ Polyfermentacin SCD is another bacteriocin produced by *B. polyfermenticus* that has shown narrow spectrum activity against certain bacteria as well as yeasts and molds and has a mass of approximately 14.3 kilodaltons.²⁰

Lantibiotics are a group of polycyclic compounds that are formed by the posttranslational modification of serine and threonine residues. These residues are dehydrated and then the thiol group of cysteine residues are added in intramolecular reactions to form lanthionine and methyllanthionine bridges.²¹ *B. subtilis* produces many lantibiotics including subtilin, ericin, and

mersacidin, among others.²² Subtilin is by far the most widely studied of this group of secondary metabolites. It is composed of 32 amino acids and has activity against mostly Gram-positive species as well as many pathogenic fungi.²³ Another group of secondary metabolites that has been isolated from *Bacillus* species are the lipopeptides (**Figure 4**).¹⁷ Lipopeptides consist of a short fatty acid chain linked to a linear or cyclized peptide.²⁴ Certain lipopeptides have exhibited antimicrobial, immunosuppressant, and cytotoxic activity.²⁴⁻²⁶

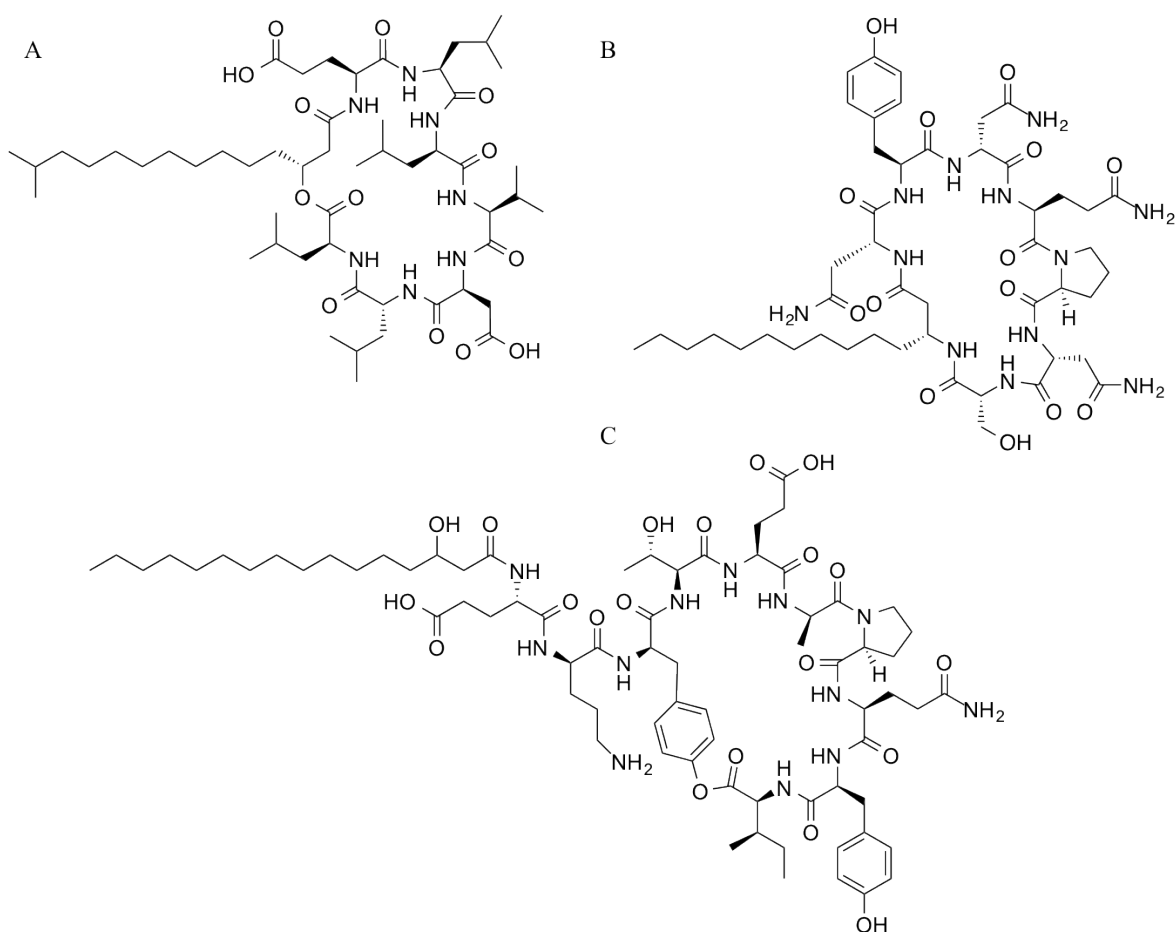


Figure 4 Representative examples of the families of lipopeptides produced by *Bacillus* spp. (A) surfactins, (B) iturins, and (C) fengycins.

The three groups of lipopeptides produced by *Bacillus* spp. are the surfactins, iturins, and fengycins. These groups are defined by the number of amino acids within the cyclized peptide

moiety. Variants within groups are established by having different amino acid residues at different positions or differences in the lipid tail.²⁴ Most of these molecules also have demonstrated surfactant properties and the most widely studied lipopeptides are the surfactin group.²⁷ The surfactin group contains molecules with a heptapeptide moiety linked to a β -hydroxy fatty acid chain.²⁴ Surfactin 5 has demonstrated biosurfactant properties, as well as antiviral and antimycoplasmal activity.²⁸ The iturins contain seven cyclized amino acids and a β -amino fatty acid. They are differentiated by variations of amino acids at different positions and also by variation in the branching or length of the β -amino fatty acid.²⁹ Iturins have demonstrated activity against fungal plant pathogens including *Podospaera fusca*,²⁹ *Rhizoctonia solani*,³⁰ and a number of iturin-producing *Bacillus* species are currently in use as bio-control agents for many other fungal pathogens.³¹ The fengycin group of lipopeptides contain 10 amino acids, eight of which form a lactone via a linkage between tyrosine and isoleucine. The β -hydroxy fatty acid is linked to the peptide moiety through an amide bond with the α -amino group of glutamic acid.²⁴ Members of this group of lipopeptides have shown selective activity against filamentous fungi and certain agricultural pests.³²

Polyketides are another group of secondary metabolites that have been isolated from *B. subtilis* (**Figure 5**). Difficidin and oxydifficidin are two macrocyclic polyene lactone phosphate esters that were first isolated and characterized in 1987 from *B. subtilis*.³³ Difficidin has also been isolated from the plant-associated *B. amyloliquefaciens* and has proven activity against fire blight in orchard trees caused by *Erwinia amylovora*.³⁴⁻³⁵ Bacillaene is another polyketide that was reported from *B. subtilis* in 1995 and has also recently shown activity against *E. amylovora*.³⁴ The production of bacillaene was discovered to be through an approximately 80 kb *pksX* gene cluster that encodes an uncommon polyketide/nonribosomal peptide synthase.³⁶

Multiple copies of this synthase form a megacomplex with an expected mass of tens to hundreds of megadaltons to produce bacillaene, which contains two amide bonds and is not cyclized.³⁶ Macrolactins are a group of compounds which contain three separated diene components within a 24-membered lactone. The first macrolactin was isolated from an unidentified deep sea bacterium.³⁷ Macrolactin F was later isolated from an identified marine *Bacillus* sp. and

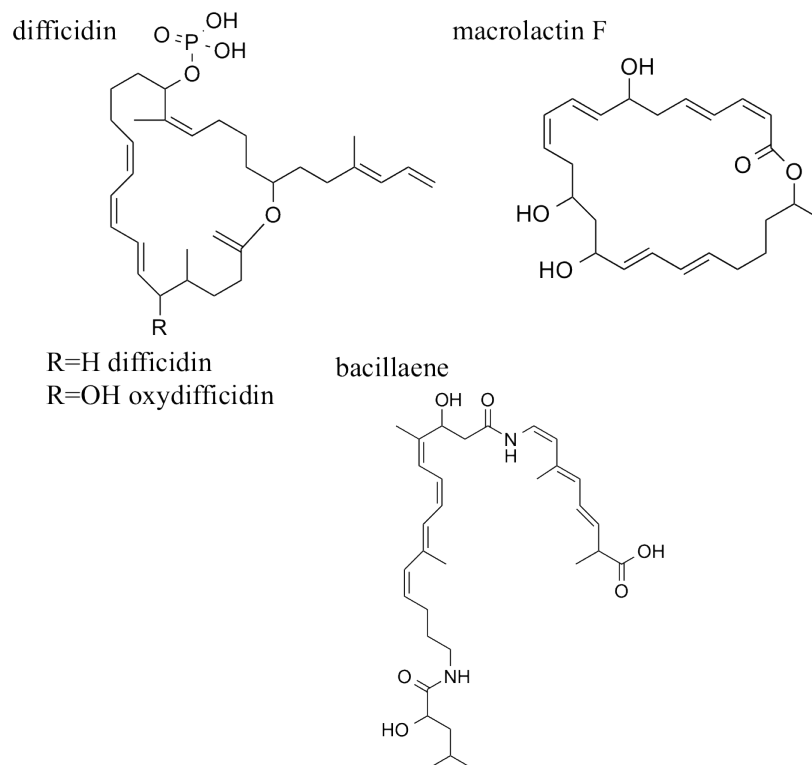


Figure 5 Representative examples of polyketides produced by *Bacillus* spp. (A) difficidin and oxydifficidin, (B) macrolactin F, and (C) bacillaene (stereochemistry unknown).

macrolactin S has also been isolated from a *Bacillus* spp. Macrolactin S showed unique activity against the *Staph. aureus* FabG protein, and 7-*O*-malonylmacrolactin A, which showed activity against MRSA and vanomycin-resistant enterococci.³⁸⁻³⁹

One of the most important polyketides from a drug discovery standpoint is rapamycin (**Figure 6**). Rapamycin was first isolated from the actinomycete *Streptomyces hygroscopicus*, which was isolated from a soil sample collected on Easter Island in the southeastern Pacific Ocean in 1975.⁴⁰⁻⁴¹ It was first reported as an antifungal product; subsequent studies

demonstrated rapamycin possessed significant activity against mammalian brain tumors⁴² and immune cells.⁴³ Investigations into the mechanism of action of rapamycin led to the discovery of *TOR 1-1* (Target of Rapamycin) and *TOR2-1* genes in *Saccharomyces cerevisiae*.⁴⁴ These genes are conserved in all eukaryotes, excepting metazoans which only contain one *TOR gene*, and are now known to code for serine/threonine protein kinases that are part of larger multiprotein complexes called TORC (TOR Complex) 1 and TORC 2.⁴⁵⁻⁴⁸ These

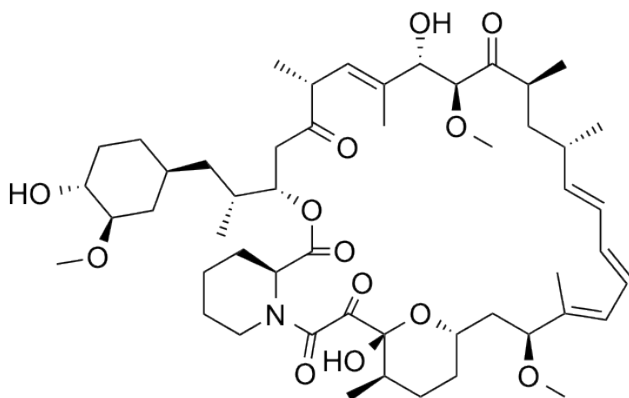


Figure 6 Rapamycin structure

kinases are master regulators of eukaryotic cells, responsible for coordinating environmental signals with cell growth.⁴⁵

For many years, it was believed that plants were resistant to rapamycin. However, it was shown that rapamycin inhibits root and leaf growth.⁴⁹ Seedling and cellular assays were used to monitor TOR kinase activity by measuring S6 kinase (S6K) phosphorylation, and showed that, in plants, rapamycin inhibited the phosphorylation of Thr-449 and Thr-455 of S6K1 and S6K2, respectively. It had previously been shown that growth of *Arabidopsis* seedlings after germination strictly relies on glucose for growth.⁵⁰ Using this newly developed assay, it was shown that glucose strongly activates TOR PK activity. Subsequently, it was shown that the presence of rapamycin had a detrimental effect on seedling growth by interfering with glucose-TOR signaling. Seedlings grown in the presence of rapamycin had underdeveloped cotyledons,

leaves, petioles, and primary and lateral roots, leading to the conclusion that reports of plant resistance to rapamycin were false.⁴⁹ A more recent paper further illustrated the importance of glucose-TOR signaling for plant development and growth.⁵¹ This study concentrated on the the photoautotrophic transition checkpoint, when a seedling transitions from acting as a heterotroph, relying on seed material, to a photoautotroph, synthesizing carbohydrates through photosynthesis. It was discovered that glucose-TOR signaling has a direct relationship to root meristem stem/progenitor cell proliferation and overall plant growth through inter-organ coordination.⁵¹ The presence or absence of rapamycin was not linked to fluctuations in levels of auxins, or cytokines, or the the maintenance of the stem cell niche, but was instead specifically linked to changes in the cell cycle of the root meristem. They discovered 1,318 up regulated and 1,050 down regulated genes related to TOR-glucose signaling. Interestingly, *tor* mutant plants did not undergo any of these transcriptome changes once again demonstrating the importance of TOR PK to plant development.⁵¹

Rapamycin has recently proved to have some anti-aging properties in mice models.⁵² Current data suggest that the prevention of cancer is responsible for life extension in mice as opposed to acting on aging itself. Rapamycin and rapamycin analogues are approved for the treatment of many different types of diseases. Rapamycin is currently approved for use in kidney transplantation and has a mechanism of action that is unique from that of other immunosuppressants including tacrolimus and cyclosporin.⁵³ These two agents act by inhibiting the transcription of calcineurin phosphatase, thus preventing the transcription of cytokines. Rapamycin exerts its effects through binding to mTOR and has the ability to synergize with other immunosuppressants.⁵³ The rapamycin analog everolimus is approved for the treatment of subependymal giant cell astrocytoma (SEGA), advanced hormone receptor-positive, HER2-

negative breast cancer, progressive neuroendocrine tumors of pancreatic origin, and advanced renal cell carcinoma.⁵⁴ Temsirolimus is another derivative which was developed to decrease immunosuppressive properties and increase solubility and is approved for advanced renal cell carcinoma.⁵⁵

Imaging mass spectrometry (IMS) is a technology that is currently finding widespread use in drug discovery for the study of biomarkers⁵⁶ and more recently the metabolism and tissue distribution of therapeutic agents.⁵⁷ IMS has also emerged in the relatively recent past as a new tool in natural products research. The use of IMS involves three basic steps, which can vary considerably depending on which ionization technique is involved. For the work presented here, all IMS data were acquired using MALDI-IMS. In MALDI-IMS, the workflow can be divided into four steps: sample preparation, matrix application, measurement, and data analysis.⁵⁸ A variety of techniques including MALDI-IMS, NMR, and LC-MS can be used to study endophyte produced metabolites.

Nicotianamine

Nicotianamine (NA) is found in all higher plants where it functions as a metal chelating compound in plant tissues, binding metal ions so they can be transferred throughout the plant.⁵⁹

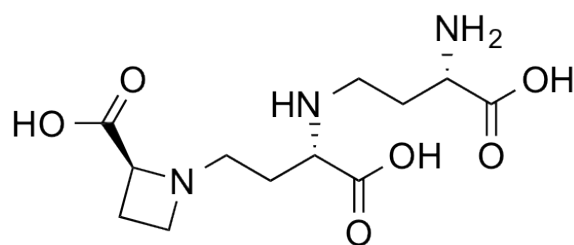


Figure 7 Nicotianamine structure

Other possible roles include protecting plants from oxidative stress.⁶⁰ Recent studies have shown that NA possesses antihypertensive effects, which are related to its ability to inhibit the angiotensin I-converting enzyme (ACE) in the renin-angiotensin system.⁶¹ Pharmacological ACE

inhibitors are widely used for the control of high blood pressure, as well as in the treatment of diabetic neuropathy and hypertensive related congestive heart failure. The ACE enzyme must bind zinc in each active site for catalytic activity, leading to speculation that NA inhibited ACE activity via zinc chelation. However, recent studies have shown that NA shows preferential inhibition towards ACE. In one study, NA had a similar inhibition rate as the known metal chelator EDTA for the zinc-containing enzyme carboxypeptidase A.⁶¹ However, NA had a 15 times higher inhibition rate for ACE than EDTA.⁶¹ NA has also shown great

Table 1 Reported Enriched Sources of Nicotianamine

Species	Reported Yield of NA ($\mu\text{mol/g fr. Wt}$)
<i>Datura metel</i>	0.12
<i>Lycium chinense</i>	0.69
<i>Solanum melongena</i>	0.05
<i>Lycopersicon esculentum</i> (tomato)	0.05
<i>Nicotiana tabacum</i> B. Y. (tobacco)	0.05
<i>N. glutinosa</i> (tobacco)	0.07
<i>N. rustica</i> (tobacco)	0.19
<i>N. arentsii</i> (tobacco)	0.12
<i>N. alata</i> (tobacco)	0.03
<i>N. debneyi</i> (tobacco)	0.13
<i>Zea mays</i>	0.02
<i>Rohdea japonica</i>	trace
<i>Fagus silvatica</i> (beechnuts)	Not reported
Soybeans	0.3 % aqueous extract of soybeans

promise as a replacement for EDTA as a food additive to prevent spoilage.⁶² Certain plant species have greater levels of nicotianamine in their tissue (**Table 1**).^{63,64}

Metal ions can act as catalysts for oxidative reactions that can cause spoilage in food products. EDTA is a synthetic chelator that is presently added to many food products to

sequester metal ions and prevent oxidative reactions. Utilizing NA as a natural metal chelator could allow companies to label food products as “all-natural” or organic and the market for these food products is continuing to increase.⁶⁵

Although all higher plants contain NA, two groups of plants, graminaceous and non-graminaceous, can be differentiated based on NA use. Graminaceous plants use it as a precursor in the biosynthetic production of the mugineic acid family of phytosiderophores, while non-graminaceous plants do not utilize this pathway. Graminaceous plants that thrive in iron deficient conditions show a higher degree of plasticity in regards to the NA synthase gene.⁶⁶ Another important distinction between plants with regards to NA production relates to plants involved in metal hyperaccumulation. *Thlaspi caerulescens* can thrive in soil with concentrations of nickel that would be toxic to other plants, and more NA is produced and resistance to high nickel soil concentrations is conferred when the NA synthase gene from *T. caerulescens* is spliced into *Arabidopsis thaliana*.⁶⁷ All of these considerations can be taken into account when deciding on source material for NA extraction. Iron deficient conditions would only need to be utilized if the plant species is both graminaceous and adaptive to iron deficient conditions. Soybeans and soy flour are readily available products which could be used to generate high yields of nicotianamine to replace EDTA in food products.

The Hepatitis C Virus

The hepatitis C virus (HCV) is responsible for chronic hepatitis C which can lead to cirrhosis of the liver and liver cancer and affects between 130-170 million people in the world today.⁶⁸ More than 350,000 people die from chronic hepatitis C annually and an estimated 3-4 million people are infected with HCV each year.⁶⁸ About 25% of people in the United States who are infected with the human immunodeficiency virus (HIV) are also infected with HCV.⁶⁸

Co-infection with HIV increases the risk of developing liver disease more than three fold.⁶⁹ There have been numerous studies showing that while HCV is primarily hepatotropic, it can also replicate in immune cells.⁷⁰

Serological tests were devised in the 1970s to detect both hepatitis A and B, leading to the discovery that an unknown, unidentified virus was responsible for many cases of viral hepatitis.⁷¹ In 1989, an immunoscreening approach which utilized a cDNA library created from clones of nucleic acids from HCV infected chimpanzees led to the identification of the hepatitis C virus.⁷² In 1991, the first detailed study of the genome reported a 9379-long nucleotide sequence with a large open reading frame (ORF) that was predicted to encode a large polyprotein containing 3011 amino acids.⁷² HCV was classified as a member of a new genus in the Flavivirus family; this family contains two other genera that encode a large polyprotein subsequently cleaved at multiple sites.⁷³ There has been a persistent problem in culturing HCV *in vitro*, prompting researchers to rely heavily on cDNA technology to study HCV. In 1993, a heterologous system using vaccinia viruses was used to elucidate the polyprotein cleavage products.⁷³ In 1997, it was formally proved that HCV is the sole causative agent of hepatitis C by infecting chimpanzees with HCV cDNA.⁷⁴

A constant barrier to HCV drug development has been the absence of successful culturing methods for detailed studies of the life cycle. There have been multiple techniques developed and refined over recent years to overcome this obstacle. One technique involves pseudotyping viral particles (HCVpp) with the E1 and E2 envelope glycoproteins to study host cell entry. Early reports using this technique utilized modified proteins which were poorly infective, however HCVpp were later reported which harbored unmodified glycoproteins and were highly infective.⁷⁵ The complete culturing of HCV (HCVcc) by transfecting hepatoma-

derived cell lines has also recently been achieved and refined, allowing for detailed studies of the HCV life cycle.⁷⁶ These new techniques have allowed for a number of directly acting antiviral (DAA) agents to be developed which target specific proteins in the life cycle. Natural products screening programs can use these targets to screen for novel inhibitors of HCV.

CHAPTER TWO:
SECONDARY METABOLITE PRODUCTION FROM A *BACILLUS AMYLOLIQUEFACIENS*
ENDOPHYTE OF *PLATANUS OCCIDENTALIS*

Endophytes are microbes that inhabit plant tissue without causing disease. One of the functions of endophytes as part of a symbiotic mutualism with plants involves participating in defense mechanisms whereby the microbe produces antibiotics, antifungals, and growth promoting/inhibiting agents. Here, we show that a *Bacillus amyloliquefaciens* endophyte produces rapamycin for its plant host *Platanus occidentalis* and this molecule is then possibly biotransformed to yield a putative rapamycin analog. MALDI-IMS of the endophyte colonies and extraction and purification of liquid endophyte cultures showed rapamycin production by *B. amyloliquefaciens*. Extraction of host tissue produced the putative rapamycin analogue. Iturin A₃ production was indicated by LC-MS from healthy stem tissue of the host plant and from liquid fermentation of the endophyte. Thus, the endophyte and *Platanus occidentalis* host are involved in a mutualism in which the endophyte produces rapamycin which is possibly modified by the host plant and also produces iturin A₃ which could be isolated from the host plant. This is the first report of rapamycin production from a new source since its original discovery from an Easter Island soil *Streptomyces hygroscopicus* in 1975 and reveals a significant ecological role for this highly important natural product.⁴⁰⁻⁴¹ The data presented here illustrates a significant potential for discovery via silent gene expression. This is also the first report of a mutualistic relationship between *B. amyloliquefaciens* and *P. occidentalis*, a potential biomass crop for the southeastern United States.

Endophytes are microbial species which live inside of plant tissue without causing disease and all plant life is thought to harbor some species of endophytes. Endophytes have the ability to contribute to plant health in a multitude of ways.⁷⁷⁻⁷⁸ One function of endophytes is the participation in a mutualism whereby endophytic microbes produce antimicrobial and antiviral secondary metabolites that benefit the host plant as defense mechanisms while consuming plant produced carbohydrates.⁷⁹ Novel and known compounds originally isolated from plant sources, with antimicrobial, immunosuppressant, and anticancer activity have been isolated from endophytes.⁸⁰ Here, we show that a *B. amyloliquefaciens* from a common plant species produces rapamycin. The genome sequenced using Illumina software and assembled using Geneious software by mapping assembly using *B. subtilis* reference sequence NC_000964.3.⁸¹⁻⁸² This has been a reference genome for more than 10 years and current annotations suggest *B. subtilis* is an epiphyte.⁸¹ Interestingly, low sensitivity and fast speed settings on Geneious genome assembly software gave much different results and showed the *Bacillus* endophyte to be much more closely related to *B. subtilis* then when settings were changed to higher sensitivity settings (**Table 2**). The endophyte was fermented under a number of different conditions and only one certain group of culture ingredients supported the detection of rapamycin production. This was CS20 medium, a medium originally developed for the culturing of fastidious organisms.⁸³ MD5FL which had been used for rapamycin production by *S. hygrosopicus* did not support production,⁸⁴ nor did the traditional *Bacillus* Landy's medium, or CHARD2, a medium that was developed to mimic the conditions of xylem plant tissue.⁸⁵ Iturin A₃ could be shown from both endophyte cultures and *P. occidentalis* extracted stem tissue. However, rapamycin could not be detected in plant host tissue. This led to our hypothesis that rapamycin was possibly being biotransformed to a currently unknown molecule by the plant host.

Table 2 *Bacillus* genome assembly

Bacterial species	Sequence length	High quality%	Identical sites	Ambiguities	Sensitivity/speed
<i>Bacillus subtilis</i>	4,215,606	-	-	-	-
<i>Bacillus</i> endophyte	4,214,756	66.5%	25.2%	1,411,866	low/high
<i>Bacillus</i> endophyte	3,315,554	98.9%	15.3%	51,780	high/low

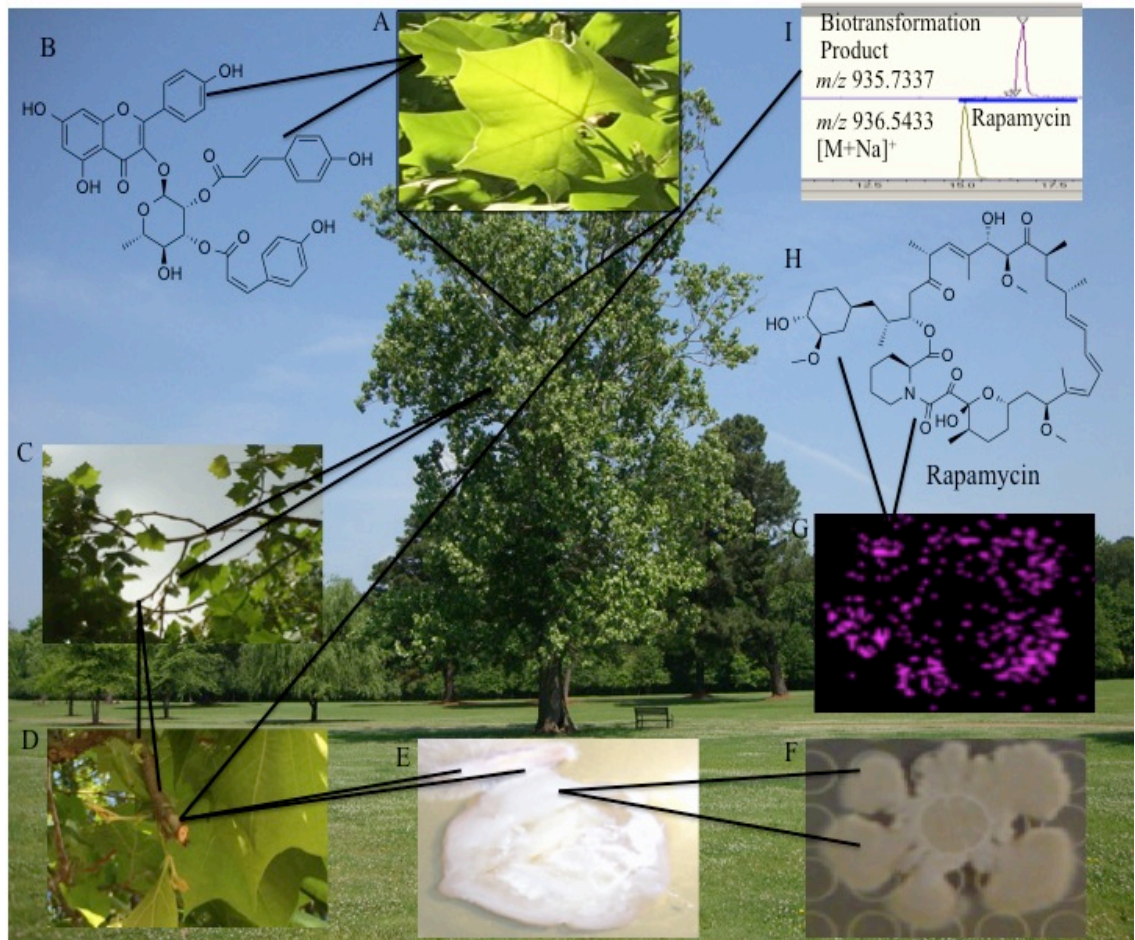


Figure 8 Production of rapamycin and possible biotransformation to a putative rapamycin analogue (A) *P. occidentalis* leaf tissue. (B) MRSA-active glycosides from leaf tissue.² (C) *P. occidentalis* stem tissue. (D) Wounded stem tissue. (E) *B. amyloliquefaciens* emerging from stem tissue. (F) Isolated *B. amyloliquefaciens* after excision from solid agar and transfer onto MALDI plate. (G) MALDI-IMS of protonated rapamycin signal from *B. amyloliquefaciens* colony. (H) Rapamycin structure. (I) LC-MS of product of putative biotransformation product and rapamycin standard.

Stem tissue material was collected from *P. occidentalis* species and, after surface

sterilization, the outer bark was removed to expose the vascular cambium layer and xylem tissue to solid malt-based agar (**Figure 8 C-E**). Within 48 hours, bacterial and fungal growth could be detected emanating from host tissue (**Figure 8 E**). The colony morphology of bacterial growth showed characteristics of *Bacillus* sp. including an undulate margin and irregular shape (**Figure 8 F**).

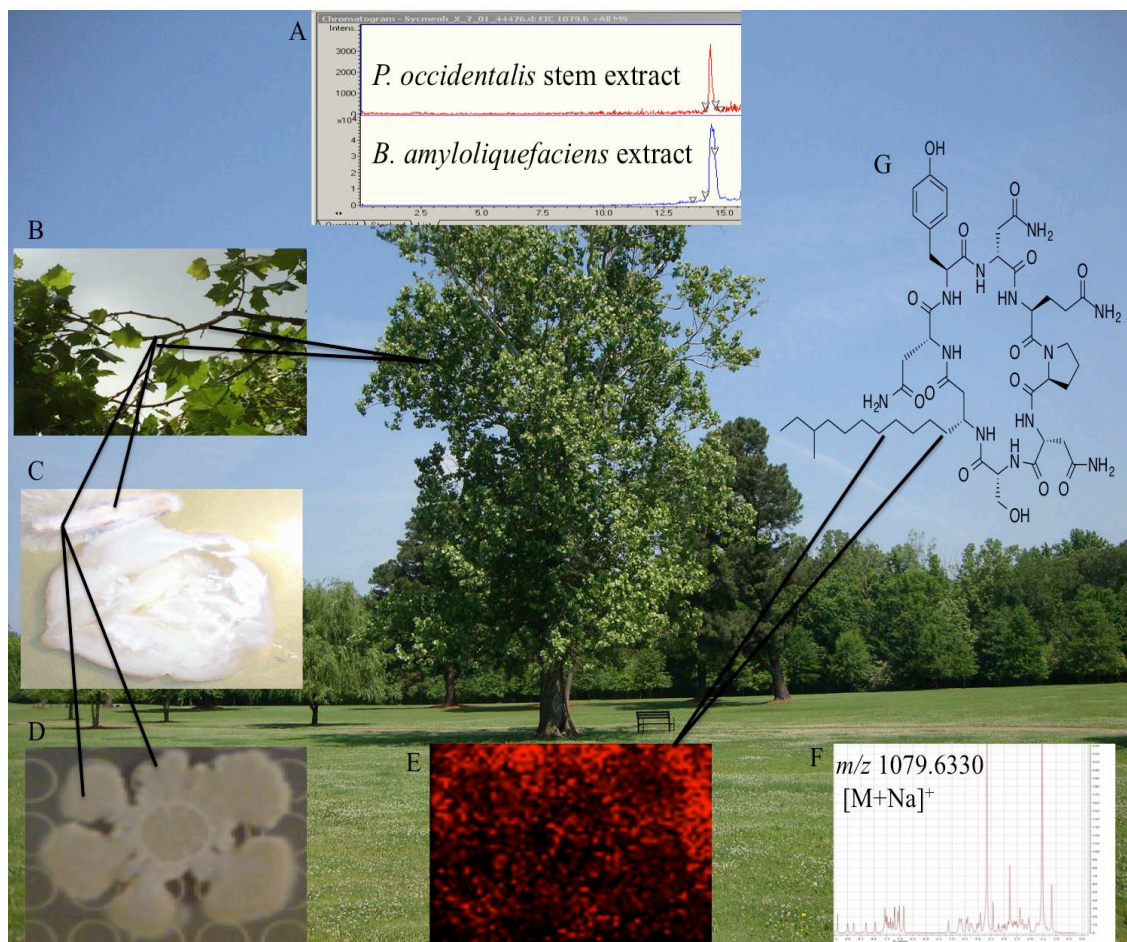


Figure 9 Isolation of iturin A₃ from *B. amyloliquefaciens* and *P. occidentalis* host. (A) EIC from LC-MS monitoring the mass for the sodium adduct for iturin A₃ at m/z 1079.6 [M+Na]⁺ from the crude ethanol extract from a *B. amyloliquefaciens* culture and methanol extract from *P. occidentalis* stem material. (B) Stems of *P. occidentalis*. (C) *B. amyloliquefaciens* emerging from stem tissue. (D) Isolated *B. amyloliquefaciens* after excision from solid agar and transfer onto MALDI plate. (E) MALDI-IMS of sodium adduct of iturin A₃ [M+Na]⁺. (F) HRMS and NMR of iturin A₃. (G) Structure of iturin A₃.

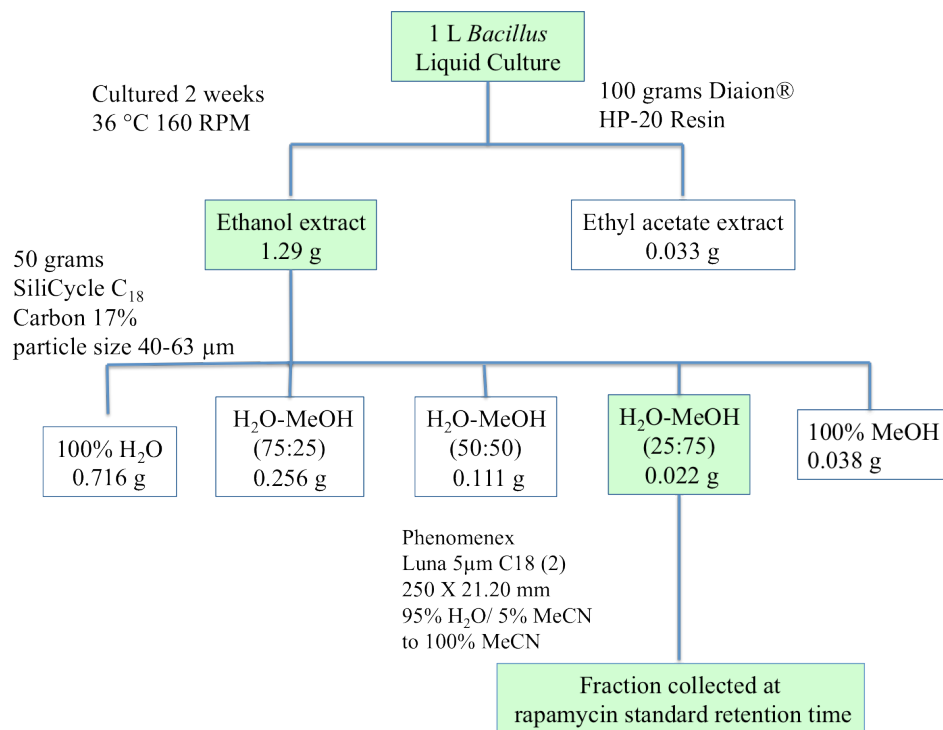


Figure 10 Isolation of rapamycin from *B. amyloliquefaciens*

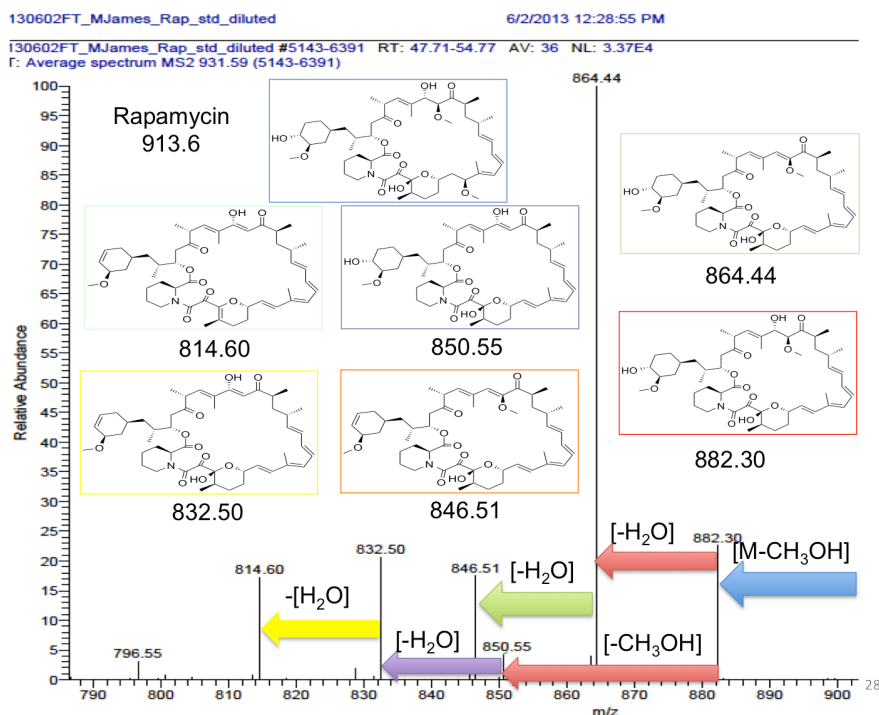


Figure 11 FTMS of rapamycin standard. Ions are rationalized by successive losses of water and methanol in certain combinations. Structures are coordinated with arrows by color.

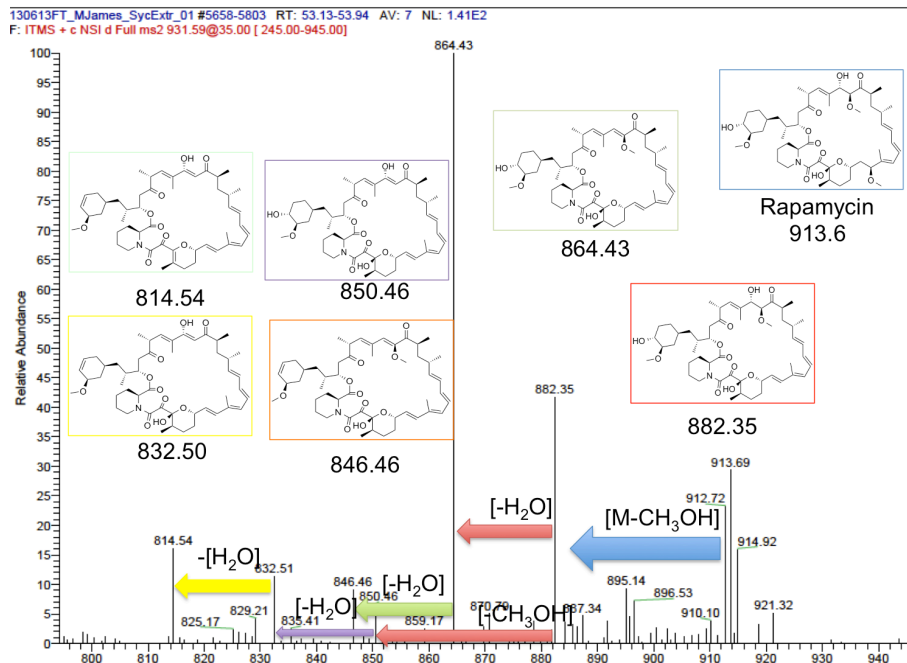


Figure 12 FTMS of purified fraction from *B. amyloliquefaciens*. Ions are rationalized by successive losses of water and methanol. Structures are coordinated with arrows by color. Ions that match rapamycin standard FTMS are highlighted.

MADLI-IMS of bacteria over seven days showed production of rapamycin with the protonated signal being detected after day two (**Figure 8 G**). Interestingly, rapamycin production clearly stayed in the boundaries of the colony which strongly contrasted with the production of iturin which was excreted from the colony (Figures 8 G & 9 E). Processed *P. occidentalis* xylem material showed a putative rapamycin analogue at m/z 935.7337 (**Figure 8 I**).

Iturin A₃ was shown from both endophytic *B. amyloliquefaciens* liquid cultures and directly from host *P. occidentalis* stem tissue (**Figure 9**). The signal for the sodium adduct of iturin A₃ was detected by LC-MS in an ethanol extract from a *B. amyloliquefaciens* culture as well as a methanol extract from processed stem material from *P. occidentalis* (**Figure 9 A**). *Bacillus* cultures were isolated directly from stem tissue and MALDI-IMS revealed the signal for the known *Bacillus* metabolite as iturin A₃ (**Figure 9 C-E**). Purification allowed for recording

NMR and HRMS data, which confirmed iturin A₃ from endophyte cultures (**Figure 9 F**).

Isolation of rapamycin from *B. amyloliquefaciens* followed the scheme shown in **Figure 10**. FTMS of liquid cultures of the *B. amyloliquefaciens* endophyte when compared to FTMS of a rapamycin standard verified that the detected signal by MALDI-IMS and LC-MS was rapamycin (**Figures 11 & 12**).

For example, it has been shown that with secondary metabolite production from filamentous fungi, it is important to have a media that is rich in amino acids, vitamins, and trace metals.⁸⁶ The carbon source can also play an important role in the secondary metabolite production of both bacteria and fungi.⁸⁷ In our studies, a media that had originally been developed for the culture of *Xylella fastidiosa* was used (**Table 3**).⁸³

Table 3 CS20 Media⁸³

Distilled H ₂ O	1 L	
Soy peptone	2.0 g	
Bacto tryptone	2.0 g	
(NH ₄) ₂ HPO ₄	0.85 g	
Hemin Cl (0.1%)	15.0 mL	
KH ₂ PO ₄		1.0 g
MgSO ₄ · 7H ₂ O	0.4 g	
L-glutamine	6.0 g	
Dextrose	1.0 g	
Starch, potato soluble	2.0 g	
L-histidine	1.0 g	
Phenol red (0.2%)	5.0 mL	
pH	6.6-6.7	

As stated previously, the colony morphology of the sample was undulate with an irregular margin which conforms with the general description of the *Bacillus* genus (**Figure 13**).¹⁰

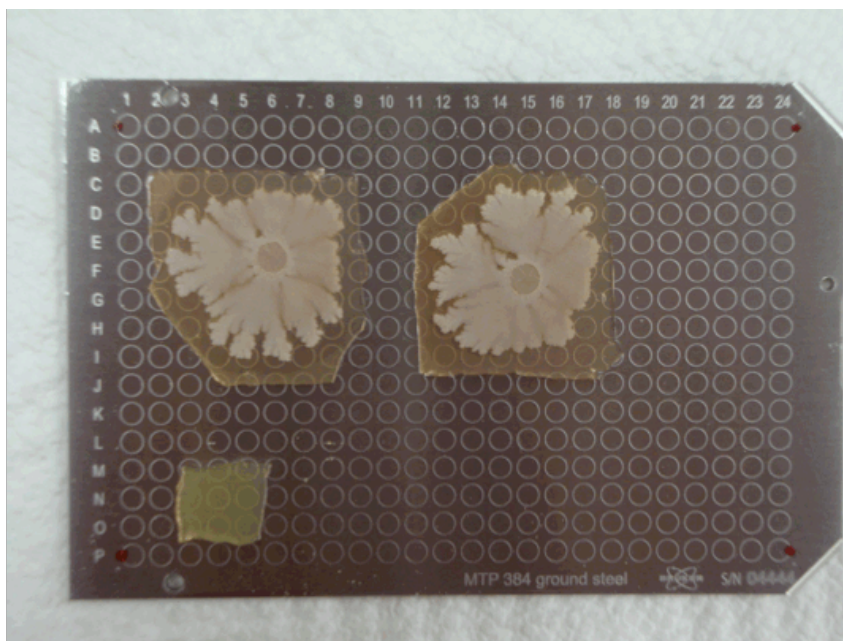


Figure 13 *B. amyloliquefaciens* morphology. The colony morphology is undulate with an irregular margin. Image taken after colonies had been transferred to MALDI plate from solid agar.

B. amyloliquefaciens colonies were grown in CS20 media⁸³ and, in order to test for bioactivity, extracts were assayed for activity against pathogenic bacteria and fungi, malaria, and leishmaniasis using the NCNPR in-house screening protocol. Although the first round of bioassay results were not encouraging, the project was continued due to the mistaken belief that we were dealing with a plant pathogen which would make the study of any secondary metabolite production, regardless of activity, important.

It was decided to continue this project, but start doing chromatography with extracts to get to higher levels of purity in hopes that more purified extracts would yield better activity. VLC with a number of different chromatography column materials including normal phase using silica gel (Silicycle Siliaflash® F60, particle size 40-63µm), size exclusion using Sephadex® LH-20, and reverse phase using C₁₈ (SiliCycle C₁₈, Carbon 17%, particle size 40-63 µm) were used. The first significant bioactivity results was retrieved from after a 1 L culturing of the

Bacillus amyloliquefaciens followed by reverse chromatography using the fractionation scheme in **Figure 14**.

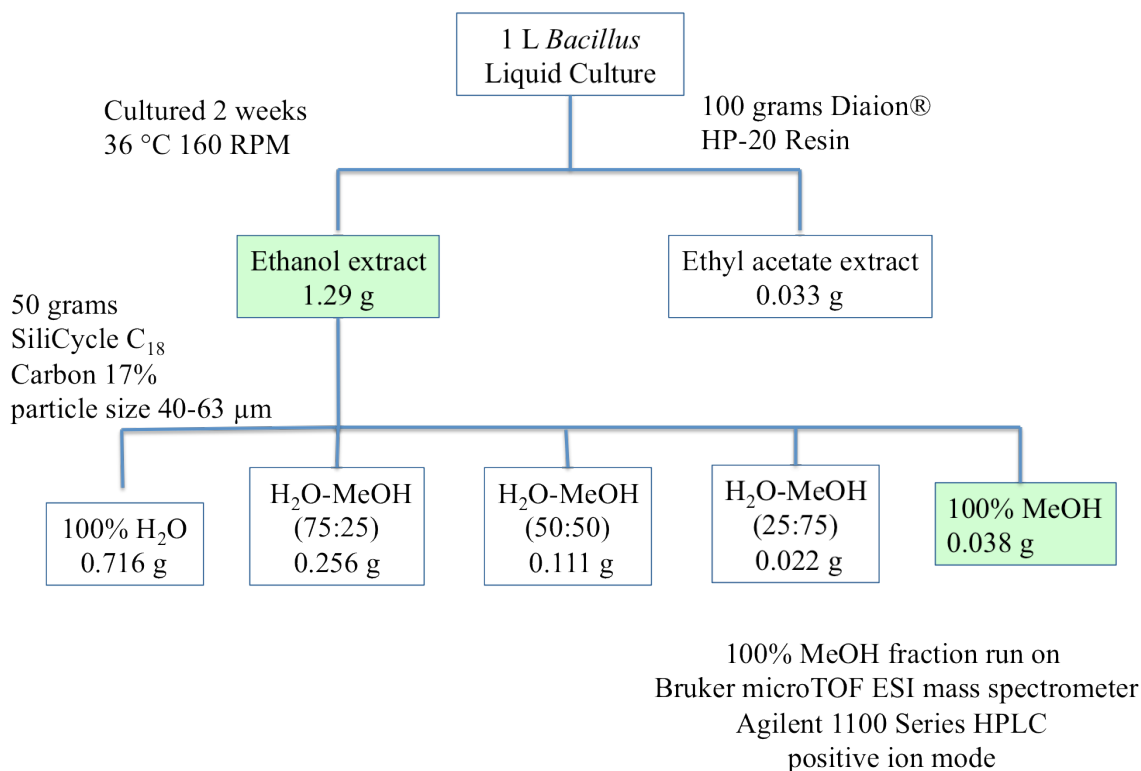


Figure 14 Culturing and purification of endophytic *Bacillus* secondary metabolites.

Table 4 MRSA and *Staph. aureus* activity

	IC ₅₀ <i>Staph aureus</i>	IC 50 MRSA
Fraction 1 (100% H ₂ O)	0	0
Fraction 2 (75% H ₂ O, 25% MeOH)	0	0
Fraction 3 (50% H ₂ O, 50% MeOH)	0	0
Fraction 4 (25% H ₂ O, 75% MeOH)	0	13.35
Fraction 5 (100% MeOH)	14.1	12.75

The IC₅₀ values for extracts 4 (25% MeOH, 75% H₂O), and 5 (100% MeOH) were significant (**Table 4**). Fraction 5 was analyzed by LC-MS. Strong signals were seen at *m/z* 1492.2 along with other signals clustered around this signal ranging from *m/z* 1461.1 to 1506.2 (**Figure 15**). These signals correlate with the known *Bacillus* metabolites the fengycins.

Fengycin lipopeptides are produced by non-ribosomal peptide synthetases (NRPSs) or through hybrid polyketide synthetases and non-ribosomal peptide synthetases (PKs/NRPSs) which can lead to multiple isoforms being produced naturally in *B. subtilis* as *B. amyloliquefaciens* extracts.⁸⁸ They possess antibacterial activity.²⁴

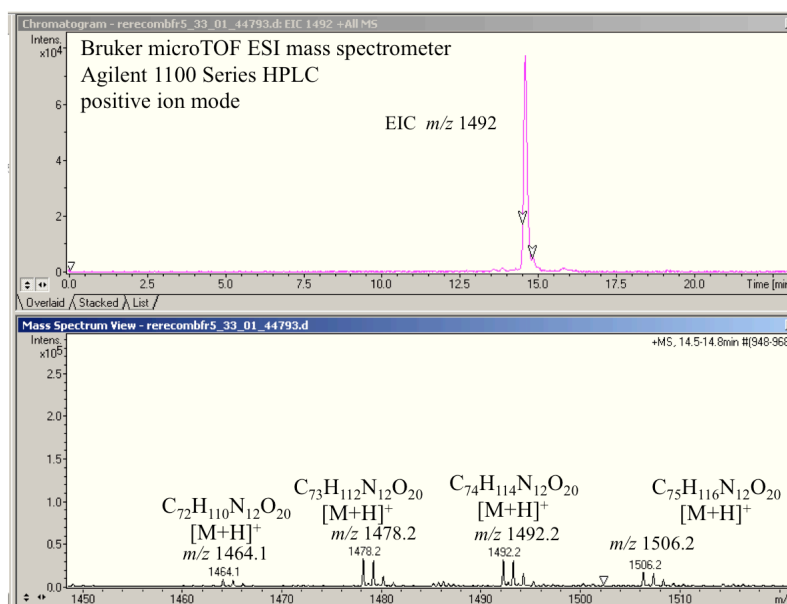


Figure 15 Fengycin ions. Formulas are noted and match a number of different fengycin isoforms.

All fengycins are decapeptides; different amino acids within the eight amino acid cyclized peptide moiety along with changes in length, branching, and saturation of the fatty acid tail are responsible for slight modifications in fengycin secondary metabolites. Members of the fengycin A family have the following amino acid sequence: Glu-Orn-Tyr-Thr-Glu-Ala-Pro-Gln-Tyr-Ile. Fengycin B isoforms have a valine substituted for alanine (**Figure 16**). Other isoforms exist and new ones continue to be discovered.⁸⁹ Rapid methods using FTMS have been developed to discern which fengycin metabolites are being observed as there can be significant overlap in $[M+H]^+$ ions from one family to another depending on amino acid substitutions and fatty acid chain composition.⁹⁰ All ions that were found have previously been reported from

fengycin-producing *Bacillus* spp.⁹¹ Another cluster of ions was seen in fraction five between m/z 1008.9 to m/z 1044.9 (**Figure 17**). These signals correlate with the known *Bacillus* secondary metabolites the surfactins.^{17,91} These are heptapeptides with some heterogeneity at different positions in the peptide moiety. All members are lactones and are linked to a fatty acid tail that can vary in length (**Figure 18**).

The final known lipopeptide family of molecules that are produced by *Bacillus* spp. are the iturins. The iturins contain seven cyclized amino acids moieties and a β -amino fatty acid. They are differentiated by variations of amino acids at different positions and also by variation in the branching or length of the β - amino fatty acid.²⁹ A cluster of signals correlating with the iturin molecules was seen by LC-MS (**Figure 19**). As with other previously discussed *Bacillus* lipopeptides, there can be significant overlap between different isoforms and homologues when trying to decipher exactly which molecule is being observed and MS/MS methods are often used for this purpose.

Fraction 5 was put through HPLC to further purify *Bacillus* metabolites (**Figure 20**). UV wavelengths of 215 nm and 254 nm were used to analyze the samples. Two sharp signals were seen at 215 nm (**Figure 21**). These correlated with two iturin homologues (**Figure 22**). HRMS and NMR showed these to be iturin A₂ and iturin A₃ (**Figure 23**). As noted previously, it is important to use MS/MS methods for full identification of iturin peptides. Therefore, only purified metabolites were assigned completely. Numerous publications dealing with lipopeptide production have assigned these metabolites using MS/MS.

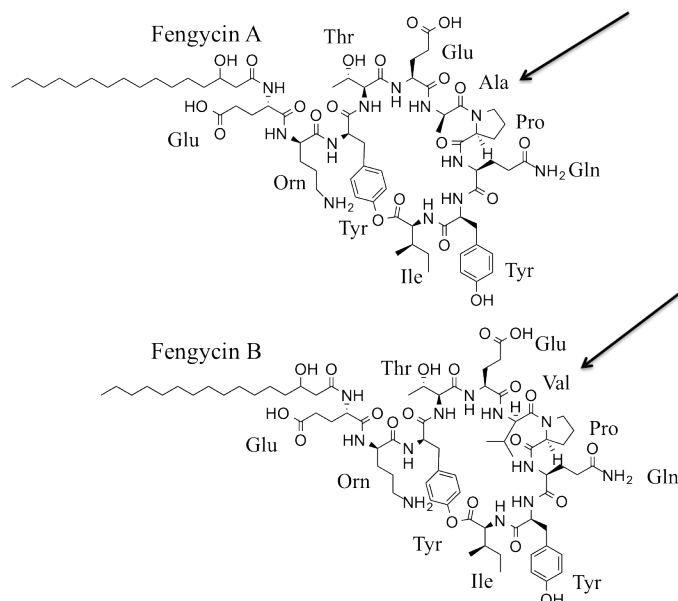


Figure 16 Fengycin isoforms (A) Fengycin A contains alanine in the indicated position. (B) Fengycin B contains valine in the indicated position. Many different members of both families are found based on differences in length and saturation in the fatty acid tail.

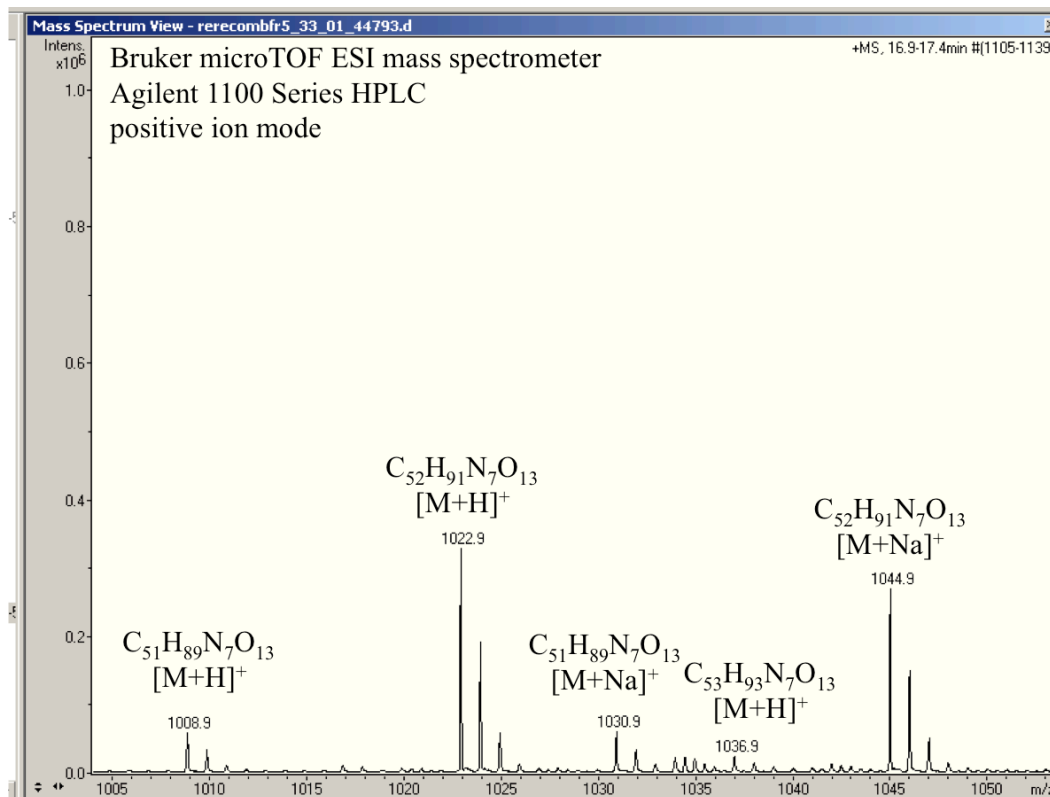


Figure 17 Surfactin ion signals. Formulas are noted and match many different surfactin isoforms.

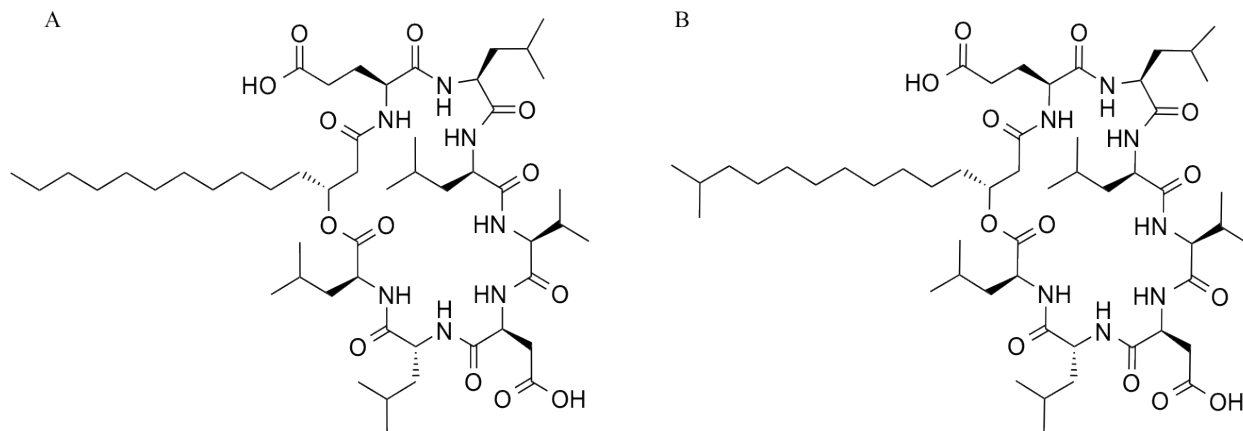


Figure 18 Surfactin homologues. (A) differs from structure (B) by a methylene unit.

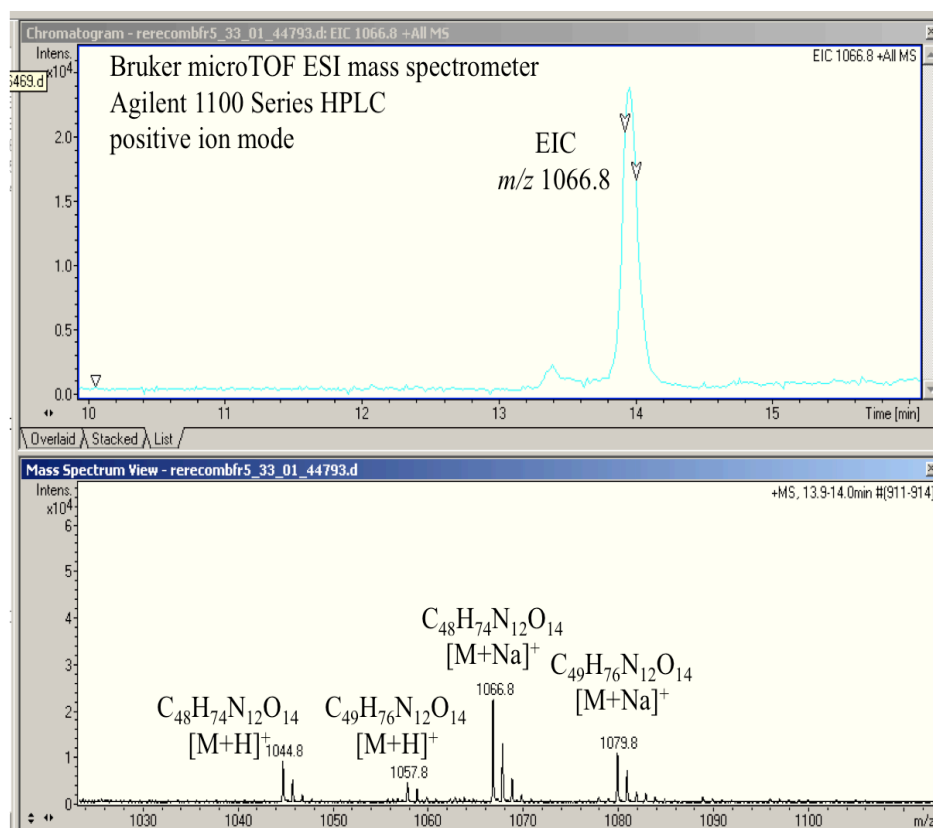


Figure 19 Iturin ions.

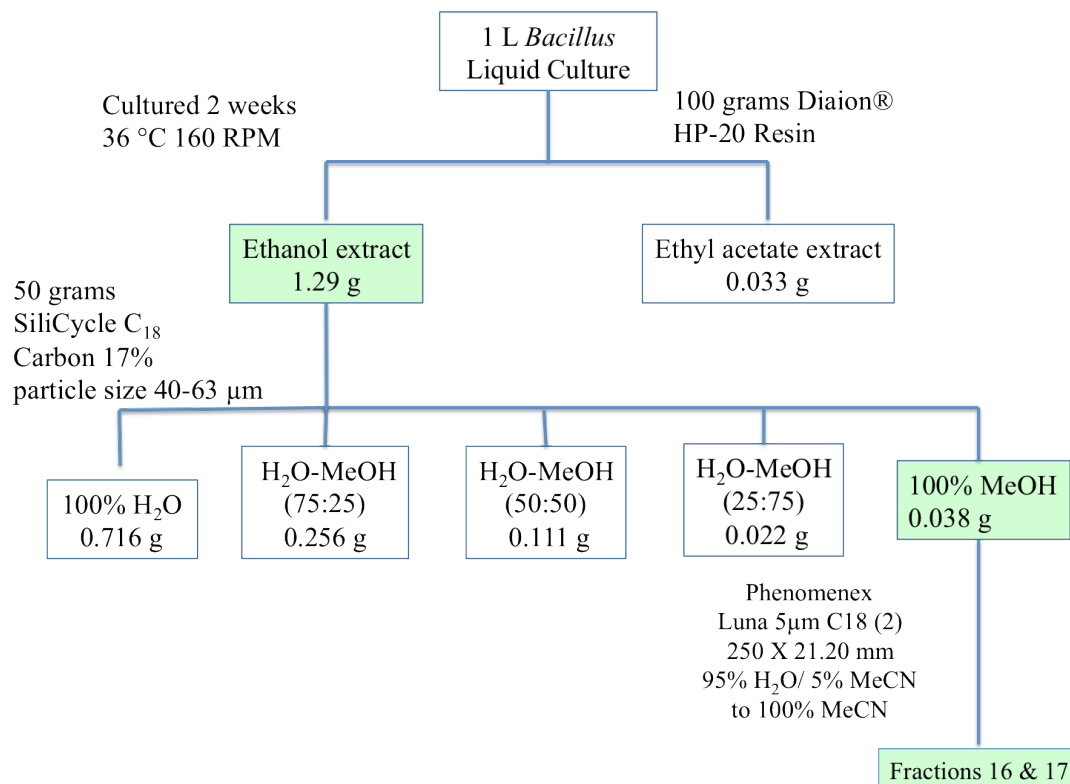


Figure 20 Iturin isolation scheme

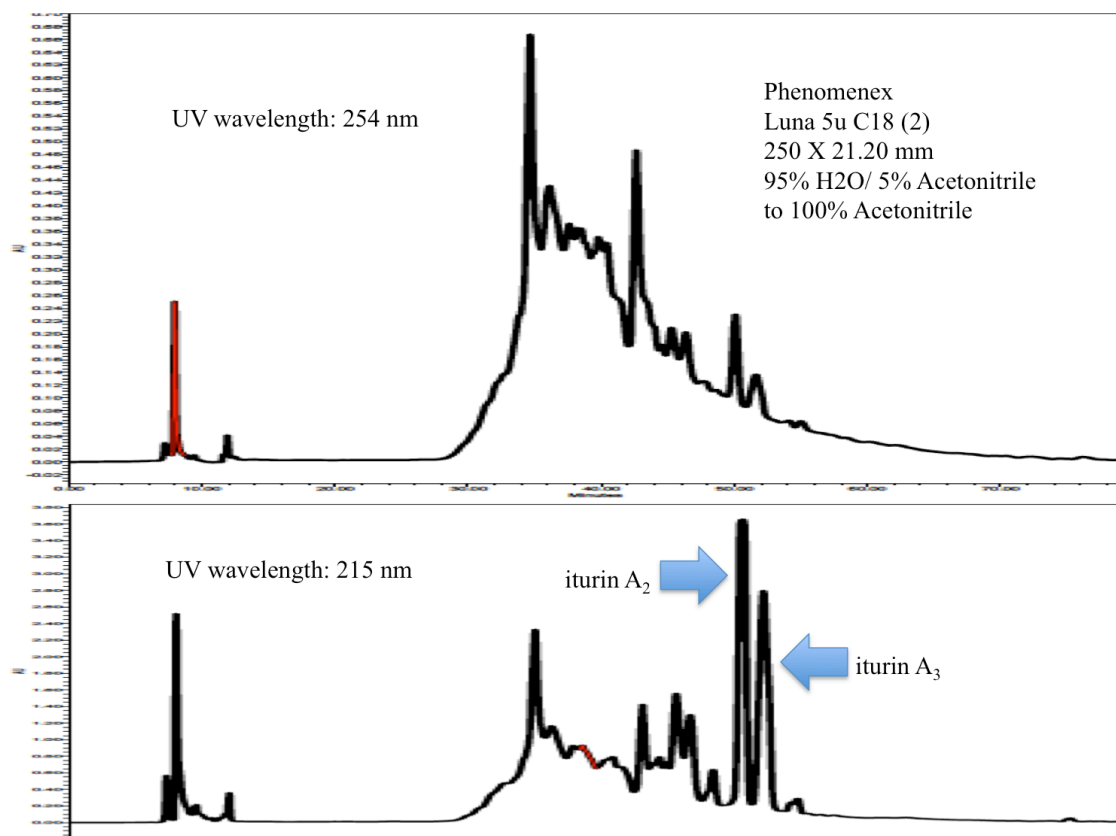


Figure 21 Purification of iturin homologues

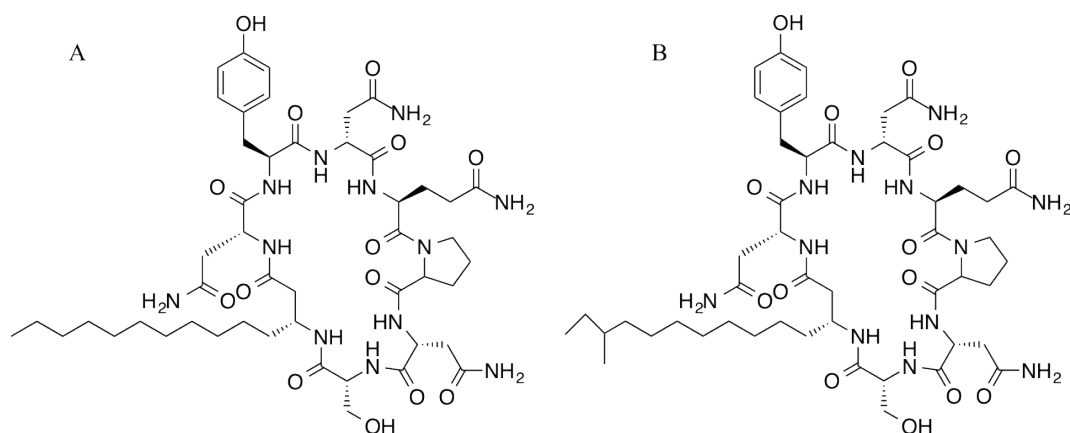


Figure 22 Iturin homologues. Structure (A) differs from structure (B) by a methylene unit. Structure (A) represents iturin A₂. Structure (B) represents iturin A₃.

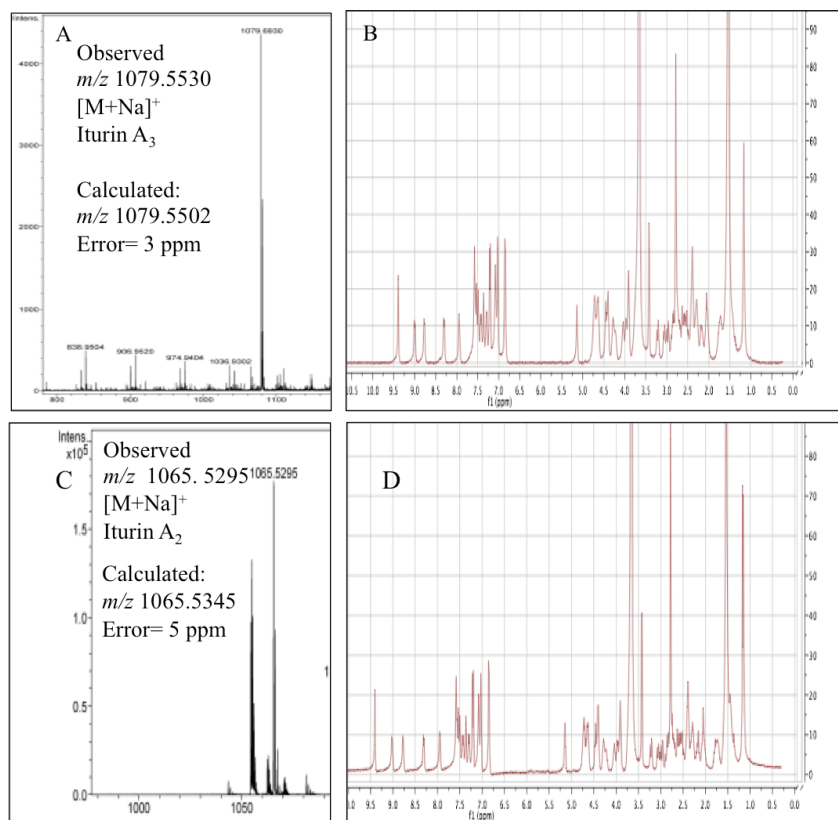


Figure 23 Purified iturin homologues. (A) HRMS for iturin A₃. (B) NMR for iturin A₃. (C) HRMS for iturin A₂. (D) NMR for iturin A₂.

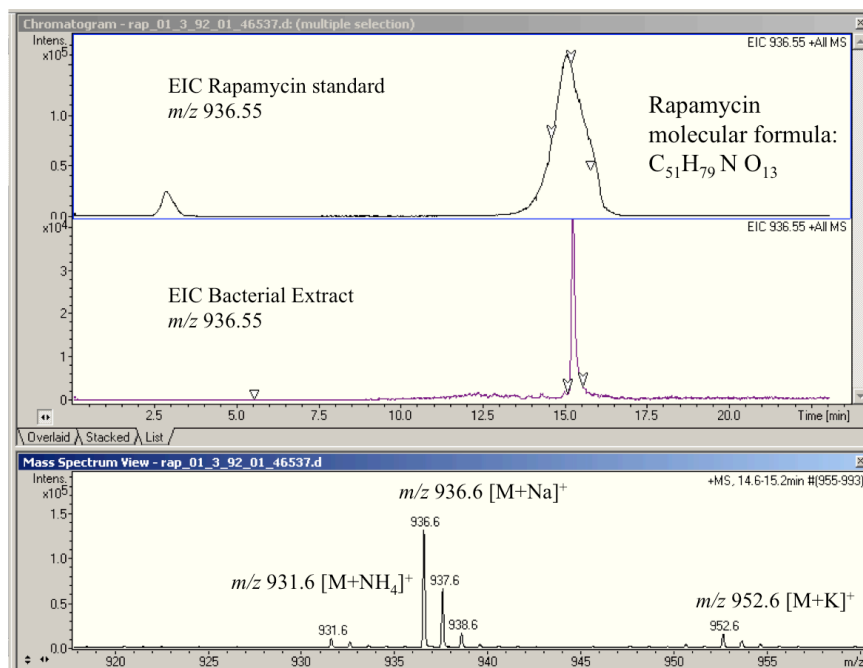


Figure 24 EIC of bacterial extract and rapamycin standard. Bottom panel shows three signals found in bacterial extract including m/z 931.6 $[M+NH_4]^+$, m/z 936.6 $[M+Na]^+$, and m/z 952.6 $[M+K]^+$ adducts.

A signal was observed in fraction 4 which correlated with the ammonium adduct of rapamycin at m/z 931.6. It was decided to use a rapamycin standard (LC Laboratories Cat. No. R-5000) to confirm that the signal was a rapamycin ammonium adduct by comparing the retention time of the standard to the ion found in the c18 fraction (**Figure 24**).

A series of MALDI-IMS experiments were performed on the *Bacillus sp.* to test for rapamycin production. In order to perform these experiments, the first step was to design the sample preparation steps so that consistent results could be obtained. This step was particularly important as sample preparation is the step that introduces the most variability and can lead to difficulty in reproducing results in MALDI-IMS.⁹² The first process that needed to be developed was to be able to excise colonies from solid agar plates and place them on a Bruker MTP 384 steel plate, being careful to not let any air bubbles form between the excised colony and the steel plate. After this technique had been developed, it was important to test different thicknesses of

agar for the colonies to grow on, as it has been proven that a thinner sample improves peak intensity as well as the signal to noise ratio.⁹³ However, the agar could not be too thin as the excised colony after matrix application had to be dehydrated prior to data acquisition and a sample that was too thin would not permit a vacuum to be applied for drying. After a period of trial and error, the following protocol was developed.

Seven CS20 agar plates were poured with days 1-5 poured with 10 mL of agar and plates for days 6 and 7 poured with 15 mL of agar. Five μL of *Bacillus* sp. containing glycerol stock was placed in the center of each of these plates and placed in an incubator at 36°C. One plate was removed every 24 hours and colonies were excised from the agar plate and placed on a Bruker MTP 384 steel plate. After a picture of the colony was taken for later overlay using imaging software, alpha-cyano-4-hydroxycinnamic acid matrix was shaken on top of the colony using a 20 μm sieve for even distribution of the matrix. The steel plate was then placed in an incubator at 36 °C for four hours. Afterwards, the plate was placed in a desiccator. The desiccator was then placed under vacuum for 5 minutes and then sealed and the plate was left inside for an additional 25 minutes. The plate was then removed and placed into a Bruker Autoflex II mass spectrometer equipped with the Compass 1.1 software suite (consisting of FlexImaging 3.0, FlexControl 2.4, and FlexAnalysis 2.4). The samples were analyzed in linear positive mode with 200 μm intervals. The spectra were collected in the m/z 700-1600 range at a 200 Hz laser frequency. After data acquisition, the data was analyzed using FlexImaging software.

The data acquired and analyzed after repeating this procedure for a time course experiment of seven days are shown in **Figure 25**. The top panel shows the bacterial colony after being placed on the steel plate before the matrix was applied (note that days 3 and 5 are

omitted as there was a problem with transferring a colony from agar to plate). The horizontal panel below this shows an ion at m/z 914.6 which correlates with the $[M+H]^+$ ion of rapamycin which has a monoisotopic mass of m/z 913.555. The third panel from the top shows the dehydration product for rapamycin at m/z 895.7. Finally, the lower panel shows the potassium adduct at m/z 952.3.

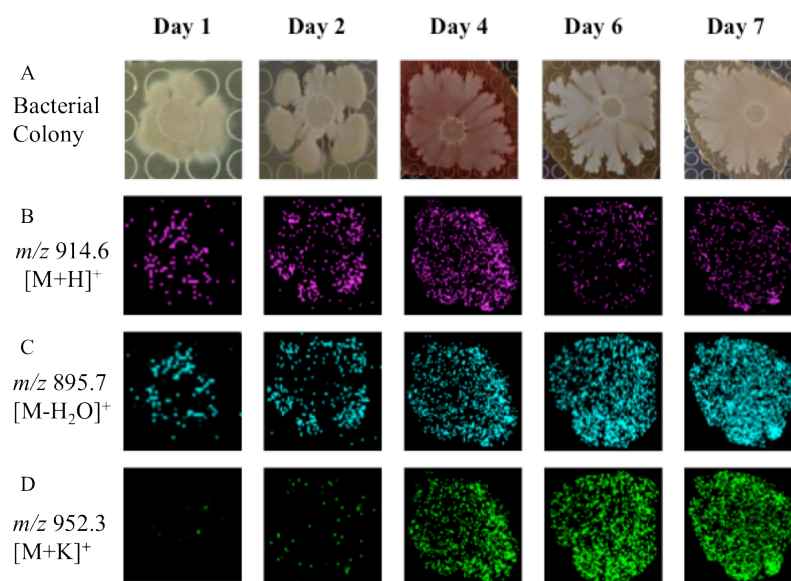


Figure 25 MADLI-IMS of *Bacillus* endophyte. Top panel shows bacterial colonies prior to matrix application. 2nd panel from top shows production of putative rapamycin signal at m/z 914.6 $[M+H]^+$. 3rd panel shows dehydration product at m/z 895.7 $[M-H_2O]^+$. 4th panel shows potassium adduct at m/z 952.3 $[M+K]^+$.

In order to confirm the mass signal was rapamycin, an attempt was made to culture enough bacterial material to generate an NMR spectrum that could be overlaid with a rapamycin standard NMR spectrum. **Figures 26** and **27** show the fermentation protocols that were followed with the highlighted fraction containing the putative rapamycin signal. In order to further test if retention times for rapamycin would match the putative rapamycin metabolite, standard rapamycin was injected on a Phenomenex Luna 5u C18(2) 250 x 21.20 RP column. A gradient was run that started 15 minutes after injection and ran over an hour from 95% H₂O/ 5% MeCN to

100% MeCN. The retention time was approximately 78 minutes. Note that UV data are not shown as rapamycin contains a weak chromophore consisting of a conjugated triene system with a peak intensity at 278 nm and the bacterial extract did not show UV absorption. Instead, the putative bacterial rapamycin molecule was isolated by using the retention time that had been shown from the standard rapamycin. Approximately 20 mgs of the fraction containing rapamycin signal were injected following the same parameters that had been used for the standard.

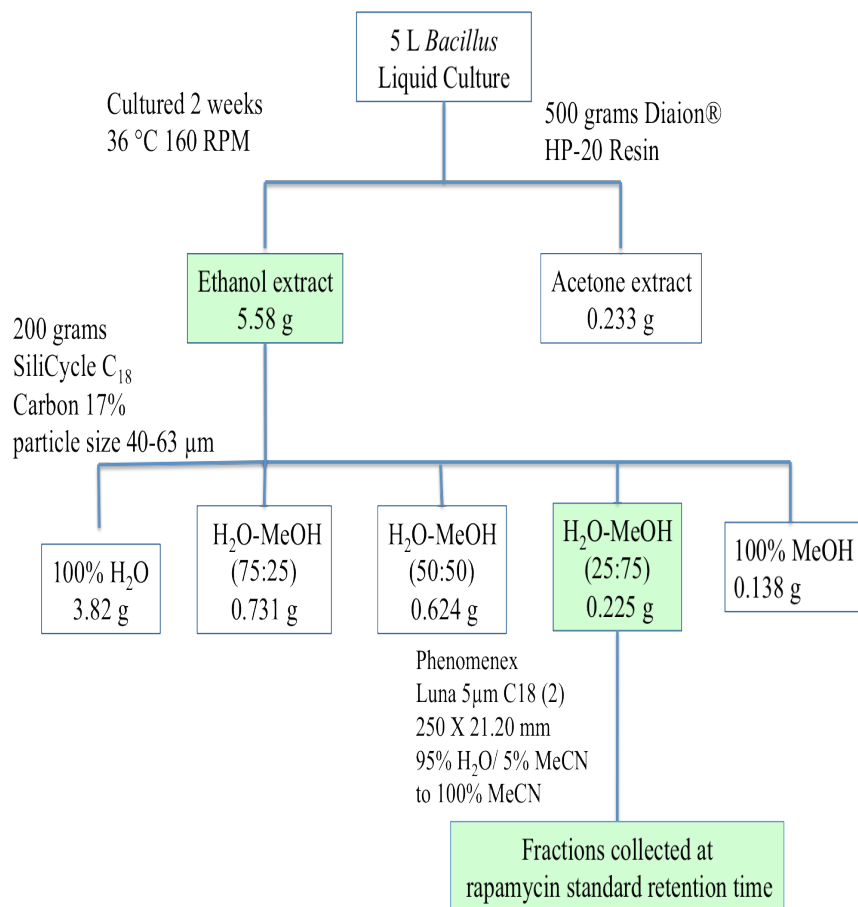


Figure 26 Isolation scheme for rapamycin

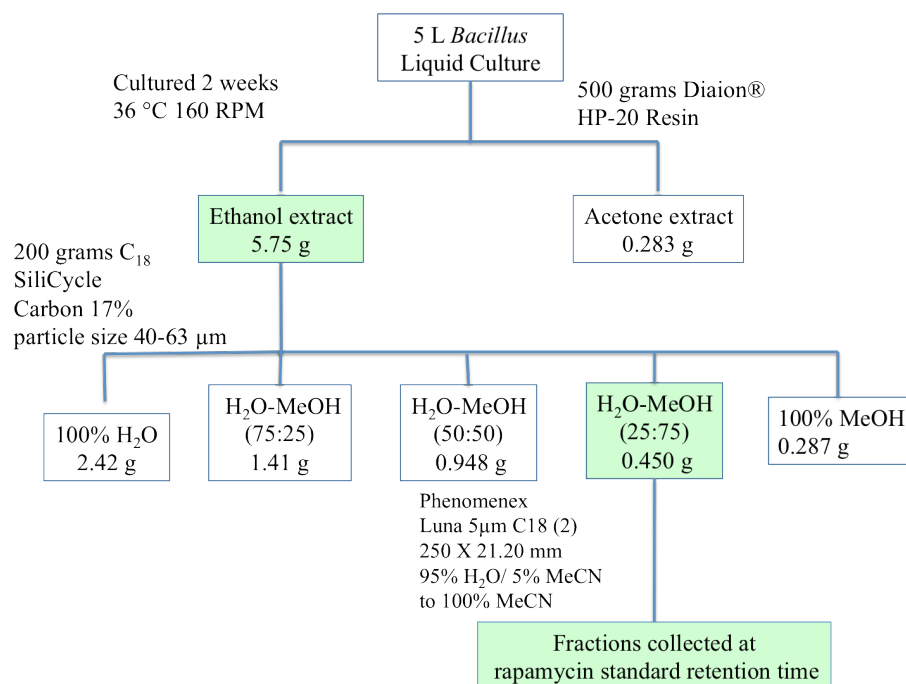


Figure 27 Isolation scheme for rapamycin

The fraction that was collected at 78 minutes could not be analyzed by NMR spectroscopy due to a low amount of material, however LC-MS confirmed that the putative rapamycin molecule from the *Bacillus* sample eluted at the same time as rapamycin. (**Figure 28**).

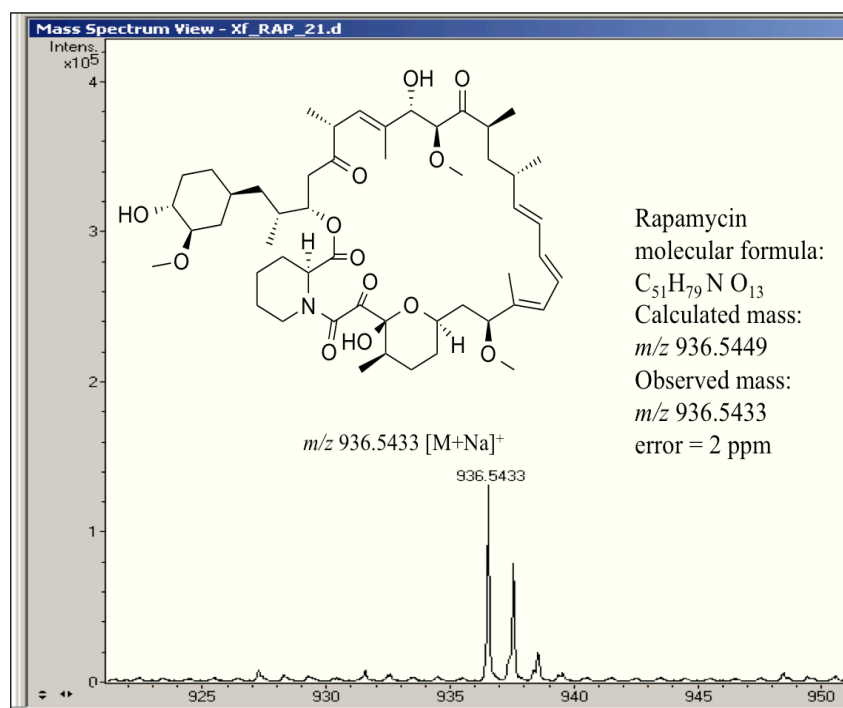


Figure 28 HRMS of rapamycin from *Bacillus* sp.

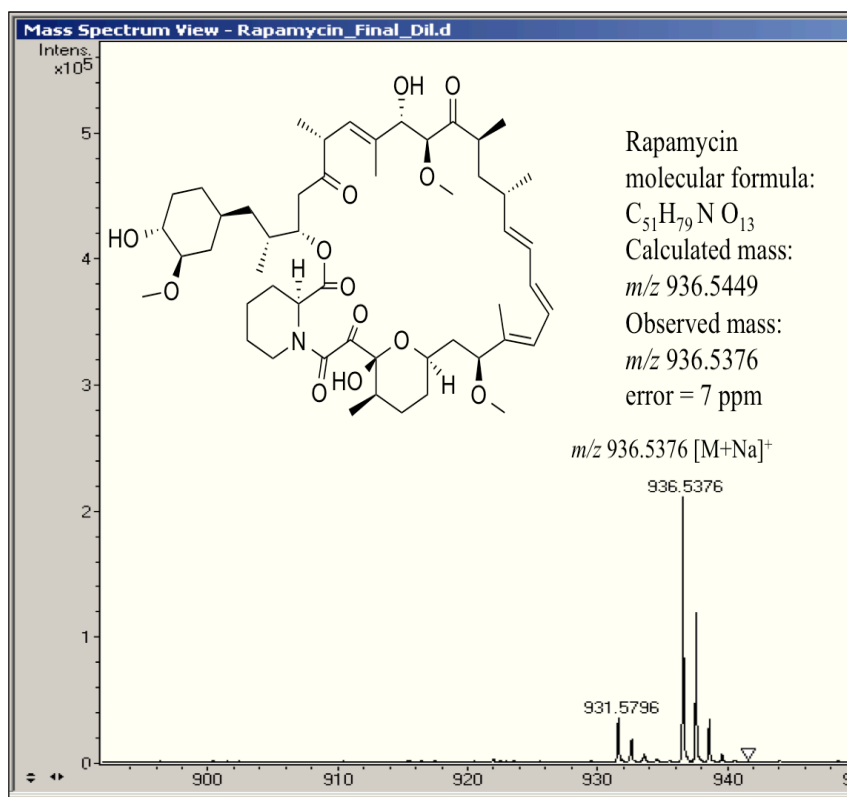


Figure 29 HRMS of rapamycin standard

Note that rapamycin standard has higher ppm value than *Bacillus* product. Both of these values were within the accepted range for error values with the rapamycin formula of $C_{51}H_{79}NO_{13}$. These values were calculated by subtracting the observed mass from the calculated mass, dividing this number by the calculated mass, and then multiplying by 10^6 . For the *Bacillus* product this equation $[(936.5449-936.5433)/936.5449] * 10^6$. For the rapamycin standard this was $[(936.5449-936.5376)/936.5449] * 10^6$.

These two molecules can be noted as identical based on these masses. However, it was important to gather NMR data to attempt to overlay the two spectra as a number of molecules can have identical monoisotopic masses. This data was gathered after multiple HPLC purifications were ran using the same procedures that have been previously outline for iturin purification.

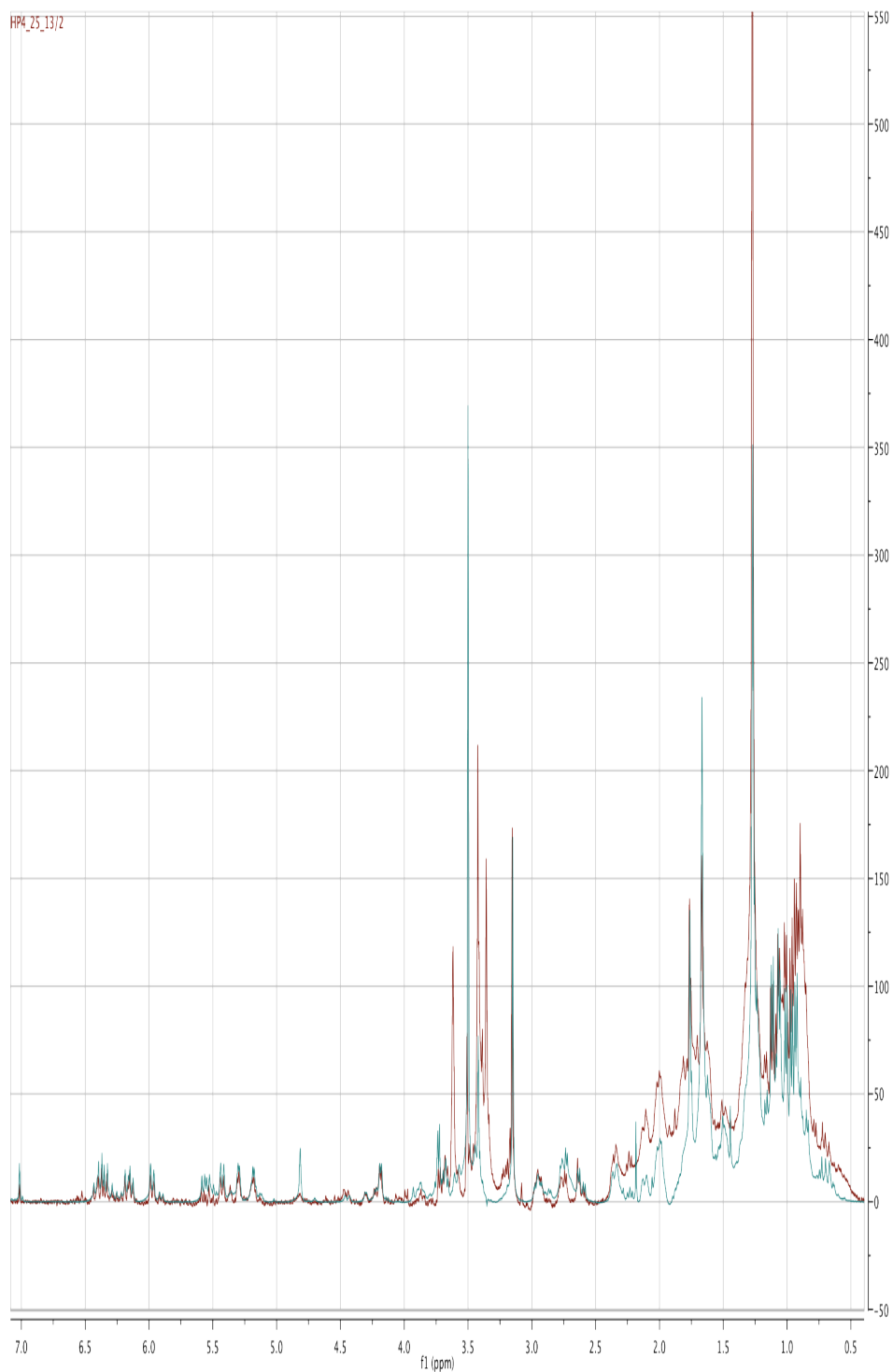


Figure 30 Rapamycin and *B. amyloliquefaciens* fraction $^1\text{H-NMR}$ overlay experiment. Green chemical shifts represent rapamycin standard (CDCl_3). Red chemical shifts represent purified metabolite from *B. amyloliquefaciens* (CDCl_3).

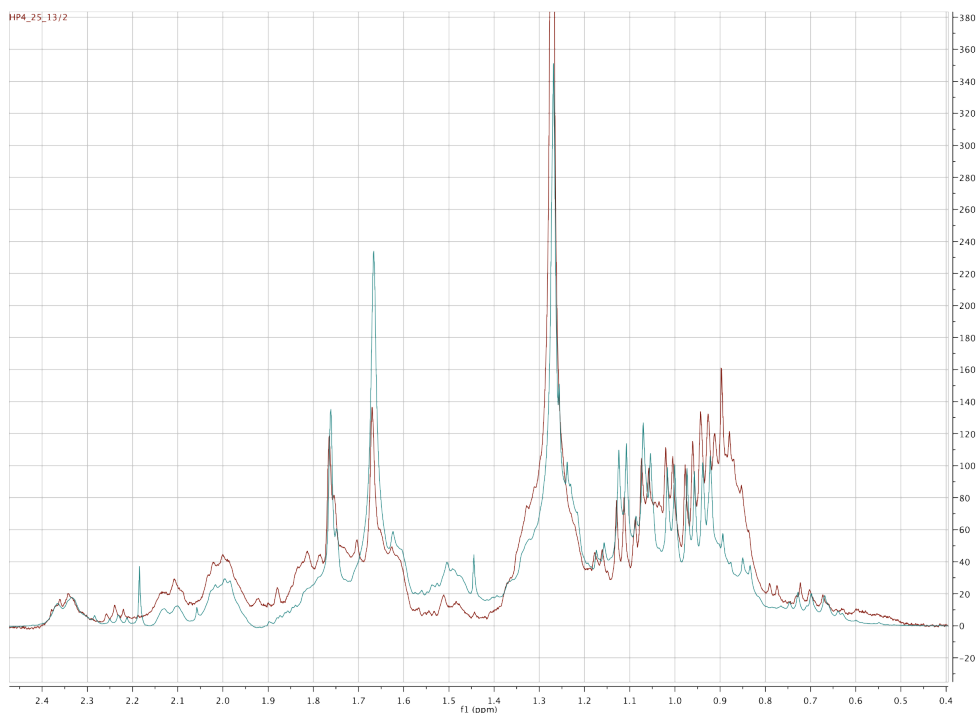


Figure 31 Rapamycin and *B. amyloliquefaciens* fraction $^1\text{H-NMR}$ overlay experiment. Green chemical shifts represent rapamycin standard (CDCl_3). Red chemical shifts represent purified metabolite from *B. amyloliquefaciens* (CDCl_3). Range is 2.4 ppm – 0.4 ppm.

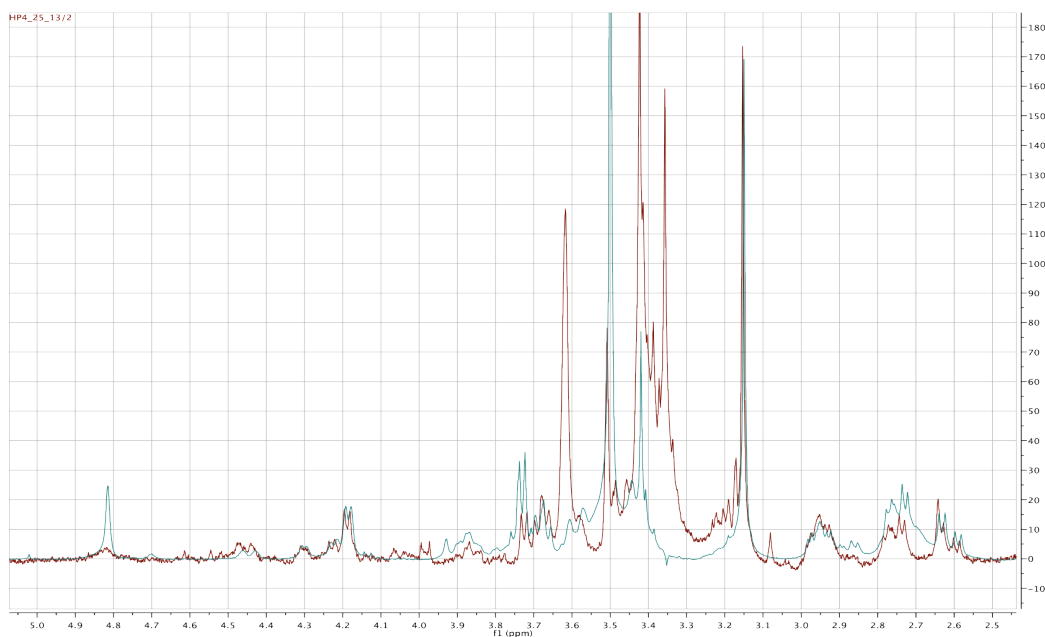


Figure 32 Rapamycin and *B. amyloliquefaciens* fraction $^1\text{H-NMR}$ overlay experiment. Green chemical shifts represent rapamycin standard (CDCl_3). Red chemical shifts represent purified metabolite from *B. amyloliquefaciens* (CDCl_3) Range is 5.0 ppm – 2.5 ppm.

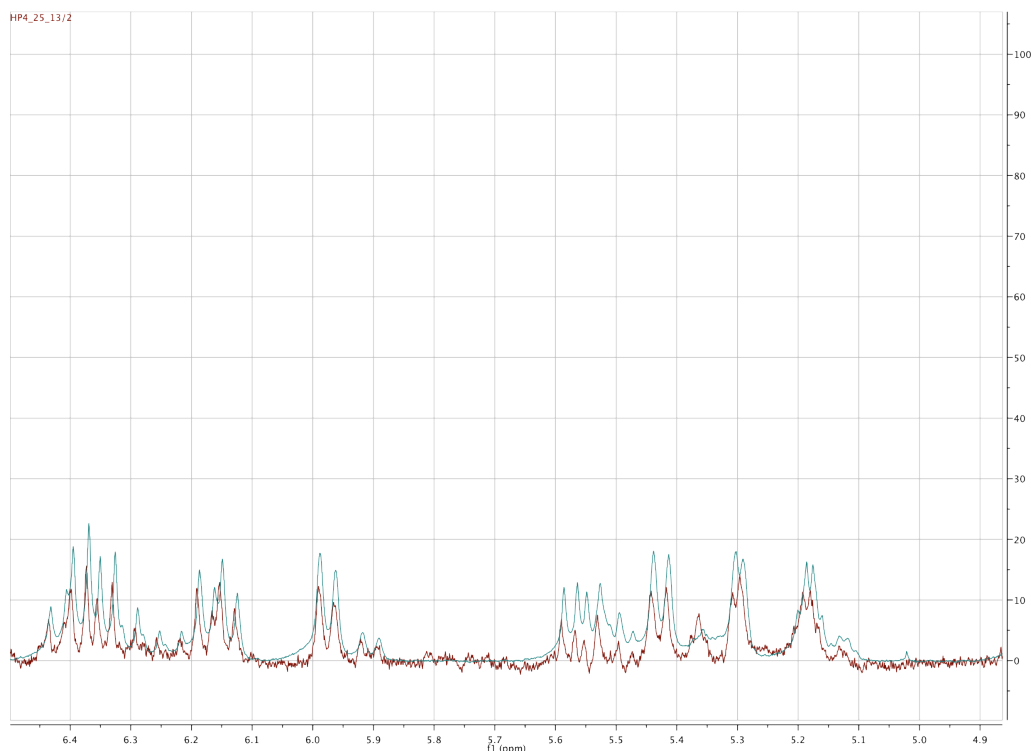


Figure 33 Rapamycin and *B. amyloliquefaciens* fraction $^1\text{H-NMR}$ overlay experiment. Green chemical shifts represent rapamycin standard (CDCl_3). Red chemical shifts represent purified metabolite from *B. amyloliquefaciens* (CDCl_3). Range is 6.4 ppm - 4.9 ppm.

HRMS is shown for the rapamycin standard to compare to the isolated rapamycin signal (**Figure 29**). After multiple purifications using HPLC, enough material was purified to obtain some NMR spectroscopic data. An overlay of rapamycin standard (green) and rapamycin from *Bacillus* sp. (red) show the same chemical shifts for many signals from both fractions (**Figure 30**). Expansions focusing on chemical shifts from 0.4 ppm to 2.4 ppm (**Figure 31**), 2.4 to 5 ppm (**Figure 32**), and 4.9 to 6.4 ppm (**Figure 33**) clearly show signals that are overlain between rapamycin and the *B. amyloliquefaciens* product. Another experiment was done to further understand the relationship between the endophyte and the host *P. occidentalis*. *P. occidentalis* tissue was extracted and analyzed by LC-MS in order to test whether or not metabolites that had been located in bacterial extracts could also be found in plant host tissue. Three *P. occidentalis* extracts analyzed were analyzed: healthy leaf tissue, leaf tissue from a plant host infected with

Xylella fastidiosa, and wood tissue from a healthy specimen. Each tissue sample was extracted successively with hexanes, chloroform, and methanol.

Table 5 Extracts of *P. occidentalis* tissue

	Hexanes ext.(mg)	Chloroform ext. (mg)	Methanol ext.(mg)
Symptomatic leaf (1.06 g)	7.3	6.1	3.8
Asymptomatic leaf (0.892 g)	6.4	5.5	4.5
Asymptomatic stem tissue (1 g)	2.4	1.9	9.6

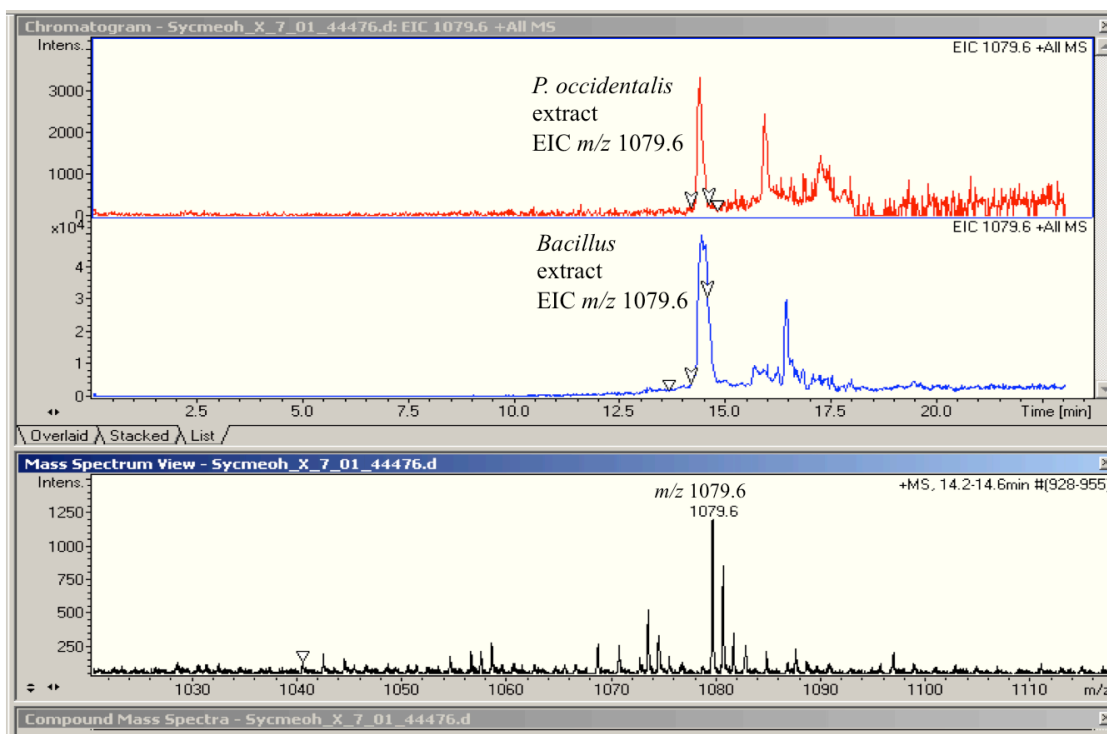


Figure 34 Overlay of two extracted ion chromatograms of *P. occidentalis* extract and endophytic extract. The m/z 1079.6 signal matches with previously purified iturin A₃.

The total weights for these extracts are collated in **Table 5**. These extracts were analyzed using LC-MS. The MeOH extract shared the same signal at m/z 1079.6 and the same retention

time (Figure 34). This was the same signal that had previously been purified and solved by NMR and HRMS as iturin A₃.

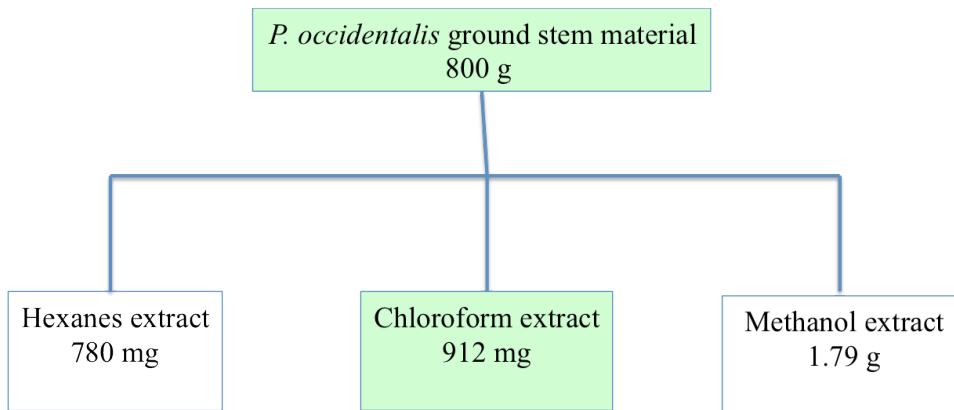


Figure 35 Extraction of *P. occidentalis* wood material

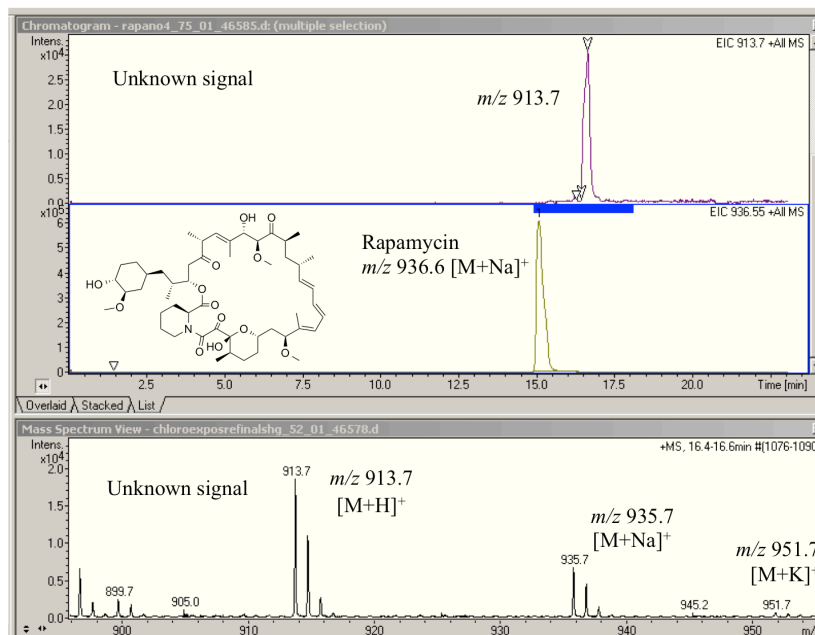


Figure 36 Two EICs of putative rapamycin analog and rapamycin. Top panel shows EIC of m/z 913.7 from chloroform extract from *P. occidentalis* and middle panel shows EIC of sodium adduct of rapamycin at m/z 936.6 $[M+Na]^+$. Bottom panel shows signal for protonated signal at m/z 913.7, sodium adduct at m/z 935.7 and potassium adduct at m/z 951.7 for unknown.

In order to complete a set of challenge experiments using MALDI-IMS, *P. occidentalis* wood material was ground to a fine sawdust material and extracted successively with hexanes,

chloroform, and methanol (**Figure 35**). Although no rapamycin adduct signals were found in any of the *P. occidentalis* wood extracts, another signal was found in the chloroform extract which was very close in mass to the rapamycin signal (**Figure 36**). In order to establish if this was a rapamycin analogue, the chloroform extract was further purified following the procedure outlined in **Figure 37**. After purification, 5 mg of the purified extract was further resolved by HPLC monitoring the UV absorption maximum for rapamycin at 278 nm (**Figure 38**).

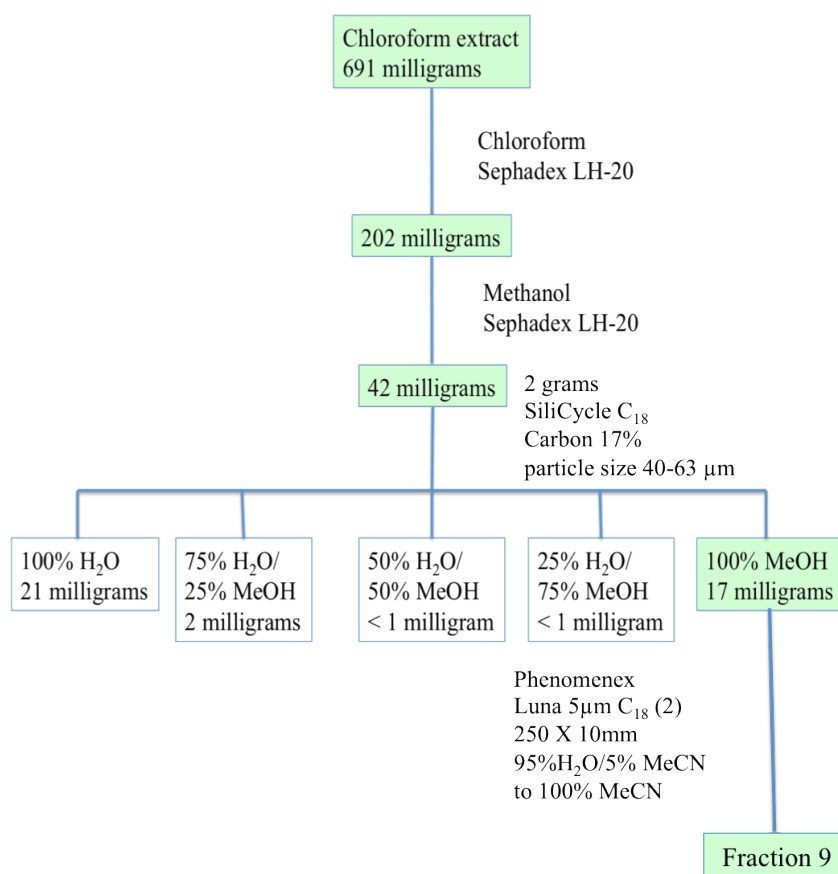


Figure 37 Isolation of putative rapamycin analogue

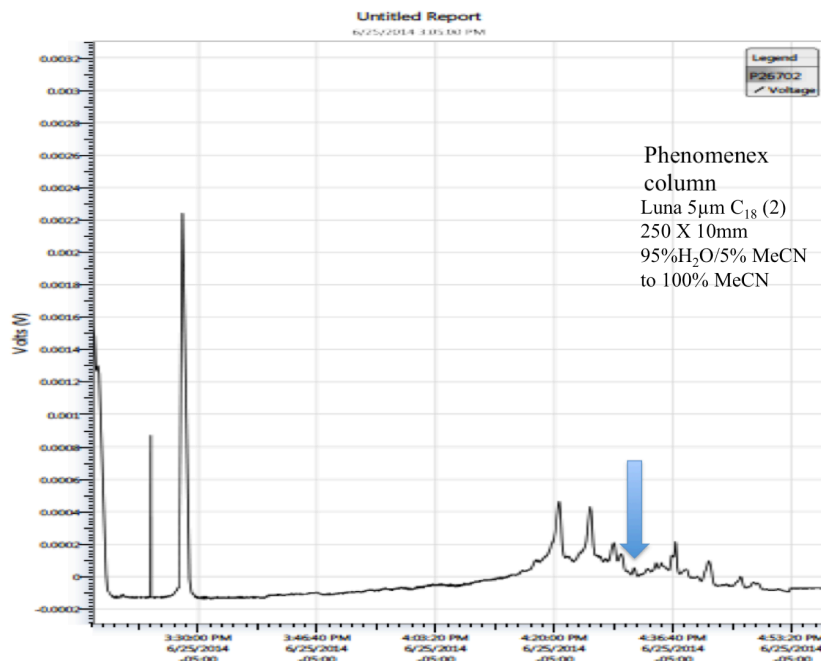


Figure 38 Putative rapamycin analogue purification. UV wavelength is 278 nm.

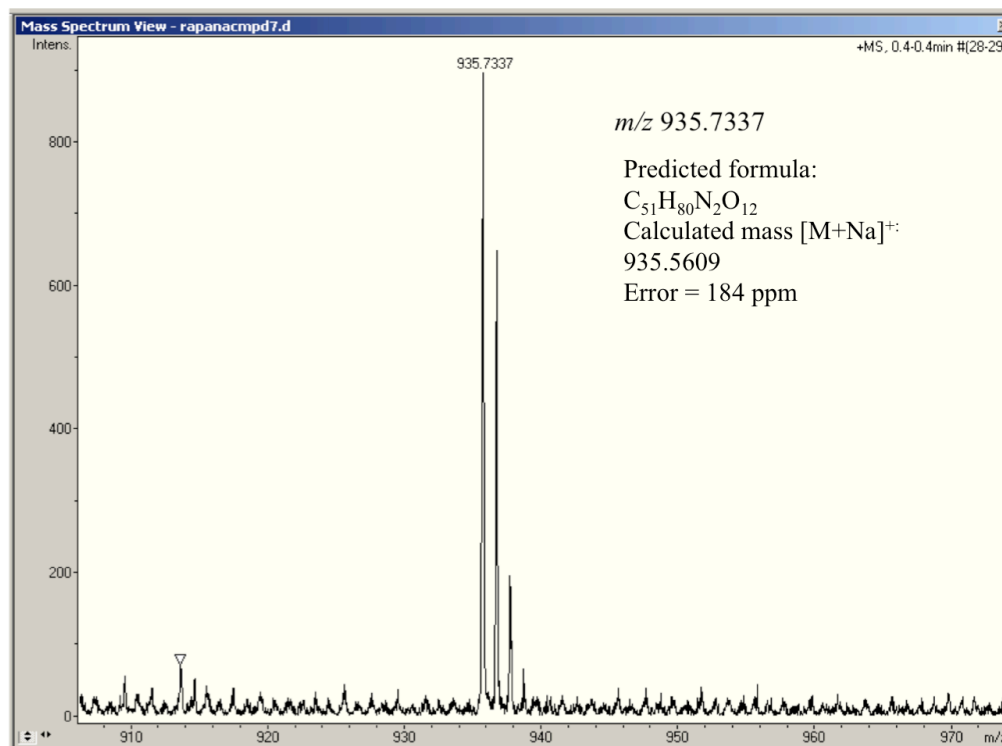


Figure 39 HRMS of putative rapamycin analog.

Fractions were analyzed after HPLC by direct injection and the indicated signal contained the putative rapamycin analogue. HRMS for this signal was gathered and this fraction was

submitted for FTMS (**Figure 39**).

As was seen in earlier parts of this thesis and is documented in numerous publications, achieving reliable microbial production of secondary metabolites can be problematic. One of the strategies for trying to help solve this problem is to try and develop an understanding of how the plant host regulates secondary metabolite production from the endophyte. A series of experiments was designed using MALDI-IMS to test if extracts of *P. occidentalis* would up-regulate iturin metabolites that had been characterized from the *Bacillus* sp. There was a significant risk that the solvent used for extraction (either hexanes, chloroform, methanol) would cause problems in bacterial growth and lead to differences in secondary metabolite production that could be interpreted as the *P. occidentalis* host regulating the *Bacillus* sp. endophyte as a false positive. Therefore, the first experiment was a time course experiment that involved plating a 5 μ L *B. amyloliquefaciens* glycerol stock onto a series of seven different CS20 plates and surrounding these newly plated colonies with 10 μ L of each solvent at approximately the same distance from different sides of the colony. These plates were incubated at 36 °C and monitored for growth. After four days bacteria had grown over all three solvents. The bacterial margin did not show any variability depending on whether or not it expanded over the areas where solvents had been placed and iturin production was uniform throughout the colony area (**Figure 40**). The next step was to test the extracts to see that, when the endophyte colony came into contact with one or more of the host plant extracts, iturin production increased. This was done by designing a time course experiment which involved plating 5 μ L of glycerol stock of the endophyte in the center of 5 different CS20 solid agar plates. These were then surrounded by the three different *P. occidentalis* extracts on three different sides of the colony. Extracts were generated by successively extracting host wood material with hexanes, chloroform, and methanol (**Figure 41**).

These extracts were re-dissolved in the original solvent using a pre-calculated volume so that 10 μ L of liquid extract would equal half a milligram of extract. These were placed in such a way so that, over the five day period, the bacterial colony would expand to eventually come in contact with the extracts. It was important to have the extracts placed sufficiently far away to allow for imaging the colony before it reached the extracts but also not too far away as to prevent the colony reaching the extracts in 5 days. On day one the colony is expanding but has not yet reached the edge of any of the extracts and the intensity of iturin production is fairly uniform throughout the colony and outside the colony (**Figures 42 & 43**). On day three there the colony has come closer to all extracts and there seems to be a slight increase in iturin intensity as a solid band as it is coming into contact with the chloroform extract (**Figures 44 & 45**).

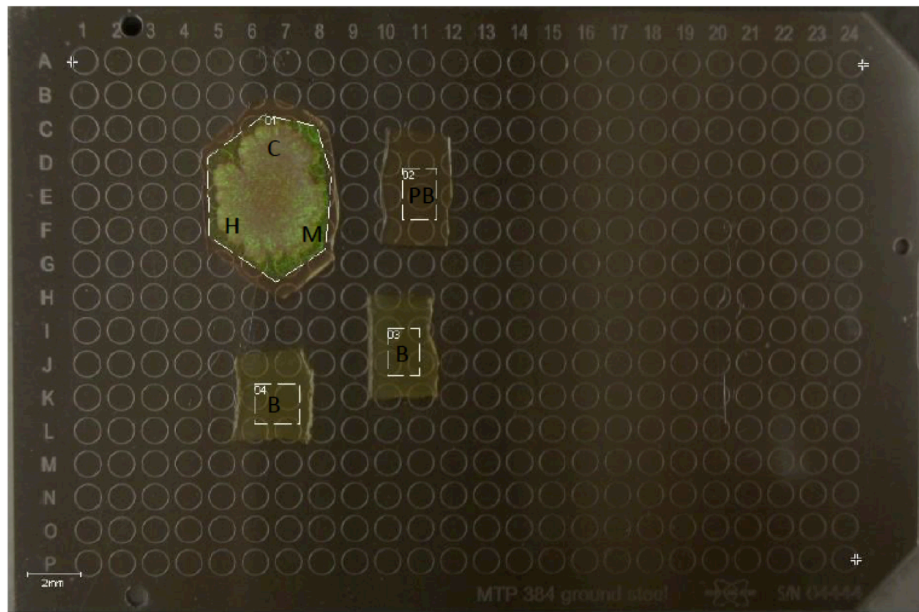


Figure 40 MALDI-IMS iturin blank run. *Bacillus* sp. were analyzed by MALDI-IMS to ascertain if solvents affected either iturin production or *Bacillus* growth. Iturin signal is shown as green. (H) hexanes, (C) chloroform, (M) is methanol. (PB) is agar piece that bacterial colony was extracted from. (B) is a separate agar plate of same media composition.

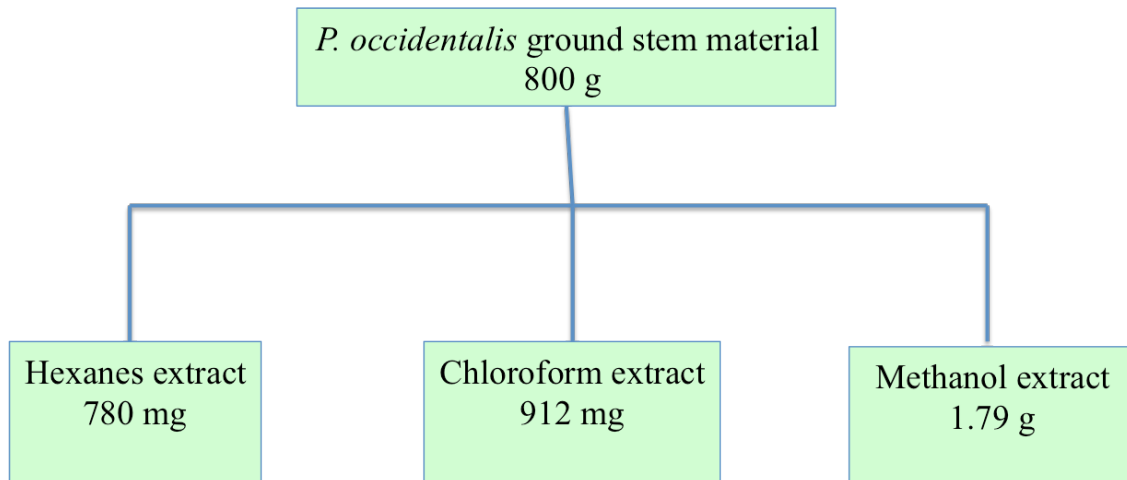


Figure 41 Extraction of *P. occidentalis* for MALDI-IMS challenge experiment

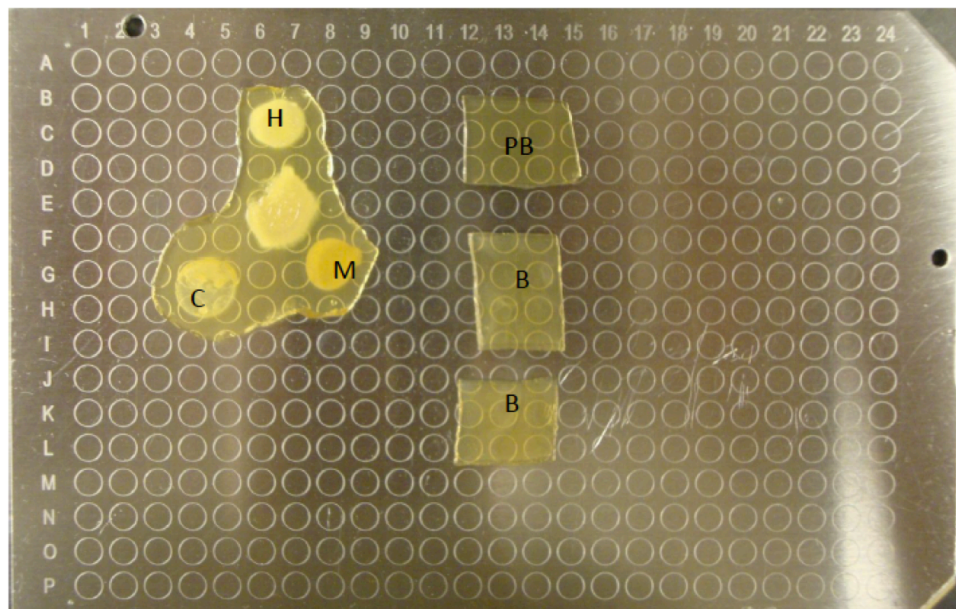


Figure 42 *Bacillus* sp. colony surrounded by host *P. occidentalis* extracts. (H) is hexane extract, (C) is chloroform extract, (M) is methanol extract. Colony and extracts were excised after one day. (PB) is agar piece that bacterial colony was extracted from. (B) is a separate agar plate of same media composition.

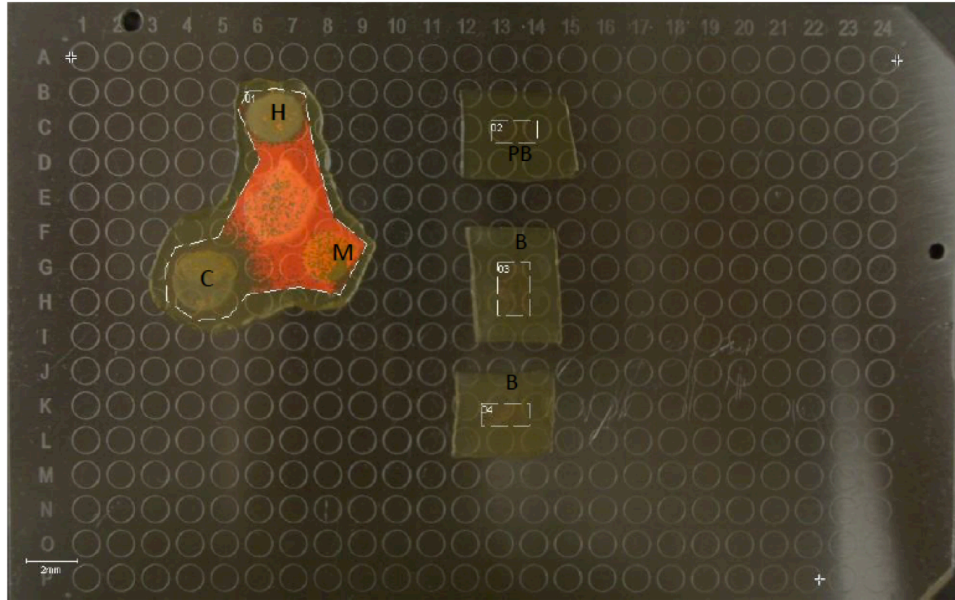


Figure 43 Day one iturin production. Iturin intensity is relatively uniform throughout with the exception that more signals are found excreted from the colony. Hexanes and chloroform extracts possibly inhibit iturin production. (PB) is agar piece that bacterial colony was extracted from. (B) is a separate agar plate of same media composition.

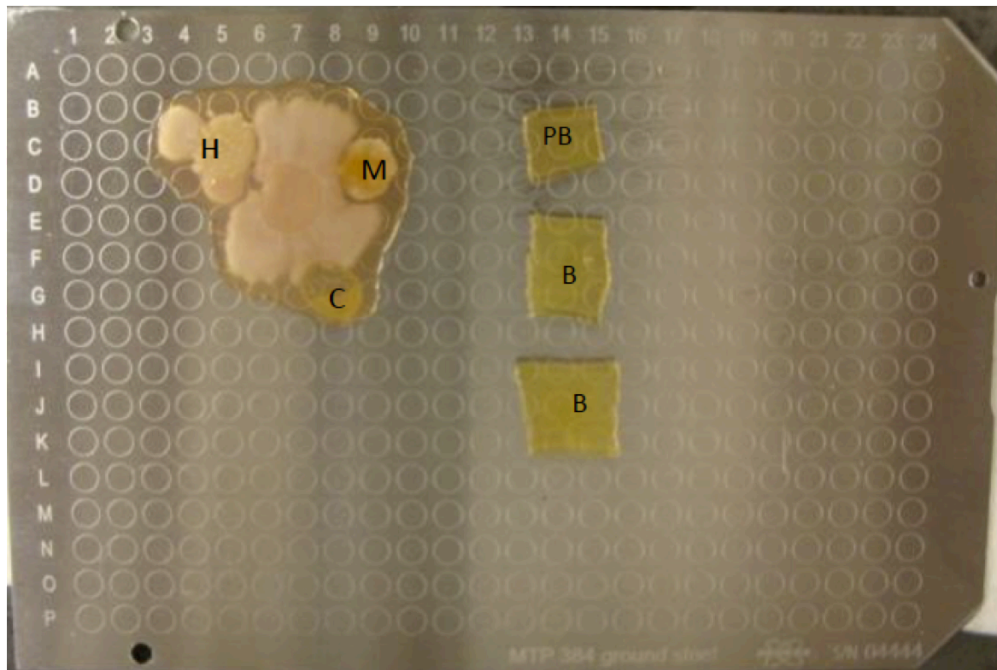


Figure 44 *Bacillus* sp. colony surrounded by host *P. occidentalis* extracts. (H) is hexane extract, (C) is chloroform extract, (M) is methanol extract. Colony and extracts were excised after three days.

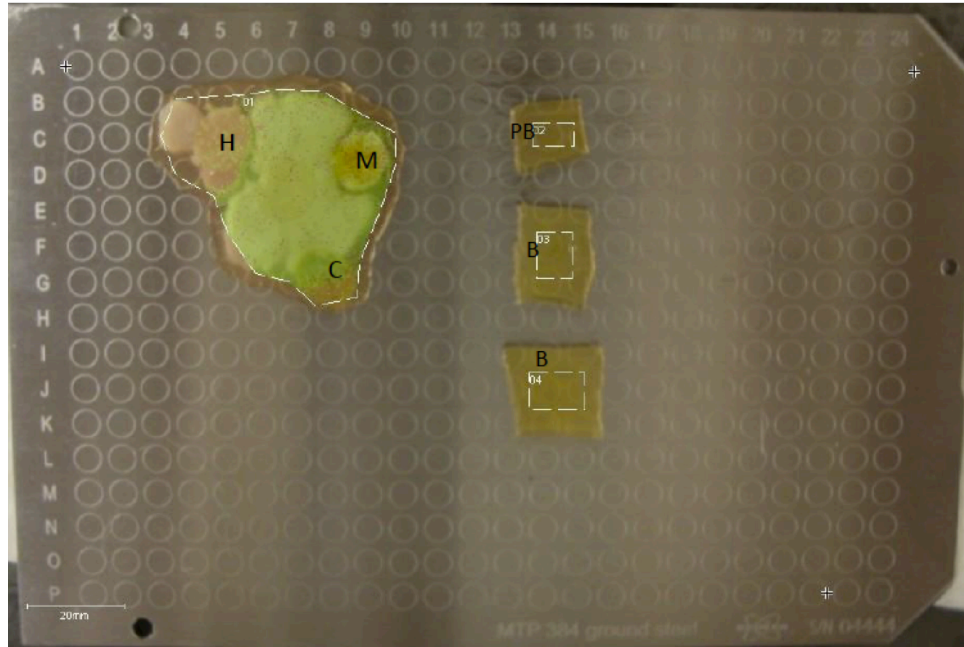


Figure 45 Day three iturin production. There is slight increase in iturin intensity as the *Bacillus* colony comes into contact with the chloroform extract.

A clear increase in iturin production can be seen on day four after the *Bacillus* extract has come into contact with the chloroform extract (**Figure 46**). This is seen clearly by representing the data in a different fashion using a heat map-like representation. The inset shows which colors represent higher intensities with blue being the lowest intensity and red being the highest. All throughout the colony the intensity of the signals is mostly uniformly blue with higher intensities interspersed throughout the colony. However, as the *Bacillus* colony comes into contact with the chloroform extract, the signals are clearly much more intense with more areas of green and there is red interspersed within green (**Figure 46**). These results suggest something within the host chloroform extract is eliciting iturin production from *B. amyloliquefaciens*.

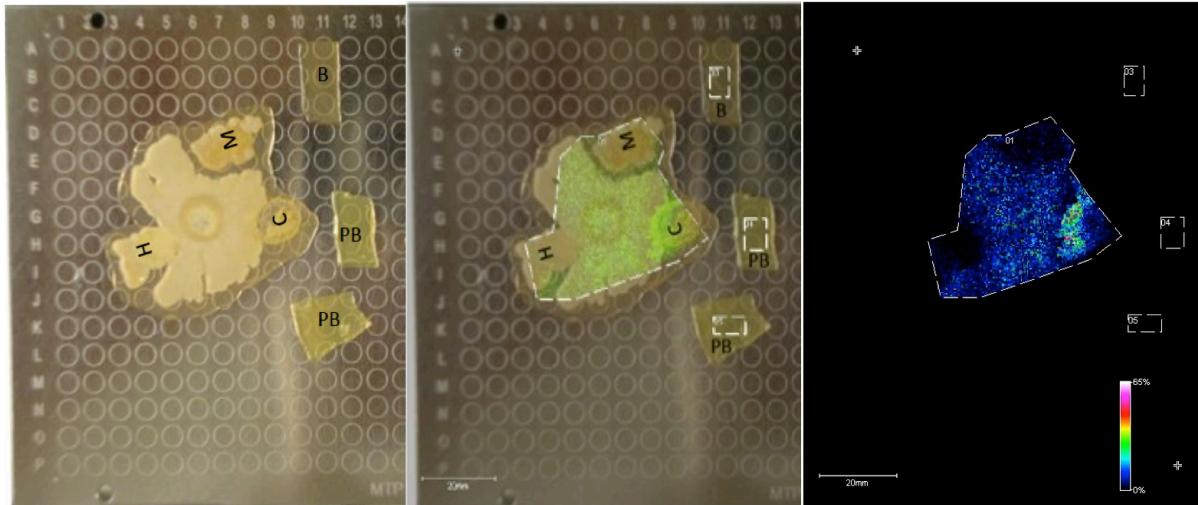


Figure 46 Day four iturin production. The left panel shows the *B. amyloliquefaciens* colony coming into contact with the chloroform extract. The middle panel shows there is a substantial increase in iturin intensity as the *Bacillus* colony comes into contact with the chloroform extract. This is highlighted by using a heat-map representation in the right panel. The inset shows how color relates to intensity.

CHAPTER THREE:
PURIFICATION OF NICOTIANAMINE FROM SOY FLOUR

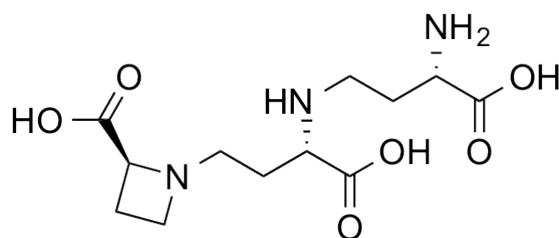


Figure 47 Nicotianamine structure

Nicotianamine is a chelator of metals found in plants that has the ability to replace EDTA in food products to prevent spoilage.⁶² Because nicotianamine is ubiquitous among plant species, options for finding a viable source are broad. After searching for nicotianamine production and yields, soybeans and soybean products were chosen for the initial attempt to isolate significant amounts. The samples that were retrieved for analysis included whole commercially produced soybeans from five different hybrid species of whole soybeans and soy flour.

Whole soybean analysis. The commercially available Asgrow 4531 strain soybeans (1.785 kg) from Monsanto-Asgrow brand markets in Leland, MS, were ground and soaked in 8 L warm water (40 °C) for roughly 20 hours, and subjected to sonication. The aqueous extract (6 L) was removed from the soybean material by use of mesh wiring filtration. Using a 1 M HCl solution, the pH of the resulting aqueous extract was adjusted to 4.5 to precipitate proteins. Using centrifugation, the proteins from the pellet were removed from the aqueous extract. A total of 5.5 L of supernatant was recovered and subsequently concentrated to 2.25 L using rotary evaporation. 2.25 L of ethanol was added to the concentrated aqueous extract in order to precipitate the nicotianamine-containing material. The mixture was stirred and placed under

refrigeration overnight to maximize precipitation. The resulting mixture was centrifuged to separate the precipitate from the aqueous extract. The precipitate was lyophilized and yielded 15 g of dry material.

Soy flour analysis. Soy flour was obtained from a 1.5 lb (680 g) bag of Hodgson Mill soy flour exp. date 11/10/12, barcode: 0 71518 05039 9. To two 2800 mL flasks were added 200 g of the flour. Water (2500 mL) was added to each and the pH was adjusted to 9 using sodium hydroxide and set to stir at 25 °C. The suspension was filtered using wire mesh filtration and the pH was adjusted to 4.5. The aqueous extract was centrifuged and the protein-containing pellet was removed. Ethanol was added to the supernatant at a concentration of 80%. The resulting solution was centrifuged and the nicotianamine-containing pellet was removed. The material was lyophilized to yield 12.4 g of dry material and nicotianamine was detected by LC-MS and compared to material generated from whole soybeans.

Table 6 Calibration of NA using LC-MS

Nicotianamine (ng)	Area	Average area	RSD
210	1350	1224	9.34
	1195		
	1127		
420	3579	3679	6.03
	3933		
	3524		
1050	9600	10248	5.47
	10565		
	10578		
2100	22021	22486	6.63
	24154		
	21284		
4200	39385	41203	5.59
	40431		
	43794		

*RSD (%)=((std dev*100)/mean)

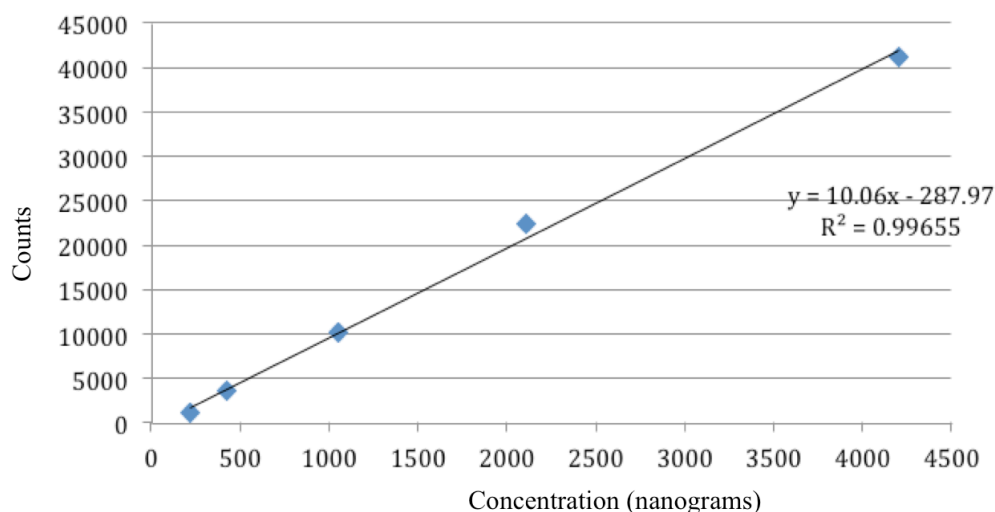


Figure 48 Calibration curve for nicotianamine

The first step in being able to quantify the yield of nicotianamine using LC-MS was to create a calibration curve using a nicotianamine standard. Five different concentrations were used and each concentration was run three times (**Table 6**). The average of three runs for each concentration were used to create a calibration curve which could be used to compare all future extracts for highest yielding methods (**Figure 48**). Another important piece of data to generate was the detection limits of the LC-MS as well as the HRMS. The detection limits were found to be approximately 4.2 ng (**Figure 49**) and the HRMS showed an $[M+H]^+$ ion at m/z 304.1431. (**Figure 50**).

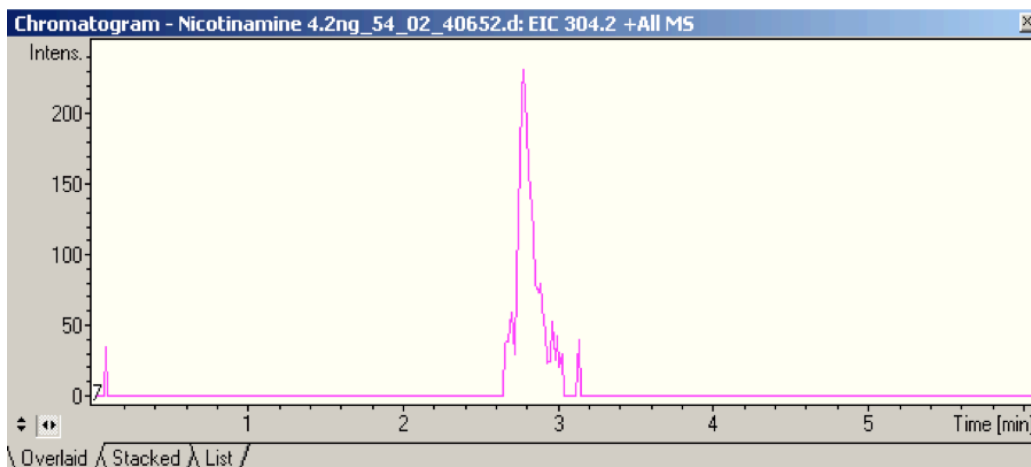


Figure 49 Detection limits of nicotianamine. 4.2 ng was the lowest amount that could be detected.

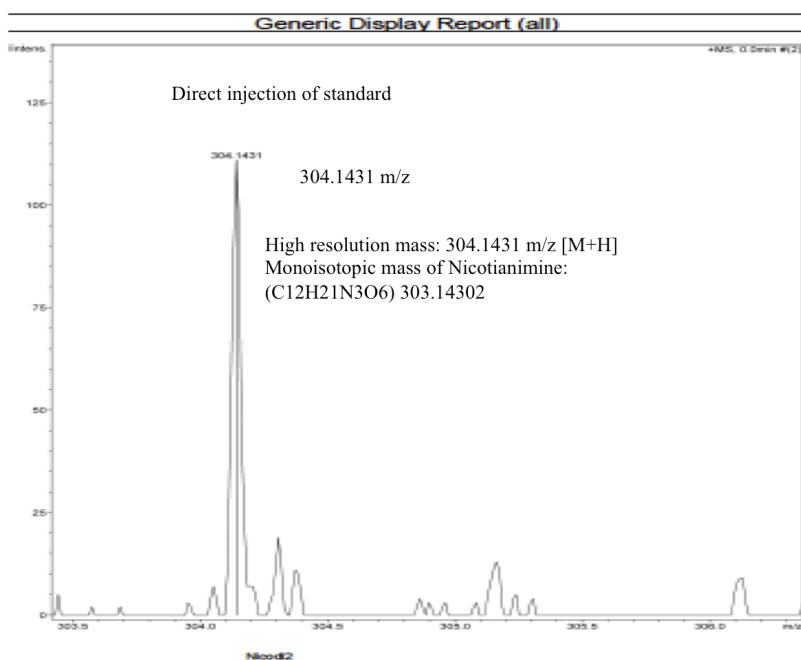


Figure 50 HRMS of nicotianamine.

After this data had been gathered, the yield from the two different sources could be quantified. A comparison of the yield between whole soybeans and soy flour, which had been defatted, proved that soy flour was the optimal soy resource. The ionization intensity of the extracted $[M+H]^+$ ion at m/z 304.1431 for nicotianamine is shown for the whole soy precipitate, soy flour precipitate and

the nicotianamine standard (**Figure 51**). The integration intensity of extracted ion m/z 304.1431 m/z for 20 μg soy flour precipitate, 20 μg whole soy precipitate, and 50 ng of pure nicotianamine standard was 621051, 228178, and 603387, respectively. The following equations give the percent composition of nicotianamine in the precipitate mixtures:

A. $[(50 \text{ ng pure NA} * 621051) / (603387)] / (20000 \text{ ng crude precipitate}) * 100\% = 0.26\% \text{ NA in soy flour precipitate.}$

B. $[(50 \text{ ng pure NA} * 228178) / (603387)] / (20000 \text{ ng crude precipitate}) * 100\% = 0.1\% \text{ NA in whole soy precipitate.}$

Based on this analysis, it was decided that soy flour was the best viable option to attempt to purify nicotianamine. The Kikkoman corporation describes a patented method for the

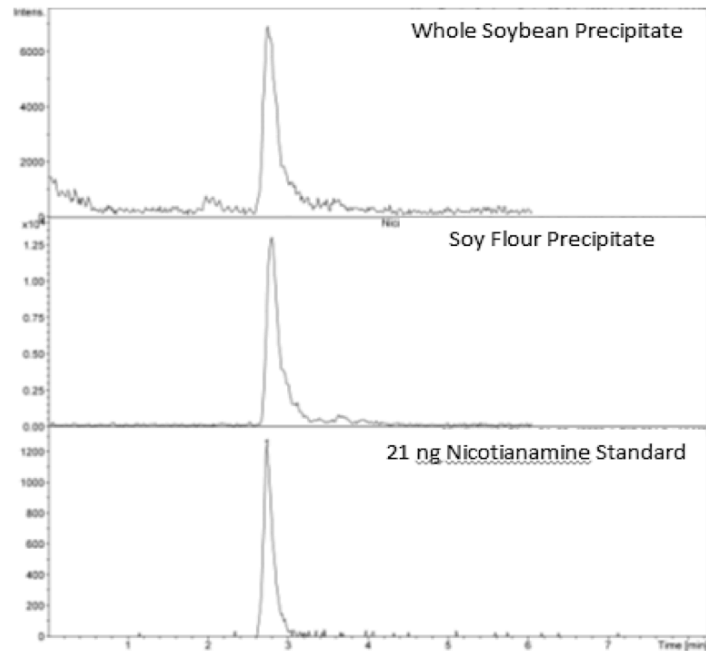


Figure 51 Comparison of nicotianamine from whole soybean precipitate, soy flour precipitate, and nicotianamine standard.

extraction of nicotianamine from soy flour which was followed, with some steps adjusted as needed (**Figure 52**).⁶⁴

Eighty grams of Hodgson's Mill soy flour was used. The first step involved adding one liter of water to this dry material and adjusting the pH to 9 using 6 M NaOH. A stir plate was used and this mixture was stirred for approximately two hours. This material was then filtered through a stainless steel sieve. The pH was then adjusted to 4.5 and the material was centrifuged at 4000 RPM for 30 minutes in order to precipitate the proteins from the solution.

Thirty grams of activated carbon was then added to this solution and it was stirred using a magnetic plate and stir bar for approximately four hours. Afterward, filter aid was added and the solution was stirred for approximately one more hour. This material was then filtered and lyophilized yielding approximately 17 grams. LC-MS quantification showed a yield of approximately 0.3% nicotianamine (**Figure 53**).

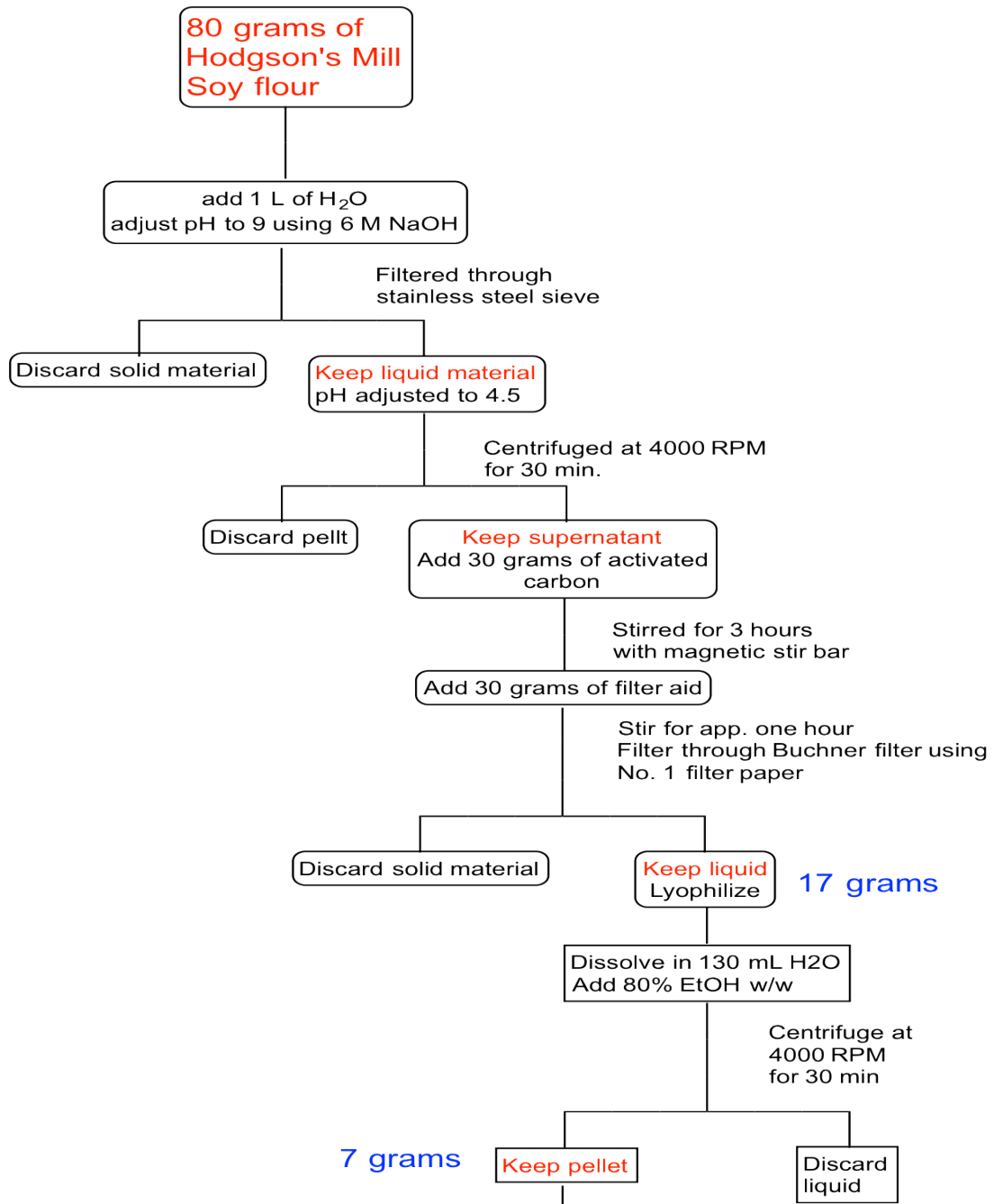


Figure 52 Nicotianamine isolation scheme

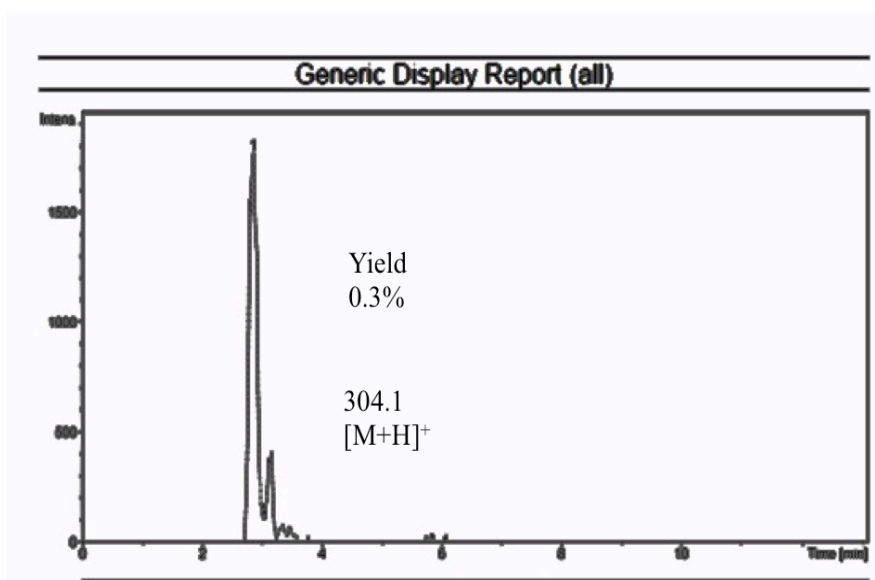


Figure 53 Yield of nicotianamine from soy flour

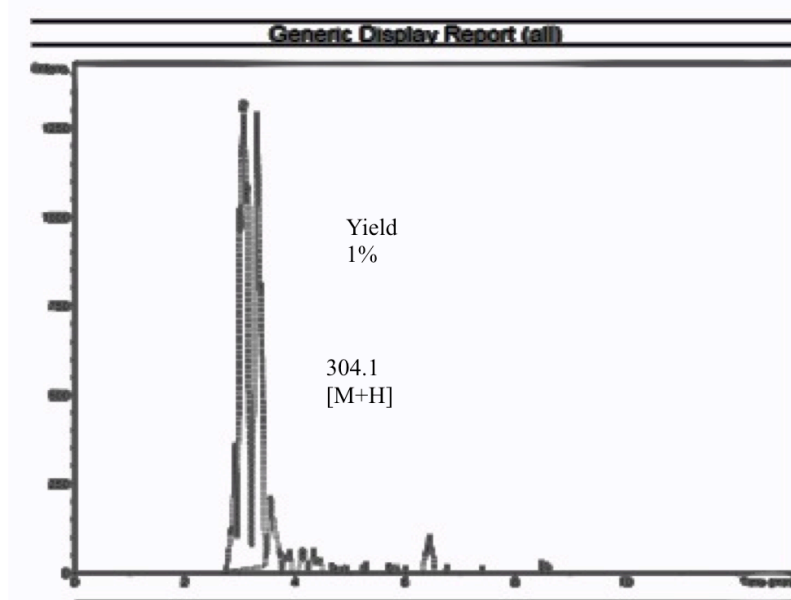


Figure 54 Yield of nicotianamine from soy flour after multiple purification steps

This freeze dried material was dissolved in 50 mL of H₂O. Next, this solution is made into an 80% solution of ethanol on a w/w basis by adding 130 mL of ethanol. This mixture was then centrifuged for 30 minutes at 4 °C at 4000 RPM. The supernatant was discarded and the pellet is kept. After lyophilization, this material contained 1.0% nicotianamine (**Figure 54**).

In order to test this material and be sure that nicotianamine was the ion signal that was being analyzed, a co-injection with the nicotianamine standard was performed (**Figure 55**).

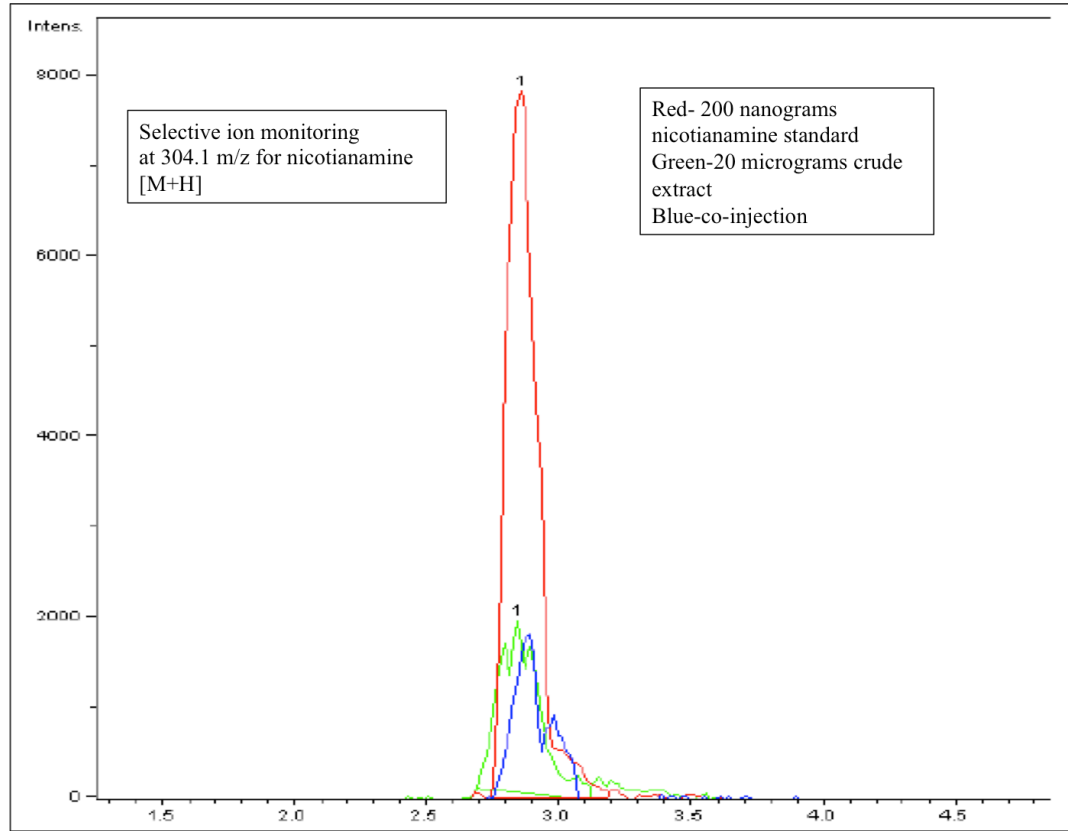


Figure 55 Co-injection of nicotianamine and extract

This scheme provides a relatively straight-forward way to purify a natural metal-chelating agent from a cheap, readily available source. Nicotianamine could replace EDTA to prevent metal-catalyzed spoilage and still enable food products to be labeled as “all-natural.”

CHAPTER FOUR: HCV REVIEW

The goal of HCV therapy is a sustained virologic response (SVR), which is achieved when HCV RNA cannot be detected in serum 24 weeks after therapy has ended. The currently prescribed therapy against HCV is a combination of ribavirin and either peginterferon alfa-2a or peginterferon alfa-2b. Less than half of patients infected with HCV genotype 1, the most prevalent genotype in patients in the United States, achieve an SVR with standard ribavirin/interferon combination therapy.⁹⁴ The FDA recently approved two protease inhibitors, telaprevir and boceprevir, for the treatment of genotype 1 HCV. Telaprevir has been shown to significantly improve the SVR in patients when administered along with the HCV standard combination therapy of ribavirin and peginterferon.⁹⁵ However, the chance that patients will discontinue therapy due to adverse side effects is also increased.⁹⁵ There have been significant differences in response to therapy based on genotype. For example, in one recent clinical study patients infected with genotype 1 showed a decrease in viral load of 4.4 log₁₀ IU/mL after two weeks of monotherapy of telaprevir; patients with genotype 4 HCV only showed a decrease of 0.9 log₁₀ IU/mL.⁹⁶ Differences in efficacy have also been noted in NS5B non-nucleoside inhibitors as well. In another recent clinical study, VCH-259, a DAA that binds to the thumb 2 site of the NS5B RdRp, was administered for 10 days to an HCV genotype 1 patient after which HCV RNA had decreased by a mean maximal of 2.5 log₁₀ IU/mL. The same conditions were tested for a patient infected with genotype 6 and no viral decline was reported.⁹⁷

The two most recent drugs approved for HCV treatment are simeprevir (Olysio®) and

sofosbuvir (Solvaldi®).⁹⁸⁻⁹⁹ Simeprevir is an NS3/4 protease inhibitor that has been shown to significantly increase SVR rates in patients with genotype 1 after 24 weeks when given in combination with interferon and ribavirin when compared to interferon and ribavirin alone or placebo.¹⁰⁰ Sofosbuvir is a RNA polymerase inhibitor that has been shown to significantly increase SVR rates in both genotype 1 and 4 patients when given with ribavirin and interferon.¹⁰¹ Interestingly, sofosbuvir has also shown efficacy in genotype 1 patients in combination with ribavirin but without interferon.¹⁰² This represents a major step forward as interferon side effects often stop patients from continuing a full regiment of HCV. However, the cost of these new drugs can be a major issue for certain segments of the population, especially for people in developing countries. The giant steps forward in knowledge of the HCV life cycle played a huge role in the development of these new agents and have also allowed for screening of natural product leads for HCV.

HCV is an enveloped virus containing a lipid bilayer that surrounds the nucleocapsid. E1 and E2 are two structural glycoproteins that are anchored in the lipid bilayer and participate in host cell receptor binding. Recent studies have shown that E1 and E2 are stabilized by covalent disulfide bridges once exported to the bilayer and that glycosylation of certain sites are vital for both infectivity and evading the host immune response.¹⁰³ There have been numerous studies attempting to elucidate the mechanism for HCV binding. The low-density lipoprotein receptor (LDL-R),¹⁰⁴ the cell receptor CD81,¹⁰⁵ the human scavenger receptor class B type I (Sr-BI),¹⁰⁶ and claudin-1,¹⁰⁷ a protein involved in tight-junction cell-to-cell adhesion, have all been studied to understand their roles in HCV entry.

The HCV genome is composed of a ~9600 bp length, positive sense strand mRNA that is translated by a negative strand intermediate. The genome includes: a 5' non-coding region

(NCR) that contains the internal ribosome entry site (IRES), the ORF that encodes the single polyprotein, and the 3' NCR.¹⁰⁸ The IRES directs translation of HCV mRNA by a mechanism that is distinct from host cell eukaryotic translation.¹⁰⁹ The HCV ORF encodes, starting from the 5' end: the core nucleocapsid; the E1 and E2 envelope proteins; the p7 ion channel; the NS2-3 protease; the NS3 serine protease and RNA helicase; the NS4A polypeptide; the NS4B and NS5A proteins; and the NS5B RNA-dependent RNA polymerase (RdRp).¹¹⁰ The developing polyprotein is processed by both the host endoplasmic reticulum signal peptidase and the NS2-3 protease and the NS3-4A serine protease.¹¹⁰ The polyprotein product contains a signal sequence between the core nucleocapsid encoding region and the E1 envelope coding region which directs it to the host endoplasmic reticulum (ER) membrane.¹¹¹ After the E1 region has been translocated into the endoplasmic reticulum, the core protein is cleaved and processed and subsequently associates with lipid droplets.¹¹¹ The E1 and E2 proteins are glycosylated by the host ER and ER chaperones are involved in proper E1 and E2 folding.¹¹²

The p7 ion channel has been shown to be vital for infectivity using mutational studies, and also for virion assembly by interacting with the NS2 and E1 proteins.¹¹³ Another possible role for this protein may be to regulate pH in intracellular compartments of the host cell.¹¹⁴

HCV relies on two proteases; the first, NS2-3, is responsible for a single cleavage at the NS2/NS3 junction. The next protease, the NS3-4A serine protease and RNA helicase complex, is responsible for cleavage between the NS3/4A cofactor (self-cleavage), and between the NS4A/4B, NS4B/5A, and NS5A/5B proteins.^{73,115}

The NS4B protein is involved in forming the membranous network where HCV replication takes place,¹¹⁶ while the NS5A proteins has proven to contain RNA binding properties,¹¹⁷ be involved in alpha-interferon resistance,¹¹⁸ and possibly contribute to liver

steatosis.¹¹⁹ The final protein in the ORF sequence is the NS5B RNA-dependent RNA polymerase (RdRp), which is responsible for synthesizing a negative-strand template from the original positive oriented strand to facilitate positive strand replication, and is used in HCV classification.

Less is known about HCV packaging and assembly, but there has been a number of studies published in this area in recent years.¹²⁰ One study has suggested that HCV co-opts the cellular production and release of very-low-density-lipoproteins (VLDL), which, through a kind of mimicry, allows HCV to persist.¹²¹ One particular protein involved in VLDL production that seems to be important in HCV production is apolipoprotein E.¹²² Other proteins that have been implicated in HCV production are heat shock cognate protein 70,¹²³ annexin A2,¹²⁴ and diacylglycerol acyltransferase-1.¹²⁵

Plant Derived HCV Natural Product Inhibitors

The HCV NS3-4A protease as emerged has a primary target for DAA agents. Four new iridoid glucosides were recently isolated from *Anarrhinum orientale*, a plant in the order Lamiales. Iridoids are monoterpene glycosides which are widely found in Lamiales.¹²⁶ One of these newly isolated iridoids (**1**), had an IC₅₀ value of 100 μM against the NS3 protease (**Figure 42**). This compound also showed selectivity for the HCV NS3-4A protease as the IC₅₀ values for the human trypsin protease were above 200 μM.¹²⁶

A recent study that screened more than 150 plants with reported medicinal properties for anti-HCV activity showed activity in the methanol extract of the root bark of species in the *Morus* genus.¹²⁷ Bioassay-guided fractionation yielded five known 2-arylbenzofuran derivatives from the original extract. Four of these compounds mulberroside C, moracin P, moracin O, and moracin M, showed inhibitory activity against HCV, with moracin P and moracin O showing

potent activity. Moracin P (**2**) had an IC_{50} value of 35.6 μ M and moracin O (**3**) an IC_{50} of 80.8 μ M in a Huh-7 cell replicon assay. These compounds were further tested for specific activity against NS3-4A helicase activity. Moracin O had an IC_{50} of 42.9 μ M, while moracin P showed an IC_{50} of 27.0 μ M.¹²⁷

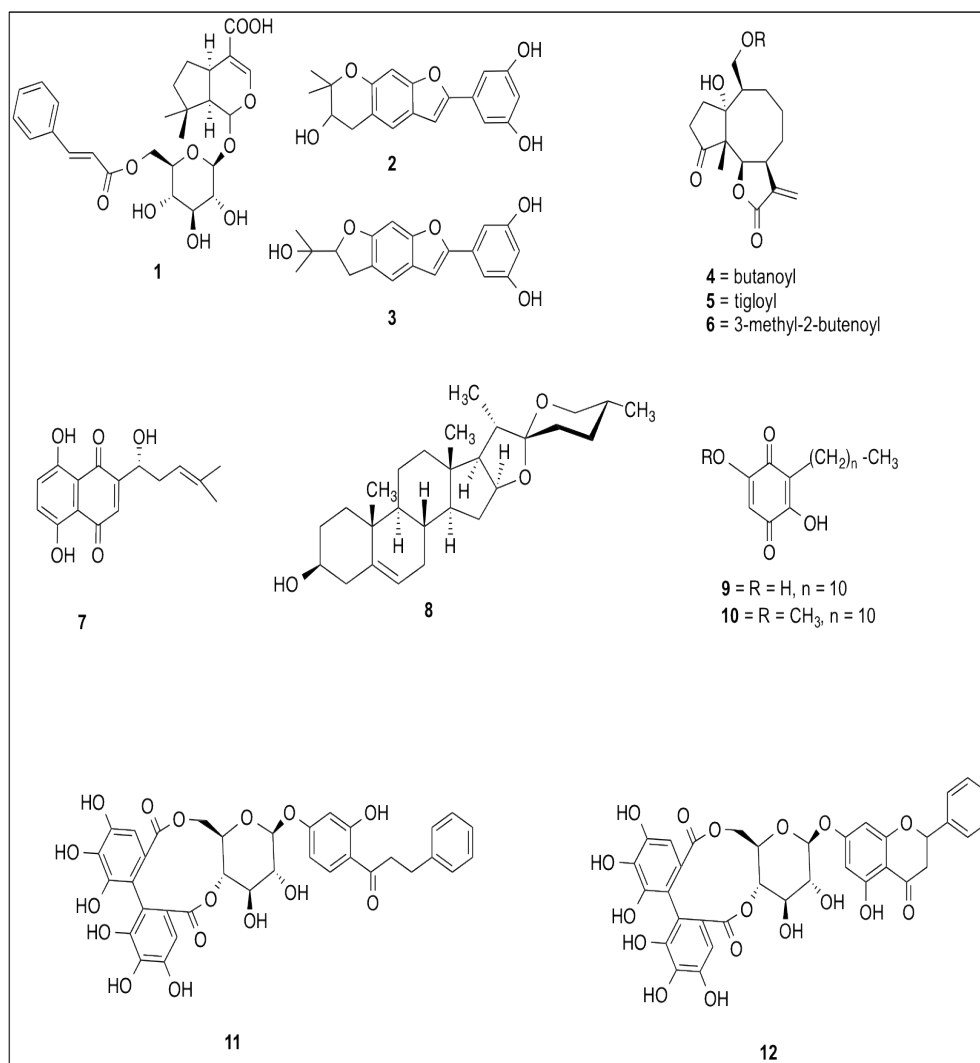


Figure 56 Plant-derived inhibitors of HCV

Another recent study screened a natural product compound library derived from American and African flora for anti-HVC activity and found HCV inhibition in extracts of the aerial parts of *Parthenium hispitum*.¹²⁸ Bioassay guided fractionation yielded a series of pseudoguaianolides, a group of sesquiterpene lactones, three of which (**4-6**) yielded primary

inhibition of HCV above 90% at a 2 μM concentration.¹²⁸ Shikonin (**7**) is a naphthoquinone derivative that has been isolated from *Arnebia euchroma* in past studies and shown activity against HIV-1 *in vitro* and has antiangiogenic and antitumorigenic properties.¹²⁹ It was recently tested against HCV and had an EC_{50} value of 0.025 $\mu\text{g}/\text{mL}$.¹³⁰ Further cytotoxicity test proved the selectivity index of shikonin to be relatively high at 43.56 ($\text{CC}_{50}/\text{EC}_{50}$).¹³⁰

Diosgenin (**8**) is a steroidal sapogenin that has been isolated from tubers in the genus *Dioscorea*. A recent study that tested diosgenin against HCV using an enhanced green fluorescent protein reporter based assay demonstrated an EC_{50} value of 3.8 μM .¹³¹ Further experiments using Western blot analysis showed that diosgenin had an additive effect when administered with interferon-alpha on inhibition of the HCV NS3-4A protease.¹³¹

Another large scale screening procedure which utilized plants used in traditional medicine in Sudan yielded two benzoquinones that showed significant activity against the HCV protease.¹³² These two compounds, embelin (**9**) and 5-*O*-methylembelin (**10**) were isolated from the fruit of an *Embelia schimperi* species. Embelin gave an IC_{50} of 21 μM , while 5-*O*-methylembelin gave a reported IC_{50} of 46 μM when tested for inhibitory activity against the HCV NS3-4A protease.¹³²

Another study, this time involving screening plants from Peru, yielded two new polyphenolic compounds that showed significant activity against the HCV NS3-4A protease.¹³³ Both compounds were isolated from the methanol extract of *Stylogone cauliflora*. SCH 644342 (**11**) showed an IC_{50} value of 0.8 μM , while SCH 644343 (**12**) gave an IC_{50} value of 0.3 μM .¹³³

Microbial Derived HCV Inhibitors

In 1996, a new quinone compound, SCH 68631 (**13**), was isolated from the fermentation broth of a soil microorganism isolated from a forested area in Nepal (**Figure 43**).¹³⁴ The original

material was extracted with ethyl acetate and a biphasic solvent partitioning system was used for further purification. The active fraction was then subjected to HPLC. SCH 68631 gave an IC value of 2.5 $\mu\text{g}/\text{mL}$ when tested against the NS3-4A protease.¹³⁴

Another novel compound from a soil microorganism was isolated in 1999 that showed high anti-HCV activity. *Penicillium griseofulvum* is a fungus that was isolated from a desert ecosystem in Arizona.¹³⁵ The fermentation broth of this organism was extracted with ethyl acetate and then purified using liquid partitioning and HPLC, yielding SCH 351633 (**14**), a novel bicyclic hemiketal lactone. This new compound gave an IC_{50} value of 3.8 $\mu\text{g}/\text{mL}$ when tested against the HCV NS3-4A protease.¹³⁵

Marine Derived HCV Natural Products Inhibitors

Manoalide (**15**) is sesterpenoid first isolated from the sponge *Luffariella variabilis*.¹³⁶ It was recently screened for antiviral activity and was shown to inhibit the ATPase, RNA binding, and helicase activities of the HCV NS3 protease.¹³⁶

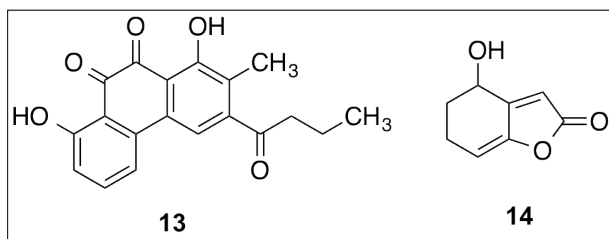


Figure 57 Microbial-derived HCV inhibitors

The discorhabdins are a group of pyrroloiminoquinone alkaloids derived from sponge species in the genus *Latrunculia*. Two compounds in this class have shown potent activity in an HCV replicon assay.¹³⁷ Discorhabdin A (**16**) had an EC_{50} value above 90% at concentrations less than 10 μM .¹³⁷

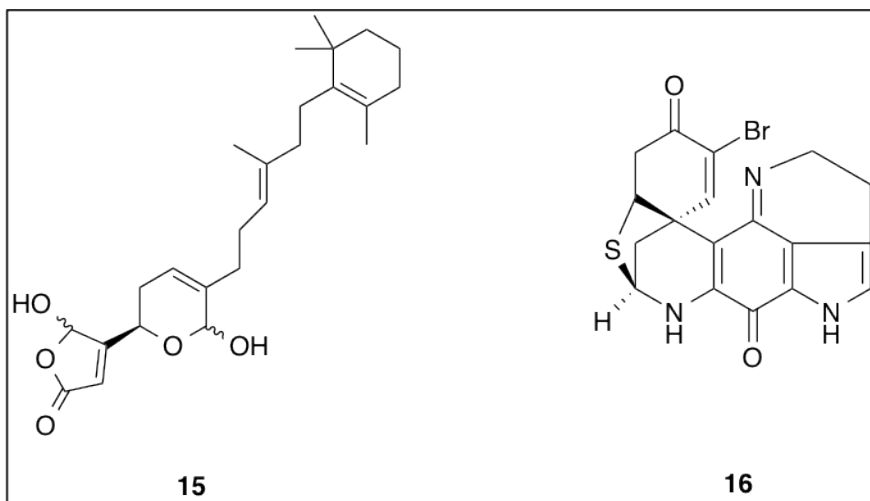


Figure 58 Marine-derived inhibitors of HCV

CHAPTER FIVE: CONCLUSIONS

Platanus occidentalis and Bacillus amyloliquefaciens

Endophytes are bacterial and fungal symbionts that reside in plant tissue without causing disease and numerous studies have proven these microbes are engaged in a symbiotic relationship with the host plant. The functions that the endophytes provide for the host are varied and studies on the ecology of endophytes are still ongoing, but the nature of these relationships has been elucidated in many host plant species and is of great importance to many important agricultural crops. For example, endophytes that reside in the leaves of *Theobroma cacao* enhance host defenses against the pathogen *Phytophthora palmivora*.¹³⁸ In rice (*Oryza sativa*), endophytes regulate resources to optimize root growth while root hairs are being established.¹³⁹ Another recent study showed that in wheat (*Triticum* spp.), endophytes help host plants to adapt to heat and drought conditions.¹⁴⁰

Bacillus spp. of bacteria are known to produce a diverse set of secondary metabolites including lantibiotics, lipopeptides, polyketides, and others.¹⁷ Rapamycin is a polyketide molecule which is of major interest due to wide-ranging activity including antitumor⁴² and immunosuppressant activities⁴³ and research into the efficacy of rapamycin against many human ailments is ongoing. Here we have increased the knowledge base in regards to this important molecule in a number of ways. We have shown that another species other than *Streptomyces hygroscopicus* produces this important molecule. The fact that a *Bacillus* species produces rapamycin could have wide ranging effects in the pharmaceutical industry as *Bacillus* species are

historically very amenable to genetic engineering. Typically, drug molecules that are produced by microbial species have been modified and engineered to increase production of the molecule of interest. Actinomycetes are known to be much more difficult to grow than *Bacillus* spp. and thus this strain of *B. amyloliquefaciens* could be a viable alternative to develop. Genetic engineering methods for increasing production would need to be developed in order to compete with current rapamycin producers.

Another finding that is important to rapamycin research is the possible discovery of a rapamycin analogue. One of the many reasons the original report of rapamycin was such an important discovery was not in regards to the molecule itself, but was due to the fact that this led to the discovery of Target of Rapamycin (TOR) protein kinases.⁴⁴ TOR is important in both primary and clinical biology; in primary biology, it is the main controller of cellular growth and aging in eukaryotic cells that coordinates environmental signals with the appropriate response.¹⁴¹ As mentioned previously, TOR proteins are part of at least two protein complexes, TORC (Target of Rapamycin Complex) 1 and TORC2. Interestingly, rapamycin only binds to TOR that is part of TORC1 and thus analogues would be of high interest to test binding differences in these different complexes. TORC1 signaling is thought to be overactive in a majority of cancers, so any differences in binding or subsequent activity in TOR as part of TORC1 would be of substantial interest as well.⁴⁵ Although there have been substantial leaps in knowledge with regards to TORC1 and TORC2 signaling and activation, this is still an active area of research.⁴⁵ If the putative rapamycin analogue binds to either complex in a distinct manner, this could assist biochemical investigations of these pathways.

Another way that this work has contributed to the study of secondary metabolites is by demonstrating the need for future investigations into silent gene expression from microbial

species. Natural products are responsible for greater than 70% of antibiotics and 55% of antiviral medications.¹⁴² Most of these were discovered in the 1940s and 1950s in what is now heralded as the Golden Age of Antibiotics.¹⁴³ A number of strategies have been developed in order to try and elicit or activate silent gene clusters that are not active under normal laboratory conditions.¹⁴³ Here, we show a *Bacillus* species from the very common *P. occidentalis* has the ability to produce rapamycin, a secondary metabolite that was first discovered on Easter Island, 2000 miles of the coast of Chile. This shows how a deeper understanding of silent gene expression, and also the chemical ecology underlying the endophyte-host plant relationship, will be important for future drug discovery efforts.

Perhaps the most intriguing part of this work was the possible biotransformation of the rapamycin metabolite by the host plant. Rapamycin has been shown to be detrimental to plant growth, yet also contains strong antifungal activity that the host plant could utilize to ward off pests. It will be of great interest to determine if the putative analogue is also detrimental to plant growth and how overall binding to rapamycin sensitive proteins is affected by structure changes. Certain *Bacillus* spp. are known to be plant growth promoters.¹⁴⁴ Owing to the wide ranging effects of rapamycin on TOR there are many different hypotheses that could be developed to explain rapamycin production by *Bacillus* spp. and the subsequent putative biotransformation product.

The MALDI-IMS challenge experiment demonstrates an important, innovative way to try and understand plant-endophyte relationships and host regulation of endophyte-produced secondary metabolites. *B. thuringiensis* (*Bt*) has been used in the past in agriculture and other applications due to its ability to produce insecticidal proteins.¹⁵ Efforts have been underway to improve production of these proteins and to increase the ability of *Bt* to act as a biopesticide

using genetic manipulation.¹⁴⁵ As mentioned previously, *Bacillus* spp. produce the antifungal lipopeptide iturins and these molecules have proven activity against a number of agricultural pathogens including those associated with powdery mildew and root rot.²⁹ There is a proven link between the level of iturin production from endophytic *Bacillus* spp. and the ability of *Triticum* spp. to fight the fungal infection *Fusarium* head blight.¹⁴⁶ An understanding of how the plant hosts regulate the production of this lipopeptide could be an important component in developing methods to increase the output of iturin production in the field. Understanding host regulation of endophyte-produced natural products is also an important facet of natural product drug research.

Nicotianamine

There has been a general trend in the market place towards all-natural or organic foods.⁶⁵ Food industries that attempt to provide products which are packaged as “all-natural” can encounter significant problems when attempting to prevent long term food spoilage. Ethylenediaminetetraacetic acid (EDTA) is a common metal chelator that is added to food products to prevent spoilage. As a synthetic product, addition of this agent disables food companies of the ability to label their products as all-natural or organic, even if strict protocols to growing all natural or organic foods have been followed.

Nicotianamine is a natural metal chelating agent which presents a viable alternative to EDTA in the food industry. Here, we show that nicotianamine can be obtained from readily available soy flour. This soy flour was easier to manage and contained a higher yield of nicotianamine when compared to a trial that used whole soybeans. In addition, although patented methods contained a variety of methods for nicotianamine purification, here we report that ethanol precipitation after activated carbon treatment was a vastly improved strategy due to lowering the amount of ethanol needed for precipitation. This is particularly important to food

conglomerates which might produce soy products in certain areas of their overall business plan and could use resources that are already available to produce a natural replacement for EDTA.

The Hepatitis C Virus

The hepatitis C virus (HCV) is responsible for chronic hepatitis C, which can lead to cirrhosis of the liver and hepatocellular carcinoma. This is a major health concern as an estimated 130-170 million people worldwide are infected with HCV.⁶⁸ More than 350,000 people die from chronic HCV related diseases annually every year, with an estimated 3-4 million new individuals infected each year.⁶⁸ Co-infection with HIV is also a major concern as this increases the chances of liver disease three fold.⁶⁹

Here, we review natural products that have shown *in vitro* HCV activity. The latest findings on HCV proteins and the HCV life cycle are reviewed as well. The discovery of the HCV virus and the elucidation of its life cycle has happened in relatively recent times. Difficulties in culturing this virus was the major hurdle in discovering the etiologic agent of hepatitis C. These difficulties have largely been overcome and permitted novel screening techniques of natural products against different targets of HCV. As demonstrated in this review, natural products are an important source of active metabolites against new targets for HCV

EXPERIMENTAL SECTION

Glycerol Stocks: There were a total of six glycerol stocks supplied by Dr. Mohammed Ibrahim. Glycerol stock labeled Xf1 was used to make multiple other glycerol stocks by plating 5 μ L of Xf1 glycerol stock on solid agar and allowing it to grow at 36 °C for 48 hours. Colonies were then streaked using sterile technique into 10:5 milliliters of liquid CS20 media. Tubes were shaken for approximately 48 hours at 36 °C at 160 RPM in a New Brunswick Series 25 Incubator Shaker. These cultures were used for creating a total of 30 glycerol stocks by removing 600 μ L of media and adding to Eppendorf tubes and mixing with 400 μ L of 60% glycerol stock solution. Glycerol stocks were placed in Thermo Fisher Scientific -86 °C freezer.

Endophyte isolation: *P. occidentalis* stem material was surface sterilized using 80% EtOH for 4 minutes under bio-hood under sterile conditions. Bio-hood was UV irradiated prior to endophyte isolation. Outer bark was peeled off using knife and forceps that had been soaked in 80% EtOH for ten minutes and flamed. Inner layer of bark tissue and exposed inner stem were placed directly on malt agar. Agar plates were sealed with Parafilm® in bio-hood. Plates were incubated at 36 °C for 48 hours. Bacterial growth emerged directly from exposed stem material. Bacterial colonies growing directly from exposed stem were sub-cultured under sterile conditions. Sub-cultured plates were used to make (10) 5 mL liquid cultures using sterile conditions. 5 mL liquid cultures were shaken at 160 RPM and 36 °C for 24 hours. Glycerol stocks were made by pipetting 600 μ L of liquid culture and 400 μ L of 80% glycerol into Eppendorf tubes. Tubes were placed in -80 °C freezer for storage.

HP-20 extractions: The first step in testing secondary metabolite production was to plate 5 μ L of glycerol stock on solid agar CS20 plates. After 48 hours of growth at 36 °C, cultures were streaked from plates under sterile conditions into 2:5 mL tubes of liquid CS20 media. In the first extraction process, 2:100mL cultures were inoculated using the 5 mL starter cultures. Cultures were removed and sonicated in a Branson 8510 Ultrasonic Cleaner for one hour. Afterwards, cultures were centrifuged in an ThermoIEC Centra CL3R centrifuge for 10 minutes at 4000 RPM. The cell pellet was subsequently discarded. HP-20 Diaion resin beads (10 g) were added to each of the 100 mL flasks and flasks were put back in the shaker for 12 hours. HP-20 beads were filtered using a Buchner funnel and Whatman No. 1 filter paper. The liquid was subsequently discarded and 100 mL of EtOH was passed over beads followed by 100 mL of EtOAc. Note that for all subsequent extractions the amount of liquid used for each solvent was equal to the original amount of culture that was fermented. Each extract was evaporated in a Büchi R-200 Rotavapor in conjunction with a Büchi B-490 heating bath. In order to complete evaporation, samples were placed in a Savant Speed-Vac SC210A in conjunction with an FTS 8L vapor trap.

NPNCR Bioassays: The general procedure was as follows. Crude extracts were tested in a primary screen which used a concentration of 50 μ g/mL and tests extracts in duplicate. Percent inhibitions were calculated relative to positive and negative controls. A total of 5 pathogenic bacteria and 5 pathogenic fungi were used for screening. These include: *C. albicans*, *C. glabrata*, *C. krusei*, *A. fumigatus*, and *C. neoformans* in the fungal category, and: *Staph. aureus*, MRSA, *E. coli*, *P. aeruginosa*, and *M. intracellulare* in the bacterial category. The amount of crude material that was submitted was in the range of 10-90 mg of material. This work was

completed under a grant by NIH, NIAID, Division of AIDS, grant number: AI 27094.

Screenings were performed by Ms. Marsha A. Wright and reported by Dr. Melissa Jacob.

LC-MS. Samples were prepared by dissolving 1 mg of material into 1 mL of MeOH. Samples were run using a 20 μ L injection volume. Method used ran a gradient of 80% H₂O/20% MeOH to 100% MeOH over a period of 24 minutes. Each solvent had 0.05% formic acid added prior to being used with a binary pump.

Challenge Experiment *P. occidentalis* wood was processed into sawdust. Wood was lyophilized using a Labconco® FreeZone 2.5 L Freeze Dry System. This material was then extracted with hexanes, chloroform, and methanol using a total of three extractions for each solvent. The material was then covered with solvent and placed in a Branson 8510 Ultrasonic Cleaner for one hour, filtered through a Buchner funnel, and the solvent evaporated a Büchi rotary evaporator R-200 used in conjunction with a Büchi B-490 heating bath. The same procedure was repeated a second time using the same solvent and the same material. For the third extraction, the same procedure was followed, with the exception that after sonication the material was left in solvent overnight for approximately 24 hours before extraction using the Buchner funnel. Following rotary evaporation, all extracts were placed in a Savant Speed-Vac SC210A in conjunction with an FTS 8L vapor trap to remove solvent. The glycerol stock (5 μ L) was placed in the center of 5 different CS20 solid agar plates. These were then surrounded by the three different *P. occidentalis* extracts on three different sides of the colony. These extracts were re-dissolved in the original solvent with using a pre-calculated volume so that 10 μ L of liquid extract would equal half a milligram of extract. These were placed in such a way so that over the 5 day period, the bacterial colony would expand to eventually come into contact with the extracts. It was important to have the extracts placed sufficiently far away which would

allow for imaging the colony before it reached the extracts but also not too far away which would prevent the colony reaching the extracts in five days.

Genome Assembly *Bacillus* sp. was sequenced by collaborators at University of Maryland and submitted as two fastq files (R1 and R2). Geneious software was used for assembly. Mapping assembly was used with NCBI reference sequence *Bacillus subtilis* NC_000964.3. Sensitivity settings were set to medium.

BIBLIOGRAPHY

1. Nesom, G. American Sycamore. <http://plants.usda.gov/java/factSheet> (accessed January 9).
2. Ibrahim, M. A.; Mansoor, A. A.; Gross, A.; Ashfaq, M. K.; Jacob, M.; Khan, S. I.; Hamann, M. T., Methicillin-resistant *Staphylococcus aureus* (MRSA)-active metabolites from *Platanus occidentalis* (American Sycamore). *Journal of Natural Products* **2009**, *72* (12), 2141-4.
3. Nikolaou, N.; Angelopoulos, K.; Karagiannidis, N., Effects of drought stress on mycorrhizal and non-mycorrhizal cabernet sauvignon grapevine, grafted onto various rootstocks. *Experimental Agriculture* **2003**, *39* (03), 241-252.
4. Zeng, R.-S., Disease resistance in plants through mycorrhizal fungi induced allelochemicals. In *Allelochemicals: Biological Control of Plant Pathogens and Diseases*, Inderjit; Mukerji, K. G., Eds. Springer Netherlands: **2006**; Vol. 2, pp 181-192.
5. Wang, B.; Qiu, Y. L., Phylogenetic distribution and evolution of mycorrhizas in land plants. *Mycorrhiza* **2006**, *16* (5), 299-363.
6. Wilson, D., Endophyte -- the evolution of a term, and clarification of its use and definition. *Oikos* **1995**, *73* (2), 274-276.
7. Crawford, K. M.; Land, J. M.; Rudgers, J. A., Fungal endophytes of native grasses decrease insect herbivore preference and performance. *Oecologia* **2010**, *164* (2), 431-44.
8. Siegel, M. R.; Bush, L. P., Defensive Chemicals in Grass-Fungal Endophyte Associations. In *Phytochemical Diversity and Redundancy in Ecological Interactions*, Romeo, J.; Saunders, J.; Barbosa, P., Eds. Springer US: **1996**; Vol. 30, pp 81-119.
9. Strobel, G. A., Endophytes as sources of bioactive products. *Microbes and Infection* **2003**, *5* (6), 535-544.
10. Claus, D.; Berkely, R., Genus *Bacillus* Cohn 1872. In *Bergey's Manual of Systematic Bacteriology* Sneath, P., Ed. William and Winkins: Baltimore **1986**; pp 1105-1139.
11. Earl, A. M.; Losick, R.; Kolter, R., Ecology and genomics of *Bacillus subtilis*. *Trends in Microbiology* **2008**, *16* (6), 269-75.
12. Zablutowicz, R.; Tipping, E.; Lifshitz, R.; Kloepper, J., Plant growth promotion mediated by bacterial rhizosphere colonizers. In *The Rhizosphere and Plant Growth*, Keister, D.; Cregan, P., Eds. Springer Netherlands: **1991**; Vol. 14, pp 315-326.
13. Hong, H. A.; Khaneja, R.; Tam, N. M. K.; Cazzato, A.; Tan, S.; Urdaci, M.; Brisson, A.; Gasbarrini, A.; Barnes, I.; Cutting, S. M., *Bacillus subtilis* isolated from the human gastrointestinal tract. *Research in Microbiology* **2009**, *160* (2), 134-143.
14. Kunst, F.; Ogasawara, N.; Moszer, I.; Albertini, A. M.; Alloni, G.; Azevedo, V.; Bertero, M. G.; Bessieres, P.; Bolotin, A.; Borchert, S.; Borriss, R.; Boursier, L.; Brans, A.; Braun, M.; Brignell, S. C.; Bron, S.; Brouillet, S.; Bruschi, C. V.; Caldwell, B.; Capuano, V.; Carter, N. M.; Choi, S. K.; Codani, J. J.; Connerton, I. F.; Danchin, A.; et al., The complete genome sequence of the gram-positive bacterium *Bacillus subtilis*. *Nature* **1997**, *390* (6657), 249-56.
15. Schnepf, E.; Crickmore, N.; Van Rie, J.; Lereclus, D.; Baum, J.; Feitelson, J.; Zeigler, D. R.; Dean, D. H., *Bacillus thuringiensis* and its pesticidal crystal proteins. *Microbiol Mol Biol Rev* **1998**, *62* (3), 775-806.
16. Chen, X. H.; Koumoutsi, A.; Scholz, R.; Eisenreich, A.; Schneider, K.; Heinemeyer, I.; Morgenstern, B.; Voss, B.; Hess, W. R.; Reva, O.; Junge, H.; Voigt, B.; Jungblut, P. R.; Vater, J.; Sussmuth, R.; Liesegang, H.; Strittmatter, A.; Gottschalk, G.; Borriss, R., Comparative analysis of the complete genome sequence of the plant growth-promoting bacterium *Bacillus amyloliquefaciens* FZB42. *Nat Biotechnol* **2007**, *25* (9), 1007-14.

17. Sansinenea, E.; Ortiz, A., Secondary metabolites of soil *Bacillus* spp. *Biotechnol Lett* **2011**, *33* (8), 1523-38.
18. Pattnaik, P.; Kaushik, J. K.; Grover, S.; Batish, V. K., Purification and characterization of a bacteriocin-like compound (Lichenin) produced anaerobically by *Bacillus licheniformis* isolated from water buffalo. *J Appl Microbiol* **2001**, *91* (4), 636-45.
19. Le Marrec, C.; Hyronimus, B.; Bressollier, P.; Verneuil, B.; Urdaci, M. C., Biochemical and genetic characterization of coagulatin, a new antilisterial bacteriocin in the pediocin family of bacteriocins, produced by *Bacillus coagulans* I(4). *Applied and Environmental Microbiology* **2000**, *66* (12), 5213-20.
20. Lee, K. H.; Jun, K. D.; Kim, W. S.; Paik, H. D., Partial characterization of polyfermentacin SCD, a newly identified bacteriocin of *Bacillus polyfermenticus*. *Letters in Applied Microbiology* **2001**, *32* (3), 146-51.
21. Willey, J. M.; van der Donk, W. A., Lantibiotics: peptides of diverse structure and function. *Annu Rev Microbiol* **2007**, *61*, 477-501.
22. Stein, T., *Bacillus subtilis* antibiotics: structures, syntheses and specific functions. *Mol Microbiol* **2005**, *56* (4), 845-57.
23. Salle, A. J.; Jann, G. J., Subtilin-an antibiotic produced by *Bacillus subtilis*. I. action on various organisms. *Experimental Biology and Medicine* **1945**, *60* (1), 60-64.
24. Raaijmakers, J. M.; De Bruijn, I.; Nybroe, O.; Ongena, M., Natural functions of lipopeptides from *Bacillus* and *Pseudomonas*: more than surfactants and antibiotics. *FEMS Microbiology Reviews* **2010**, *34* (6), 1037-1062.
25. Cameotra, S. S.; Makkar, R. S., Recent applications of biosurfactants as biological and immunological molecules. *Curr Opin Microbiol* **2004**, *7* (3), 262-6.
26. Pirri, G.; Giuliani, A.; Nicoletto, S.; Pizzuto, L.; Rinaldi, A., Lipopeptides as anti-infectives: a practical perspective. *cent.eur.j.biol.* **2009**, *4* (3), 258-273.
27. Arima, K.; Kakinuma, A.; Tamura, G., Surfactin, a crystalline peptidolipid surfactant produced by *Bacillus subtilis*: Isolation, characterization and its inhibition of fibrin clot formation. *Biochemical and Biophysical Research Communications* **1968**, *31* (3), 488-494.
28. Carrillo, C.; Teruel, J. A.; Aranda, F. J.; Ortiz, A., Molecular mechanism of membrane permeabilization by the peptide antibiotic surfactin. *Biochim Biophys Acta* **2003**, *1611* (1-2), 91-7.
29. Romero, D.; de Vicente, A.; Rakotoaly, R. H.; Dufour, S. E.; Veenig, J.-W.; Arrebola, E.; Cazorla, F. M.; Kuipers, O. P.; Paquot, M.; Pérez-García, A., The iturin and fengycin families of lipopeptides are key factors in antagonism of *Bacillus subtilis* toward *Podospaera fusca*. *Molecular Plant-Microbe Interactions* **2007**, *20* (4), 430-440.
30. Asaka, O.; Shoda, M., Biocontrol of *Rhizoctonia solani* Damping-Off of Tomato with *Bacillus subtilis* RB14. *Applied and Environmental Microbiology* **1996**, *62* (11), 4081-5.
31. Emmert, E. A. B.; Handelsman, J., Biocontrol of plant disease: a (Gram-) positive perspective. *FEMS Microbiology Letters* **1999**, *171* (1), 1-9.
32. Vanittanakom, N.; Loeffler, W.; Koch, U.; Jung, G., Fengycin--a novel antifungal lipopeptide antibiotic produced by *Bacillus subtilis* F-29-3. *J Antibiot (Tokyo)* **1986**, *39* (7), 888-901.
33. Wilson, K. E.; Flor, J. E.; Schwartz, R. E.; Joshua, H.; Smith, J. L.; Pelak, B. A.; Liesch, J. M.; Hensens, O. D., Difficidin and oxydifficidin: novel broad spectrum antibacterial antibiotics produced by *Bacillus subtilis*. Isolation and physico-chemical characterization. *J Antibiot (Tokyo)* **1987**, *40* (12), 1682-91.

34. Chen, X. H.; Scholz, R.; Borriss, M.; Junge, H.; Mogel, G.; Kunz, S.; Borriss, R., Difficidin and bacilysin produced by plant-associated *Bacillus amyloliquefaciens* are efficient in controlling fire blight disease. *Journal of Biotechnology* **2009**, *140* (1-2), 38-44.
35. Patel, P. S.; Huang, S.; Fisher, S.; Pirnik, D.; Aklonis, C.; Dean, L.; Meyers, E.; Fernandes, P.; Mayerl, F., Bacillaene, a novel inhibitor of procaryotic protein synthesis produced by *Bacillus subtilis*: production, taxonomy, isolation, physico-chemical characterization and biological activity. *J Antibiot (Tokyo)* **1995**, *48* (9), 997-1003.
36. Butcher, R. A.; Schroeder, F. C.; Fischbach, M. A.; Straight, P. D.; Kolter, R.; Walsh, C. T.; Clardy, J., The identification of bacillaene, the product of the PksX megacomplex in *Bacillus subtilis*. *Proc Natl Acad Sci U S A* **2007**, *104* (5), 1506-9.
37. Gustafson, K.; Roman, M.; Fenical, W., The macrolactins, a novel class of antiviral and cytotoxic macrolides from a deep-sea marine bacterium. *Journal of the American Chemical Society* **1989**, *111* (19), 7519-7524.
38. Romero-Tabarez, M.; Jansen, R.; Sylla, M.; Lünsdorf, H.; Häussler, S.; Santosa, D. A.; Timmis, K. N.; Molinari, G., 7-O-malonyl macrolactin A, a new macrolactin antibiotic from *Bacillus subtilis* active against methicillin-resistant *Staphylococcus aureus*, vancomycin-resistant enterococci, and a small-colony variant of *Burkholderia cepacia*. *Antimicrob Agents Chemother* **2006**, *50* (5), 1701-1709.
39. Sohn, M. J.; Zheng, C. J.; Kim, W. G., Macrolactin S, a new antibacterial agent with FabG-inhibitory activity from *Bacillus* sp. AT28. *J Antibiot (Tokyo)* **2008**, *61* (11), 687-91.
40. Vezina, C.; Kudelski, A.; Sehgal, S. N., Rapamycin (AY-22,989), a new antifungal antibiotic. I. Taxonomy of the producing streptomycete and isolation of the active principle. *J Antibiot (Tokyo)* **1975**, *28* (10), 721-6.
41. Sehgal, S. N.; Baker, H.; Vezina, C., Rapamycin (AY-22,989), a new antifungal antibiotic. II. Fermentation, isolation and characterization. *J Antibiot (Tokyo)* **1975**, *28* (10), 727-32.
42. Houchens, D. P.; Ovejera, A. A.; Riblet, S. M.; Slagel, D. E., Human brain tumor xenografts in nude mice as a chemotherapy model. *European Journal of Cancer and Clinical Oncology* **1983**, *19* (6), 799-805.
43. Thomson, A. W.; Turnquist, H. R.; Raimondi, G., Immunoregulatory functions of mTOR inhibition. *Nature Reviews Immunology* **2009**, *9* (5), 324-37.
44. Heitman, J.; Movva, N.; Hall, M., Targets for cell cycle arrest by the immunosuppressant rapamycin in yeast. *Science* **1991**, *253* (5022), 905-909.
45. Loewith, R., A brief history of TOR. *Biochem Soc Trans* **2011**, *39* (2), 437-42.
46. Loewith, R.; Jacinto, E.; Wullschleger, S.; Lorberg, A.; Crespo, J. L.; Bonenfant, D.; Oppliger, W.; Jenoe, P.; Hall, M. N., Two TOR complexes, only one of which is rapamycin sensitive, have distinct roles in cell growth control. *Mol Cell* **2002**, *10* (3), 457-68.
47. Wedaman, K. P.; Reinke, A.; Anderson, S.; Yates, J., 3rd; McCaffery, J. M.; Powers, T., Tor kinases are in distinct membrane-associated protein complexes in *Saccharomyces cerevisiae*. *Mol Biol Cell* **2003**, *14* (3), 1204-20.
48. Wullschleger, S.; Loewith, R.; Hall, M. N., TOR signaling in growth and metabolism. *Cell* **2006**, *124* (3), 471-484.
49. Xiong, Y.; Sheen, J., Rapamycin and glucose-target of rapamycin (TOR) protein signaling in plants. *J Biol Chem* **2012**, *287* (4), 2836-42.
50. Xiao, W.; Sheen, J.; Jang, J. C., The role of hexokinase in plant sugar signal transduction and growth and development. *Plant Mol Biol* **2000**, *44* (4), 451-61.

51. Xiong, Y.; McCormack, M.; Li, L.; Hall, Q.; Xiang, C.; Sheen, J., Glucose-TOR signalling reprograms the transcriptome and activates meristems. *Nature* **2013**, *496* (7444), 181-6.
52. Harrison, D. E.; Strong, R.; Sharp, Z. D.; Nelson, J. F.; Astle, C. M.; Flurkey, K.; Nadon, N. L.; Wilkinson, J. E.; Frenkel, K.; Carter, C. S.; Pahor, M.; Javors, M. A.; Fernandez, E.; Miller, R. A., Rapamycin fed late in life extends lifespan in genetically heterogeneous mice. *Nature* **2009**, *460* (7253), 392-5.
53. Saunders, R. N.; Metcalfe, M. S.; Nicholson, M. L., Rapamycin in transplantation: a review of the evidence. *Kidney Int* **2001**, *59* (1), 3-16.
54. Pazdur, R. FDA Approval for Everolimus.
<http://www.cancer.gov/cancertopics/druginfo/fda-everolimus> (accessed June 23, 2014).
55. Pazdur, R. FDA Approval for Temsirolimus
<http://www.cancer.gov/cancertopics/druginfo/fda-temsirolimus> (accessed June 23).
56. Sanders, M. E.; Dias, E. C.; Xu, B. J.; Mobley, J. A.; Billheimer, D.; Roder, H.; Grigorieva, J.; Dowsett, M.; Arteaga, C. L.; Caprioli, R. M., Differentiating Proteomic Biomarkers in Breast Cancer by Laser Capture Microdissection and MALDI MS. *Journal of Proteome Research* **2008**, *7* (4), 1500-1507.
57. Castellino, S.; Groseclose, M. R.; Wagner, D., MALDI imaging mass spectrometry: bridging biology and chemistry in drug development. *Bioanalysis* **2011**, *3* (21), 2427-41.
58. Zaima, N.; Hayasaka, T.; Goto-Inoue, N.; Setou, M., Matrix-assisted laser desorption/ionization imaging mass spectrometry. *International Journal of Molecular Sciences* **2010**, *11* (12), 5040-5055.
59. Takahashi, M.; Terada, Y.; Nakai, I.; Nakanishi, H.; Yoshimura, E.; Mori, S.; Nishizawa, N. K., Role of nicotianamine in the intracellular delivery of metals and plant reproductive development. *The Plant Cell Online* **2003**, *15* (6), 1263-1280.
60. von Wiren, N.; Klair, S.; Bansal, S.; Briat, J. F.; Khodr, H.; Shioiri, T.; Leigh, R. A.; Hider, R. C., Nicotianamine chelates both FeIII and FeII. Implications for metal transport in plants. *Plant Physiol* **1999**, *119* (3), 1107-14.
61. Hayashi, A.; Kimoto, K., Nicotianamine preferentially inhibits angiotensin I-converting enzyme. *Journal of Nutritional Science and Vitaminology* **2007**, *53* (4), 331-336.
62. West, L.; Dinwoodie, R.; Tsui, I. Oxidation stability using natural antioxidants. 2011.
63. Noma, M.; Noguchi, M., Occurrence of nicotianamine in higher plants. *Phytochemistry* **1976**, *15* (11), 1701-1702.
64. Asai, S.; Obata, A.; Yamazaki, E.; Kinoshita, E.; Kikuchi, M. Method for preparing nicotianamine or nicotianamine-containing product. 2005.
65. Greene, C. Growth Patterns in the U.S. Organic Industry.
<http://www.ers.usda.gov/amber-waves/2013-october/growth-patterns-in-the-us-organic-industry.aspx> - .U7LQwlaXcda (accessed June 28).
66. Higuchi, K.; Watanabe, S.; Takahashi, M.; Kawasaki, S.; Nakanishi, H.; Nishizawa, N. K.; Mori, S., Nicotianamine synthase gene expression differs in barley and rice under Fe-deficient conditions. *The Plant Journal* **2001**, *25* (2), 159-167.
67. Pianelli, K.; Mari, S.; Marques, L.; Lebrun, M.; Czernic, P., Nicotianamine over-accumulation confers resistance to nickel in *Arabidopsis thaliana*. *Transgenic Research* **2005**, *14* (5), 739-748.
68. WHO Hepatitis C Fact Sheet
<http://www.who.int/mediacentre/factsheets/fs164/en/> (accessed February 10, 2012).

69. CDC <http://www.cdc.gov/hepatitis/Populations/hiv.htm> (accessed June 12).
70. Bare, P., Hepatitis C virus and peripheral blood mononuclear cell reservoirs. *World J Hepatol* **2009**, *1* (1), 67-71.
71. Houghton, M., The long and winding road leading to the identification of the hepatitis C virus. *Journal of Hepatology* **2009**, *51* (5), 939-948.
72. Choo, Q.; Kuo, G.; Weiner, A.; Overby, L.; Bradley, D.; Houghton, M., Isolation of a cDNA clone derived from a blood-borne non-A, non-B viral hepatitis genome. *Science* **1989**, *244* (4902), 359-362.
73. Grakoui, A.; Wychowski, C.; Lin, C.; Feinstone, S. M.; Rice, C. M., Expression and identification of hepatitis C virus polyprotein cleavage products. *J Virol* **1993**, *67* (3), 1385-1395.
74. Kolykhalov, A. A.; Agapov, E. V.; Blight, K. J.; Mihalik, K.; Feinstone, S. M.; Rice, C. M., Transmission of hepatitis C by intrahepatic inoculation with transcribed RNA. *Science* **1997**, *277* (5325), 570-574.
75. Bartosch, B.; Dubuisson, J.; Cosset, F.-L., Infectious hepatitis C virus pseudo-particles containing functional E1-E2 envelope protein complexes. *J Exp Med* **2003**, *197* (5), 633-642.
76. Zhong, J.; Gastaminza, P.; Cheng, G.; Kapadia, S.; Kato, T.; Burton, D. R.; Wieland, S. F.; Uprichard, S. L.; Wakita, T.; Chisari, F. V., Robust hepatitis C virus infection in vitro. *Proc Natl Acad Sci U S A* **2005**, *102* (26), 9294-9299.
77. Porrás-Alfaro, A.; Bayman, P., Hidden fungi, emergent properties: endophytes and microbiomes. *Annual Review of Phytopathology* **2011**, *49*, 291-315.
78. Rosenblueth, M.; Martínez-Romero, E., Bacterial endophytes and their interactions with hosts. *Molecular Plant-Microbe Interactions* **2006**, *19* (8), 827-837.
79. Kusari, S.; Hertweck, C.; Spiteller, M., Chemical ecology of endophytic fungi: origins of secondary metabolites. *Chem Biol* **2012**, *19* (7), 792-798.
80. Strobel, G.; Daisy, B.; Castillo, U.; Harper, J., Natural products from endophytic microorganisms. *Journal of Natural Products* **2004**, *67* (2), 257-268.
81. Barbe, V.; Cruveiller, S.; Kunst, F.; Lenoble, P.; Meurice, G.; Sekowska, A.; Vallenet, D.; Wang, T.; Moszer, I.; Medigue, C.; Danchin, A., From a consortium sequence to a unified sequence: the *Bacillus subtilis* 168 reference genome a decade later. *Microbiology* **2009**, *155* (Pt 6), 1758-75.
82. Biomatters *Geneious*, R7, available at: <http://www.geneious.com/>
83. Chang, C. J.; Walker, J. T., Bacterial leaf scorch of northern red oak: isolation, cultivation, and pathogenicity of a xylem-limited bacterium. *Plant Disease* **1988**, *72* (8), 730-733.
84. Kendrew, S. G.; Petkovic, H.; Gaisser, S.; Ready, S. J.; Gregory, M. A.; Coates, N. J.; Nur, E. A. M.; Warneck, T.; Suthar, D.; Foster, T. A.; McDonald, L.; Schlingman, G.; Koehn, F. E.; Skotnicki, J. S.; Carter, G. T.; Moss, S. J.; Zhang, M. Q.; Martin, C. J.; Sheridan, R. M.; Wilkinson, B., Recombinant strains for the enhanced production of bioengineered rapalogs. *Metab Eng* **2013**, *15*, 167-73.
85. Leite, B.; Andersen, P. C.; Ishida, M. L., Colony aggregation and biofilm formation in xylem chemistry-based media for *Xylella fastidiosa*. *FEMS Microbiology Letters* **2004**, *230* (2), 283-290.
86. Frisvad, J. C., Media and growth conditions for induction of secondary metabolite production. *Methods Mol Biol* **2012**, *944*, 47-58.

87. Ruiz, B.; Chavez, A.; Forero, A.; Garcia-Huante, Y.; Romero, A.; Sanchez, M.; Rocha, D.; Sanchez, B.; Rodriguez-Sanoja, R.; Sanchez, S.; Langley, E., Production of microbial secondary metabolites: regulation by the carbon source. *Crit Rev Microbiol* **2010**, *36* (2), 146-67.
88. Ongena, M.; Jacques, P.; Toure, Y.; Destain, J.; Jabrane, A.; Thonart, P., Involvement of fengycin-type lipopeptides in the multifaceted biocontrol potential of *Bacillus subtilis*. *Appl Microbiol Biotechnol* **2005**, *69* (1), 29-38.
89. Sang-Cheol, L.; Kim, S.-H.; Park, I.-H.; Chung, S.-Y.; Chandra, M. S.; Yong-Lark, C., Isolation, purification, and characterization of novel fengycin S from *Bacillus amyloliquefaciens* LSC04 degrading-crude oil. *Biotechnol Bioproc E* **2010**, *15* (2), 246-253.
90. Li, X. Y.; Mao, Z. C.; Wang, Y. H.; Wu, Y. X.; He, Y. Q.; Long, C. L., ESI LC-MS and MS/MS characterization of antifungal cyclic lipopeptides produced by *Bacillus subtilis* XF-1. *J Mol Microbiol Biotechnol* **2012**, *22* (2), 83-93.
91. Ongena, M.; Jacques, P., Bacillus lipopeptides: versatile weapons for plant disease biocontrol. *Trends in Microbiology* **2008**, *16* (3), 115-25.
92. Esquenazi, E.; Yang, Y.-L.; Watrous, J.; Gerwick, W. H.; Dorrestein, P. C., Imaging mass spectrometry of natural products. *Natural Product Reports* **2009**, *26* (12), 1521-1534.
93. Sugiura, Y.; Shimma, S.; Setou, M., Thin sectioning improves the peak intensity and signal-to-noise ratio in direct tissue mass spectrometry. *Journal of the Mass Spectrometry Society of Japan* **2006**, *54* (2), 45-48.
94. McHutchison, J. G.; Gordon, S. C.; Schiff, E. R.; Shiffman, M. L.; Lee, W. M.; Rustgi, V. K.; Goodman, Z. D.; Ling, M.-H.; Cort, S.; Albrecht, J. K., Interferon alfa-2b alone or in combination with ribavirin as initial treatment for chronic hepatitis C. *New England Journal of Medicine* **1998**, *339* (21), 1485-1492.
95. McHutchison, J. G.; Everson, G. T.; Gordon, S. C.; Jacobson, I. M.; Sulkowski, M.; Kauffman, R.; McNair, L.; Alam, J.; Muir, A. J., Telaprevir with peginterferon and ribavirin for chronic HCV genotype 1 infection. *New England Journal of Medicine* **2009**, *360* (18), 1827-1838.
96. Benhamou, Y.; Moussalli, J.; Ratziu, V.; Lebray, P.; Gysen, V.; de Backer, K.; Ghys, A.; van Heeswijk, R.; Vangeneugden, T.; Picchio, G.; Beumont-Mauviel, M., 10 results of a proof of concept study (C210) of telaprevir monotherapy and in combination with peginterferon alfa-2a and ribavirin in treatment-naïve genotype 4 HCV patients. *Journal of Hepatology* **2009**, *50*, Supplement 1 (0), S6.
97. Cooper, C.; Lawitz, E. J.; Ghali, P.; Rodriguez-Torres, M.; Anderson, F. H.; Lee, S. S.; Bédard, J.; Chauret, N.; Thibert, R.; Boivin, I.; Nicolas, O.; Proulx, L., Evaluation of VCH-759 monotherapy in hepatitis C infection. *Journal of Hepatology* **2009**, *51* (1), 39-46.
98. FDA Olysio (simeprevir) for the treatment of chronic hepatitis C in combination antiviral treatment.
<http://www.fda.gov/forconsumers/byaudience/forpatientadvocates/ucm377234.htm>
(accessed June 23).
99. FDA Approval of sovaldi (sofosbuvir) tablets for the treatment of chronic hepatitis C
<http://www.fda.gov/forconsumers/byaudience/forpatientadvocates/ucm377920.htm>
(accessed June 24).
100. Zeuzem, S.; Berg, T.; Gane, E.; Ferenci, P.; Foster, G. R.; Fried, M. W.; Hezode, C.; Hirschfield, G. M.; Jacobson, I.; Nikitin, I.; Pockros, P. J.; Poordad, F.; Scott, J.; Lenz, O.; Peeters, M.; Sekar, V.; De Smedt, G.; Sinha, R.; Beumont-Mauviel, M., Simeprevir Increases

Rate of Sustained Virologic Response Among Treatment-Experienced Patients With HCV Genotype-1 Infection: A Phase IIb Trial. *Gastroenterology* **2013**, *146* (2), 430-441.e6.

101. Lawitz, E.; Mangia, A.; Wyles, D.; Rodriguez-Torres, M.; Hassanein, T.; Gordon, S. C.; Schultz, M.; Davis, M. N.; Kayali, Z.; Reddy, K. R.; Jacobson, I. M.; Kowdley, K. V.; Nyberg, L.; Subramanian, G. M.; Hyland, R. H.; Arterburn, S.; Jiang, D.; McNally, J.; Brainard, D.; Symonds, W. T.; McHutchison, J. G.; Sheikh, A. M.; Younossi, Z.; Gane, E. J., Sofosbuvir for previously untreated chronic hepatitis C infection. *New England Journal of Medicine* **2013**, *368* (20), 1878-1887.

102. Lawitz, E.; Poordad, F. F.; Pang, P. S.; Hyland, R. H.; Ding, X.; Mo, H.; Symonds, W. T.; McHutchison, J. G.; Membreno, F. E., Sofosbuvir and ledipasvir fixed-dose combination with and without ribavirin in treatment-naïve and previously treated patients with genotype 1 hepatitis C virus infection (LONESTAR): an open-label, randomised, phase 2 trial. *The Lancet* **2014**, *383* (9916), 515-523.

103. Vieyres, G.; Thomas, X.; Descamps, V.; Duverlie, G.; Patel, A. H.; Dubuisson, J., Characterization of the envelope glycoproteins associated with infectious hepatitis C virus. *J Virol* **2010**, *84* (19), 10159-68.

104. Agnello, V.; Ábel, G.; Elfahal, M.; Knight, G. B.; Zhang, Q.-X., Hepatitis C virus and other Flaviviridae viruses enter cells via low density lipoprotein receptor. *Proceedings of the National Academy of Sciences* **1999**, *96* (22), 12766-12771.

105. Akazawa, D.; Date, T.; Morikawa, K.; Murayama, A.; Miyamoto, M.; Kaga, M.; Barth, H.; Baumert, T. F.; Dubuisson, J.; Wakita, T., CD81 expression is important for the permissiveness of Huh7 cell clones for heterogeneous hepatitis C virus infection. *J Virol* **2007**, *81* (10), 5036-5045.

106. Zeisel, M. B.; Koutsoudakis, G.; Schnober, E. K.; Haberstroh, A.; Blum, H. E.; Cosset, F.-L.; Wakita, T.; Jaeck, D.; Doffoel, M.; Royer, C.; Soulier, E.; Schvoerer, E.; Schuster, C.; Stoll-Keller, F.; Bartenschlager, R.; Pietschmann, T.; Barth, H.; Baumert, T. F., Scavenger receptor class B type I is a key host factor for hepatitis C virus infection required for an entry step closely linked to CD81. *Hepatology* **2007**, *46* (6), 1722-1731.

107. Harris, H. J.; Davis, C.; Mullins, J. G. L.; Hu, K.; Goodall, M.; Farquhar, M. J.; Mee, C. J.; McCaffrey, K.; Young, S.; Drummer, H.; Balfe, P.; McKeating, J. A., Claudin association with CD81 defines hepatitis C virus entry. *Journal of Biological Chemistry* **2010**, *285* (27), 21092-21102.

108. Tsukiyama-Kohara, K.; Iizuka, N.; Kohara, M.; Nomoto, A., Internal ribosome entry site within hepatitis C virus RNA. *J Virol* **1992**, *66* (3), 1476-1483.

109. Otto, G. A.; Puglisi, J. D., The pathway of HCV IRES-mediated translation initiation. *Cell* **2004**, *119* (3), 369-380.

110. Moradpour, D.; Penin, F.; Rice, C. M., Replication of hepatitis C virus. *Nature Reviews Microbiology* **2007**, *5* (6), 453-63.

111. McLauchlan, J.; Lemberg, M. K.; Hope, G.; Martoglio, B., Intramembrane proteolysis promotes trafficking of hepatitis C virus core protein to lipid droplets. *EMBO Journal* **2002**, *21* (15), 3980-3988.

112. Choukhi, A.; Ung, S.; Wychowski, C.; Dubuisson, J., Involvement of endoplasmic reticulum chaperones in the folding of hepatitis C virus glycoproteins. *J Virol* **1998**, *72* (5), 3851-3858.

113. Sakai, A.; Claire, M. S.; Faulk, K.; Govindarajan, S.; Emerson, S. U.; Purcell, R. H.; Bukh, J., The p7 polypeptide of hepatitis C virus is critical for infectivity and contains

- functionally important genotype-specific sequences. *Proceedings of the National Academy of Sciences* **2003**, *100* (20), 11646-11651.
114. Wozniak, A. L.; Griffin, S.; Rowlands, D.; Harris, M.; Yi, M.; Lemon, S. M.; Weinman, S. A., Intracellular proton conductance of the hepatitis C virus p7 protein and its contribution to infectious virus production. *PLoS Pathogens* **2010**, *6* (9), e1001087.
115. Grakoui, A.; McCourt, D. W.; Wychowski, C.; Feinstone, S. M.; Rice, C. M., Characterization of the hepatitis C virus-encoded serine proteinase: determination of proteinase-dependent polyprotein cleavage sites. *J Virol* **1993**, *67* (5), 2832-2843.
116. Egger, D.; Wölk, B.; Gosert, R.; Bianchi, L.; Blum, H. E.; Moradpour, D.; Bienz, K., Expression of hepatitis C virus proteins induces distinct membrane alterations including a candidate viral replication complex. *J Virol* **2002**, *76* (12), 5974-5984.
117. Huang, L.; Hwang, J.; Sharma, S. D.; Hargittai, M. R. S.; Chen, Y.; Arnold, J. J.; Raney, K. D.; Cameron, C. E., Hepatitis C virus nonstructural protein 5A (NS5A) is an RNA-binding protein. *Journal of Biological Chemistry* **2005**, *280* (43), 36417-36428.
118. Lan, K.-H.; Lan, K.-L.; Lee, W.-P.; Sheu, M.-L.; Chen, M.-Y.; Lee, Y.-L.; Yen, S.-H.; Chang, F.-Y.; Lee, S.-D., HCV NS5A inhibits interferon-alpha signaling through suppression of STAT1 phosphorylation in hepatocyte-derived cell lines. *Journal of Hepatology* **2007**, *46* (5), 759-767.
119. Shi, S. T.; Polyak, S. J.; Tu, H.; Taylor, D. R.; Gretch, D. R.; Lai, M. M. C., Hepatitis C virus NS5A colocalizes with the core protein on lipid droplets and interacts with apolipoproteins. *Virology* **2002**, *292* (2), 198-210.
120. Bartenschlager, R.; Penin, F.; Lohmann, V.; André, P., Assembly of infectious hepatitis C virus particles. *Trends in Microbiology* **2011**, *19* (2), 95-103.
121. Gastaminza, P.; Cheng, G.; Wieland, S.; Zhong, J.; Liao, W.; Chisari, F. V., Cellular determinants of hepatitis C virus assembly, maturation, degradation, and secretion. *J Virol* **2008**, *82* (5), 2120-9.
122. Chang, K.-S.; Jiang, J.; Cai, Z.; Luo, G., Human apolipoprotein E is required for infectivity and production of hepatitis C virus in cell culture. *J Virol* **2007**, *81* (24), 13783-13793.
123. Parent, R.; Qu, X.; Petit, M. A.; Beretta, L., The heat shock cognate protein 70 is associated with hepatitis C virus particles and modulates virus infectivity. *Hepatology* **2009**, *49* (6), 1798-809.
124. Backes, P.; Quinkert, D.; Reiss, S.; Binder, M.; Zayas, M.; Rescher, U.; Gerke, V.; Bartenschlager, R.; Lohmann, V., Role of annexin A2 in the production of infectious hepatitis C virus particles. *J Virol* **2010**, *84* (11), 5775-89.
125. Herker, E.; Harris, C.; Hernandez, C.; Carpentier, A.; Kaehlcke, K.; Rosenberg, A. R.; Farese, R. V., Jr.; Ott, M., Efficient hepatitis C virus particle formation requires diacylglycerol acyltransferase-1. *Nature Medicine* **2010**, *16* (11), 1295-8.
126. Salah El Dine, R.; Abdel Monem, A. R.; El-Halawany, A. M.; Hattori, M.; Abdel-Sattar, E., HCV-NS3/4A protease inhibitory iridoid glucosides and dimeric foliamenthic acid derivatives from *Anarrhinum orientale*. *Journal of Natural Products* **2011**, *74* (5), 943-8.
127. Lee, H. Y.; Yum, J. H.; Rho, Y. K.; Oh, S. J.; Choi, H. S.; Chang, H. B.; Choi, D. H.; Leem, M. J.; Choi, E. J.; Ryu, J. M.; Hwang, S. B., Inhibition of HCV replicon cell growth by 2-arylbenzofuran derivatives isolated from mori cortex radicis. *Planta Med* **2007**, *73* (14), 1481-5.

128. Hu, J.-F.; Patel, R.; Li, B.; Garo, E.; Hough, G. W.; Goering, M. G.; Yoo, H.-D.; O'Neil-Johnson, M.; Eldridge, G. R., Anti-HCV bioactivity of pseudoguaianolides from *Parthenium hispidum*. *Journal of Natural Products* **2007**, *70* (4), 604-607.
129. Chen, X.; Yang, L.; Zhang, N.; Turpin, J. A.; Buckheit, R. W.; Osterling, C.; Oppenheim, J. J.; Howard, O. M. Z., Shikonin, a component of Chinese herbal medicine, inhibits chemokine receptor function and suppresses human immunodeficiency virus type 1. *Antimicrob Agents Chemother* **2003**, *47* (9), 2810-2816.
130. Li, H. M.; Tang, Y. L.; Zhang, Z. H.; Liu, C. J.; Li, H. Z.; Li, R. T.; Xia, X. S., Compounds from *Arnebia euchroma* and their related anti-HCV and antibacterial activities. *Planta Med* **2012**, *78* (1), 39-45.
131. Wang, Y. J.; Pan, K. L.; Hsieh, T. C.; Chang, T. Y.; Lin, W. H.; Hsu, J. T., Diosgenin, a plant-derived saponin, exhibits antiviral activity in vitro against hepatitis C virus. *Journal of Natural Products* **2011**, *74* (4), 580-4.
132. Hussein, G.; Miyashiro, H.; Nakamura, N.; Hattori, M.; Kakiuchi, N.; Shimotohno, K., Inhibitory effects of sudanese medicinal plant extracts on hepatitis C virus (HCV) protease. *Phytotherapy Research* **2000**, *14* (7), 510-6.
133. Hegde, V. R.; Pu, H.; Patel, M.; Das, P. R.; Butkiewicz, N.; Arreaza, G.; Gullo, V. P.; Chan, T. M., Two antiviral compounds from the plant *Stylogne cauliflora* as inhibitors of HCV NS3 protease. *Bioorg Med Chem Lett* **2003**, *13* (17), 2925-8.
134. Chu, M.; Mierzwa, R.; Truumees, I.; King, A.; Patel, M.; Berrie, R.; Hart, A.; Butkiewicz, N.; DasMahapatra, B.; Chan, T.-M.; Puar, M. S., Structure of Sch 68631: A new hepatitis C virus proteinase inhibitor from *Streptomyces* sp. *Tetrahedron Letters* **1996**, *37* (40), 7229-7232.
135. Chu, M.; Mierzwa, R.; He, L.; King, A.; Patel, M.; Pichardo, J.; Hart, A.; Butkiewicz, N.; Puar, M. S., Isolation and structure of SCH 351633: a novel hepatitis C virus (HCV) NS3 protease inhibitor from the fungus *Penicillium griseofulvum*. *Bioorganic & Medicinal Chemistry Letters* **1999**, *9* (14), 1949-52.
136. Salam, K. A.; Furuta, A.; Noda, N.; Tsuneda, S.; Sekiguchi, Y.; Yamashita, A.; Moriishi, K.; Nakakoshi, M.; Tsubuki, M.; Tani, H.; Tanaka, J.; Akimitsu, N., Inhibition of hepatitis C virus NS3 helicase by manoalide. *Journal of Natural Products* **2012**, *75* (4), 650-4.
137. Na, M.; Ding, Y.; Wang, B.; Tekwani, B. L.; Schinazi, R. F.; Franzblau, S.; Kelly, M.; Stone, R.; Li, X. C.; Ferreira, D.; Hamann, M. T., Anti-infective discorhabdins from a deep-water Alaskan sponge of the genus *Latrunculia*. *Journal of Natural Products* **2010**, *73* (3), 383-7.
138. Herre, E. A.; Mejía, L. C.; Kyllö, D. A.; Rojas, E.; Maynard, Z.; Butler, A.; Van Bael, S. A., Ecological implications of anti-pathogen effects of tropical fungal endophytes and mycorrhizae. *Ecology* **2007**, *88* (3), 550-558.
139. Rodriguez, R. J.; Freeman, D. C.; McArthur, E. D.; Kim, Y. O.; Redman, R. S., Symbiotic regulation of plant growth, development and reproduction. *Commun Integr Biol* **2009**, *2* (2), 141-3.
140. Hubbard, M.; Germida, J. J.; Vujanovic, V., Fungal endophytes enhance wheat heat and drought tolerance in terms of grain yield and second-generation seed viability. *J Appl Microbiol* **2014**, *116* (1), 109-22.
141. Loewith, R.; Hall, M. N., Target of rapamycin (TOR) in nutrient signaling and growth control. *Genetics* **2011**, *189* (4), 1177-201.

142. Newman, D. J.; Cragg, G. M., Natural products as sources of new drugs over the 30 years from 1981 to 2010. *Journal of Natural Products* **2012**, 75 (3), 311-335.
143. Seyedsayamdost, M. R., High-throughput platform for the discovery of elicitors of silent bacterial gene clusters. *Proceedings of the National Academy of Sciences* **2014**.
144. Nautiyal, C. S.; Srivastava, S.; Chauhan, P. S.; Seem, K.; Mishra, A.; Sopory, S. K., Plant growth-promoting bacteria *Bacillus amyloliquefaciens* NBRISN13 modulates gene expression profile of leaf and rhizosphere community in rice during salt stress. *Plant Physiology and Biochemistry* **2013**, 66, 1-9.
145. Sansinenea, E.; Vazquez, C.; Ortiz, A., Genetic manipulation in *Bacillus thuringiensis* for strain improvement. *Biotechnol Lett* **2010**, 32 (11), 1549-57.
146. Crane, J. M.; Gibson, D. M.; Vaughan, R. H.; Bergstrom, G. C., Iturin levels on wheat spikes linked to biological control of Fusarium Head Blight by *Bacillus amyloliquefaciens*. *Phytopathology* **2012**, 103 (2), 146-155.

VITA

Michael Christopher James graduated from the University of Knoxville Tennessee in 2010 with a Bachelor of Science in Plant Biology. During his senior year, he was awarded the Undergraduate Summer Research Stipend Award for his research under Dr. Elias Fernandez focusing on metabolism of xenobiotics. After graduation he was accepted to an internship with the Student Conservation Association focusing on floodplain easements. In August of 2011 he joined the lab of Dr. Mark Hamann in the Department of Pharmacognosy at The University of Mississippi, focusing on endophyte secondary metabolism.